A&A 510, A48 (2010)
DOI: 10.1051/0004-6361/200811184

Astronomy & Astrophysics

The Palermo *Swift*-BAT hard X-ray catalogue

II. Results after 39 months of sky survey⋆

G. Cusumano[1], V. La Parola[1], A. Segreto[1], V. Mangano[1], C. Ferrigno[1,2,3], A. Maselli[1], P. Romano[1], T. Mineo[1], B. Sbarufatti[1], S. Campana[4], G. Chincarini[5,4], P. Giommi[6], N. Masetti[7], A. Moretti[4], and G. Tagliaferri[4]

[1] INAF, Istituto di Astrofisica Spaziale e Fisica Cosmica di Palermo, via U. La Malfa 153, 90146 Palermo, Italy
e-mail: cusumano@ifc.inaf.it
[2] Institut für Astronomie und Astrophysik Tübingen (IAAT), Germany
[3] ISDC Data Centre for Astrophysics, Chemin d'Écogia 16, 1290 Versoix, Switzerland
[4] INAF – Osservatorio Astronomico di Brera, via Bianchi 46, 23807 Merate, Italy
[5] Università degli studi di Milano-Bicocca, Dipartimento di Fisica, Piazza delle Scienze 3, 20126 Milan, Italy
[6] ASI Science Data Center, via Galileo Galilei, 00044 Frascati, Italy
[7] INAF, Istituto di Astrofisica Spaziale e Fisica Cosmica di Bologna, via Gobetti 101, 40129 Bologna, Italy

Received 17 October 2008 / Accepted 23 June 2009

ABSTRACT

Aims. We present the Palermo *Swift*-BAT hard X-ray catalogue obtained from the analysis of data acquired during the first 39 months of the Swift mission.
Methods. We developed a dedicated software to perform the data reduction, mosaicking, and source detection of the BAT survey data. We analyzed the BAT dataset in three energy bands (14−150 keV, 14−30 keV, 14−70 keV), obtaining a list of 962 detections above a significance threshold of 4.8 standard deviations. The identification of the source counterparts was pursued using three strategies: cross-correlation with published hard X-ray catalogues, analysis of field observations of soft X-ray instruments, and cross-correlation with SIMBAD databases.
Results. The survey covers 90% of the sky down to a flux limit of 2.5×10^{-11} erg cm^{-2} s^{-1} and 50% of the sky down to a flux limit of 1.8×10^{-11} erg cm^{-2} s^{-1} in the 14−150 keV band. We derived a catalogue of 754 identified sources, of which ∼69% are extragalactic, ∼27% are Galactic objects, and ∼4% are already known X-ray or gamma ray emitters, whose nature has yet to be determined. The integrated flux of the extragalactic sample is ∼1% of the cosmic X-ray background in the 14−150 keV range.

Key words. X-rays: general – catalogs – surveys

1. Introduction

The study of Galactic and extragalactic sources at energies greater than 10 keV is fundamental to both the investigation of non thermal emission processes and to the study of source populations that are not detectable in the soft X-ray energy band because their emission is strongly absorbed by a thick column of gas or dust. Another major aim of deep and sensitive surveys in the hard X-ray domain is to resolve the diffuse X-ray background (CXB) and identify which class of sources represents the most significant contribution: while the CXB at energies lower than 10 keV has been almost entirely resolved (80−90%, Moretti et al. 2003; Worsley et al. 2005, 2006; Brandt & Hasinger 2005), only ∼1.5% of the CXB at higher energies can be associated with resolved sources (Ajello et al. 2008b).

Until now, the observation of the hard X-ray sky has not been performed with imaging grazing incidence telescopes because the reflectivity above 10 keV rapidly declines because of the steep decrease in the critical angle with energy. The first surveys in the hard X-ray domain were performed with detectors equipped with collimator-limited field of view: UHURU (2−20 keV; Forman et al. 1978) and HEAO1 (0.2 keV−10 MeV; Wood et al. 1984). Later, sky images for energies greater than 10 keV were produced using coded mask detectors (e.g., Fenimore & Cannon 1978; Skinner et al. 1987a): in these detectors the entrance window of the telescope is partially masked and the "shadows" of the cosmic sources are projected onto a position-sensitive detector. Dedicated algorithms are then used to reconstruct the position and intensity of the sources in the field of view and, therefore, reproduce the image of the observed sky. In the last two decades, space observatories equipped with this type of telescopes have surveyed the sky reporting detections of numerous sources emitting in the hard X-ray domain: Spacelab/XRT (Skinner et al. 1987b), MIR/KVANT/TTM (Sunyaev et al. 1991), GRANAT/ART-P (Pavlinsky et al. 1992, 1994), GRANAT/SIGMA (Cordier et al. 1991; Sunyaev et al. 1991), and *BeppoSAX*/WFC (Jager et al. 1997). Today, the IBIS-ISGRI camera (Ubertini et al. 2003; Lebrun et al. 2003) on the INTEGRAL observatory (Winkler et al. 2003) with its field of view of 8° × 8° (fully coded) is carrying out a hard X-ray survey focussing mostly on the Galactic plane in the 20−150 keV energy band with a sensitivity higher than previous observatories. The main results of this survey and the relevant source catalogues are reported in several papers (e.g. Bird et al. 2004, 2006, 2007; Bassani et al. 2006; Krivonos et al. 2007, 2005; Sazonov et al. 2007; Churazov et al. 2007).

⋆ Table 2 is also available in electronic form at the CDS via anonymous ftp to cdsarc.u-strasbg.fr (130.79.128.5) or via http://cdsweb.u-strasbg.fr/cgi-bin/qcat?J/A+A/510/A48

The Burst Alert Telescope (BAT; Barthelmy et al. 2005) onboard the *Swift* observatory (Gehrels et al. 2004), because of its large field of view (100° × 60° half coded) and large detector area (a factor of 2 greater than ISGRI), offers the opportunity to significantly increase the number of detections contributing to the luminosity of the sky in the hard X-rays allowing a substantial improvement of our knowledge of the AGN and of the cosmic hard X-ray background. The first results on the BAT survey have been presented in Markwardt et al. (2005), Ajello et al. (2008a,b), and Tueller et al. (2008). The latter presents a catalogue of sources detected in the first 9 months of the BAT survey data, identifying 154 extragalactic sources (129 at $|b| > 15°$).

To take full advantage of the BAT survey archive, we developed the dedicated software BATIMAGER (Segreto et al. 2010), which is independent from the software developed by the Swift-BAT team[1]. In this paper, we present the results obtained from the analysis of 39 months of BAT sky survey. The paper is organized as follows: in Sect. 2, we describe the BAT telescope; in Sect. 3, we describe the data set and screening criteria; in Sect. 4, we present a brief description of the code used for the analysis and illustrate our analysis strategy. In Sect. 5, we describe the survey properties. The catalogue construction and the results are reported in Sect. 6. The last section summarizes our results. The spectral properties of our extragalactic sample will be discussed in a forthcoming paper (La Parola et al. 2010, in preparation).

The cosmology adopted in this work assumes $H_0 = 70\ \mathrm{km\,s^{-1}\ Mpc^{-1}}$, $k = 0$, $\Omega_\mathrm{m} = 0.3$, and $\Lambda_0 = 0.7$. Quoted errors are at 1σ confidence level, unless stated otherwise.

2. The BAT telescope

The BAT, one of the three instruments onboard the *Swift* observatory, is a coded aperture imaging camera consisting of a 5200 $\mathrm{cm^2}$ array of $4 \times 4\ \mathrm{mm^2}$ CdZnTe elements mounted on a plane 1 m behind a 2.7 $\mathrm{m^2}$ coded aperture mask of $5 \times 5\ \mathrm{mm^2}$ elements distributed with a pseudo-random pattern. The telescope, which operates in the 14−150 keV energy range, has a large field of view (1.4 steradian half coded), and a point spread function (PSF) of 17 arcmin, and is devoted mainly to the monitoring of a large fraction of the sky for the occurrence of gamma ray bursts (GRBs). The BAT can measure their position with the accuracy (1−4 arcmin) that is necessary to slew the spacecraft towards a GRB position and bring the burst location inside the field of view of the narrow field instruments in a couple of minutes. While waiting for new GRBs, it continuously collects spectral and imaging information in survey mode, covering a fraction of between 50% and 80% of the sky every day. The data are immediately made available to the scientific community through the public Swift data archive[2].

3. Survey data set and screening criteria

We analyzed the first 39 months of the BAT survey data archive, from 2004 December to the end of 2008 February. The BAT survey data are in the form of detector plane histograms (DPH). These are three dimensional arrays (two spatial dimensions, one spectral dimension) that collect count-rate data in (typically) 5-m time bins for 80 energy channels.

The data were retrieved from the *Swift* public archive and screened out from bad quality files, excluding those files where the spacecraft attitude was unstable (i.e., with a significant variation in the pointing coordinates). The resulting dataset was pre-analyzed (see Sect. 4), to produce preliminary Detector Plane Images (DPI, obtained integrating the DPH along the spectral dimension) from where the bright sources ($S/N > 8$) and background were subtracted; very noisy DPHs, i.e., with a standard deviation significantly larger than the average value where subtracted. The list of bright sources detected in each DPH was used to identify and discard the files suffering from inaccurate position reconstruction. After cross-correlating the position of these sources with the ISGRI catalogue, the GRB positions, and the newly discovered *Swift* sources documented in literature (Markwardt et al. 2005; Ajello et al. 2008a; Tueller et al. 2008), we discarded the files where:

- the bright sources in the BAT field of view are detected more than 10 arcmin from their counterpart position (because of a star tracker loss of lock);
- the reconstructed image of at least one bright source has a strongly elongated shape (maybe due to an unrecognized slew).

After the screening based on these criteria, the usable archive has a total nominal exposure time of 72.7 Ms, corresponding to 91.2% of the total survey exposure time during the period under investigation.

4. Methodology

To perform a systematic and efficient search for new hard X-ray sources, we developed the BATIMAGER, a dedicated software that produces an all-sky mosaic directly from a list of BAT data files. A complete and detailed description of the software and its performance is presented in Segreto et al. (2010). Here we report only the details of the procedure which are relevant to this work.

4.1. The code

The BATIMAGER integrates each single DPH in a selected energy range, producing the corresponding DPI. A preliminary cleaning of the disabled and noisy pixels is performed, and the DPI is cross-correlated with the mask pattern, to identify and subtract bright sources (with $S/N > 8$). The background, modelled on a large scale from the analysis of the shadowgram residuals by performing a Principal Component Analysis (Kendall 1980), is then subtracted. A further search for bad pixels is performed, to obtain the final map of all pixels to be excluded in the following steps. A further correction is applied to take into account differences in the detection efficiency of single detector pixels, by means of a time/energy dependent efficiency map, built by stacking all the processed DPI and equalizing the average residual contribution for each pixel. The original DPI, corrected for the efficiency map and cleaned for bad pixels, is processed again, with all the contributions from the background and the bright sources identified in the previous steps computed simultaneously, to correct for cross-contamination effects. These contributions are subtracted from the DPI, that is then converted into a sky image, using the Healpix projection (Górski et al. 2005). This projection provides an equal-area pixelization on a sphere and allows the generation of an all-sky map, avoiding the distortion introduced by other types of sky projections far from the projection center. This sky map is then corrected for the occultation of Sun, Earth, and Moon. The sky maps produced from each DPI are added together, with the intensity in a given sky direction computed from the contribution from all the sky images,

[1] http://heasarc.gsfc.nasa.gov/docs/swift/analysis/
[2] http://heasarc.gsfc.nasa.gov/cgi-bin/W3Browse/swift.pl

each inversely weighted for its variance in that direction. As described above, the bright sources and background were already subtracted from each single DPI; therefore, this all-sky mosaic contains only the residual sky contribution. To correct for residual systematic effects (e.g., imperfect modelling of the source illumination pattern or of the background distribution), the all-sky S/N map is sampled on a scale significantly larger than the PSF: the local average S/N is subtracted and its measured variance used to normalize the local S/N distribution. Finally, we obtain a S/N map with zero average and unitary variance that can be used to complete a blind source detection.

4.2. Detection strategy

We created all-sky maps in three energy bands: 14−150 keV, 14−70 keV, and 14−30 keV. The source detection in the all-sky map is performed by searching for local excesses in the significance map. The source position and its peak significance are then refined with a fit restricted within a region of a few pixels, where the excess dominates over the noise distribution. Only detections with peak significance greater than 4.8 sigma are included in our list of detected sources. We found that this threshold represents the optimal value maximizing the number of detectable sources, maintaining at the same time an acceptable number of spurious detections: taking into account the total number of pixels in the all sky map and their spatial correlation, the PSF, and the Gaussian distribution of the noise, we expect 15 spurious detections above our threshold in each energy band, because of statistical fluctuations (Segreto et al. 2010). Therefore, the total number of spurious detections will be between 15 and 45 (1.6% to 4.7% of the total number of our detections, see below), the best case occurring if each noise fluctuation above the threshold appears simultaneously in all three bands, the worst case occurring if each fluctuation appears only in one energy band. A few sources (∼5%) detected with a significance slightly lower than our threshold were included in the detection list because their S/N is significantly higher than the negative excess (in modulus) of the local noise distribution.

The resulting detection catalogues (one for each of the three energy bands) were cross-correlated and merged into a single catalogue: when source candidates closer than 10 arcmin were present in the sky maps of different energy bands, they were reported in the merged catalogue as a single source candidate. We obtain a final number of 962 source candidates (detected in at least one of the three energy bands). We assume the most accurate source position to be that corresponding to the energy range with the highest detection significance.

We evaluated the hardness ratio of the detected sources as Rate(30−150 keV)/Rate(14−30 keV) (the hard rate is evaluated as the difference between the count rates in the 14−150 and in the 14−30 energy bands). In Fig. 1, we plot the hardness ratio as a function of the significance of each detected source, showing the energy range where the detection has the highest significance. Repeating the detection process in three energy bands optimizes the S/N for each source, yielding more reliable values of the source position, whose uncertainty scales inversely with the significance. Moreover, a significant subsample of sources was detected in only one of the three energy bands (56 in the 14−150 keV energy band, 38 in the 14−30 keV energy band, 78 in the 14−70 keV energy band) demonstrating that searching in different energy bands maximizes the number of detectable sources.

Figure 2 shows that the distribution of the detected sources (orange squares) versus Galactic latitude flattens for $|b| > 5$, which we shall hereafter consider to be our operational definition of the Galactic plane.

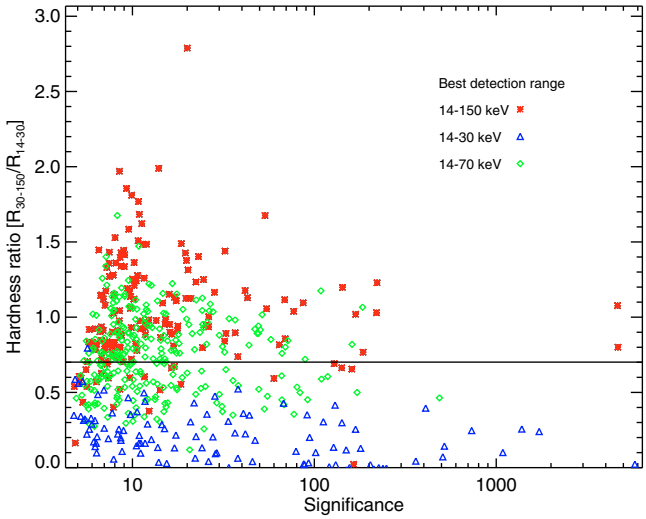

Fig. 1. Hardness ratio (defined as R(30–150)/R(14–30)) of the sources detected with BATIMAGER as a function of the best detection significance. Different symbols refer to the energy range where each source was detected at the highest S/N. The solid line is the average hardness ratio value.

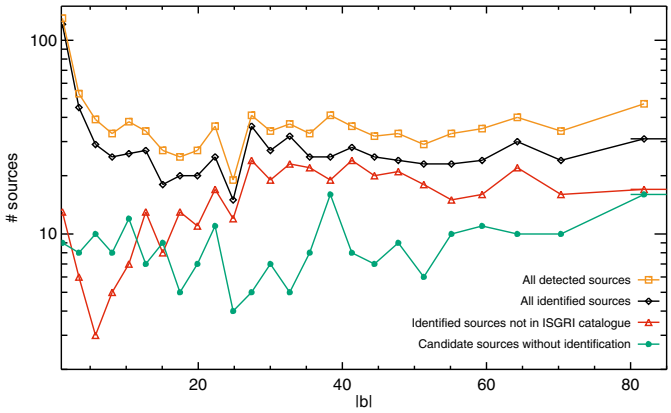

Fig. 2. Distribution of the detected sources versus Galactic latitude. Each bin corresponds to a solid angle of ∼0.50 sr.

4.3. Identification strategy

The identification of the counterpart to the BAT detections was performed following three different strategies:

A. The position of each of the 962 detected excesses was cross-correlated with the coordinates of the sources included in the INTEGRAL General Reference Catalogue[3] (v. 27), which contains 1652 X-ray emitters, and with the coordinates of the counterpart of the 48 new identifications of BAT sources already published (Markwardt et al. 2005; Tueller et al. 2008; Ajello et al. 2008a,b) and not included in the above catalogue. We adopted as a counterpart a source within a radius $R = 8.4$ arcmin from the BAT position (4 standard deviations error circle for a source detection at 4.8 standard deviations, Segreto et al. 2010). With this method, we obtained 458 identifications, 295 with $|b| > 5°$. Our choice of the error radius enabled us to maximize the associations and ensure that the number of spurious

[3] http://isdc.unige.ch/?Data+catalogs

associations were maintained to a negligible level. The number of spurious identifications due to chance spatial coincidence was evaluated using the following expression:

$$N_{\rm sp} = \frac{N \times A_R}{A} \times N_{\rm cat} \quad (1)$$

where, A_R is the selected error circle area, A is the total sky area under investigation, and N and $N_{\rm cat}$ are the number of BAT detections and of candidate counterparts in A. The above formula assumes both source distributions to be uniform over the sky. To take into account the higher density of sources on the Galactic plane, we divided the sky into two regions: $|b| \leq 5°$ (the Galactic plane, with $N = 190$, $N_{\rm cat} = 651$) and $|b| > 5°$ ($N = 772$, $N_{\rm cat} = 1049$). The number of expected spurious identifications is 2.1 within $|b| < 5°$ and 1.3 elsewhere. Since the assumption of uniform distribution could be only a crude approximation, we verified the evaluation of expected spurious associations with an alternative method: we produced a set of 962 coordinate pairs by inverting the position of the detected excesses with respect to the Galactic reference system and cross-correlated these positions with both the INTEGRAL General Reference Catalogue and the published BAT identifications. We obtained 3 spurious associations, in full agreement with the value obtained in Eq. (1).

B. We searched for observations from *Swift*/XRT containing the remaining (504) unidentified excesses in their field. We found *Swift*/XRT observations for 186 BAT source candidates. Source detection inside these X-ray images was performed using XIMAGE (v4.4). When a source was detected inside a 6.3 arcmin error circle (99.7% confidence level for a source detection at 4.8 standard deviations, Segreto et al. 2010), we first measured its hardness ratio in the 0.3−10 keV range (with 3 keV as a common boundary of the two ratio bands) and its count rate above 3 keV. We identified a source as the counterpart of a BAT detection, if at least one of the above conditions was satisfied: hardness ratio >0.5, count rate above 3 keV $>5 \times 10^{-3}$ c s^{-1}. In seven cases where two candidates, satisfying at least one of the threshold conditions, were found inside the BAT error circle, we selected the counterpart to be the closest source to the BAT position. With this method, we identified 170 source counterparts. To evaluate the number of expected spurious identifications, we collected a large sample of XRT observations of GRB fields, using only late follow-ups (where the GRB afterglow has faded) with the same exposure time distribution as the XRT pointings of the BAT sources. We searched for sources within a 6.3 arcmin error circle centered on the nominal pointing position in each of these fields, excluding any GRB residual afterglow, and satisfying at least one of the above threshold conditions. We detected 7 sources, therefore, the number of expected spurious identifications is consistent with the number of multiple XRT detections inside the BAT error circle. We also searched for field observations with other X-ray instruments (*XMM-Newton*, *Chandra*, *BeppoSAX*), finding 25 identifications, out of 30 pointings. Given the low number of available fields, the number of expected spurious identifications within this sample is irrelevant.

C. For the remaining unidentified sky map excesses (309), we searched for spatial coincidence inside an error circle of 4.2 arcmin radius (90% confidence level for a source detection at 4.8 standard deviations, Segreto et al. 2010) with sources included in the SIMBAD catalogues. The size of the search radius was fixed to 4.2 arcmin to ensure a negligible number of spurious identifications (see below). We restricted our search to the following SIMBAD object classes: cataclysmic variable (CV), high mass X-ray binaries (HXB), low mass X-ray binaries (LXB),

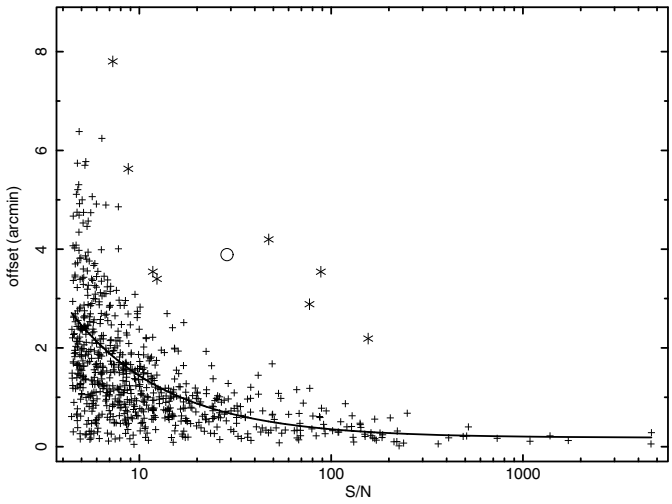

Fig. 3. Offset between the BAT position and the counterpart position as a function of the detection significance. A few values are far from the overall distribution: those marked with a star (sources number 535, 564, 565, 570, 571, 574, 584 and 586 in Table 2) are in crowded field and the reconstructed sky position suffers from the contamination of the PSF of the nearest sources; the one marked with a circle is an extended source (Coma Cluster). The solid line represents the fit to the data (excluding the few outliers) with a power law.

Seyfert 1 (Sy1), Seyfert 2 (Sy2), Blazar and BL Lac (Bla, BLL), and LINERs (LIN), for a total of 22 425 objects in the SIMBAD database. This strategy allowed us to identify 92 detections, only one source being at low Galactic latitude ($|b| < 5°$). The number of expected spurious identifications was evaluated with the two methods described by strategy *A*. According to Eq. (1), we expect 0.03 spurious identifications within $|b| < 5°$ (20 BAT detections and 391 Simbad sources in the classes of interest) and 2.7 elsewhere (289 BAT detections and 22 034 Simbad sources); using the set of 309 coordinate pairs obtained inverting with respect to the Galactic center the positions of the sources in our sample, we find 3 spurious associations, consistent with the first method. The cross-correlation between unidentified sky excess and the SIMBAD catalogue of QSOs was treated separately because the coincidence error circle of 4.2 arcmin radius results in a high number of spurious associations (9 out of 17 associations). A radius of 2 arcmin allowed us to identify 9 sources as QSOs, and to optimize the ratio of the total number of associations to the expected number of spurious associations (∼2).

In Fig. 3, we report the offsets of each BAT source with respect to its identified counterpart as a function of the detection significance (S/N). The offset versus the detection significance can be modeled with a power-law plus a constant. The best-fit equation that we obtained was:

$$\text{offset(arcmin)} = (9.1 \pm 1.6) \times (S/N)^{-0.93 \pm 0.09} + (0.21 \pm 0.03). \quad (2)$$

The constant in Eq. (2) represents the systematic error due to a residual boresight misalignment. At the detection threshold of 4.8 standard deviations, the average offset is ∼2.6 arcmin.

Figure 4 shows the distribution of the identified sources for each identification strategy as a function of the offset between the BAT position and the counterpart position. The peak of the distribution is at a lower offset for strategy *A* because the sample of the sources identified with this strategy contains the brightest objects. The peak of the distribution relevant to strategy *B* is at a lower offset than the distribution of strategy *C* because the XRT

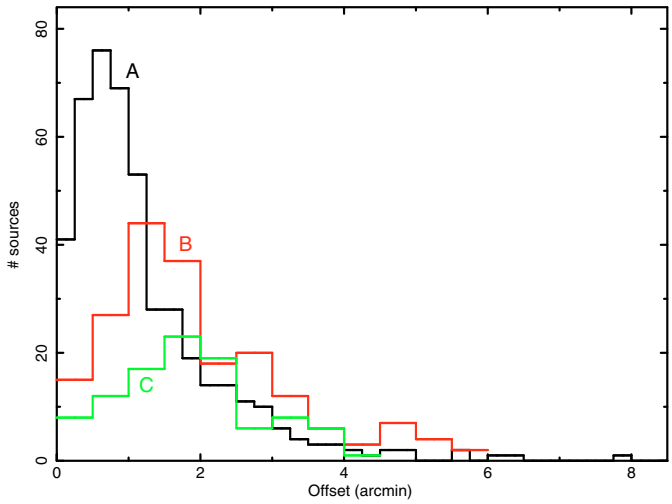

Fig. 4. Distribution of the identified sources for each identification strategy (Sect. 4.3) as a function of the offset between the BAT position and the counterpart position.

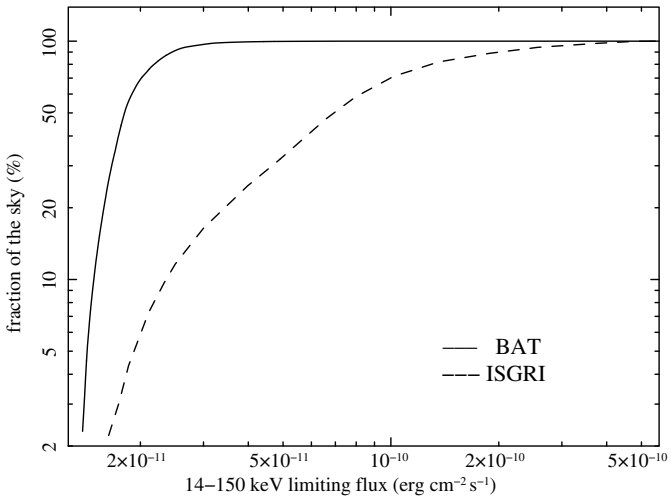

Fig. 5. Fraction of the sky covered by the *Swift*-BAT and INTEGRAL-ISGRI surveys vs. limiting flux.

follow-up observations were performed on the more significant still unidentified source candidates.

All the identifications obtained with the three strategies (754) were merged into the final catalogue reported in Table 2 (see Sect. 6), where a flag indicates the identification method for each source. Figure 2 shows the distribution of all identified sources (black diamonds) as a function of the Galactic latitude.

A set of 208 detections could not be associated with a counterpart. These source candidates have a detection significance of between 4.8 and 14 standard deviations and a flux in the 14–150 keV band of between 6.7×10^{-12} and 2.7×10^{-11} erg cm^{-2} s^{-1}. Thirty-three sources out of 208 are detected in all the three enegy bands, and 63 in two energy bands. The unidentified detections are distributed quite uniformly across the sky (Fig. 2, green circles), 190 sources out of 208 being located above the Galactic plane ($|b| > 5°$).

5. Sky coverage and limiting flux

Figure 5 shows the sky coverage, defined as the fraction of the sky covered by the survey as a function of the detection limiting flux. The limiting flux for a given sky direction is calculated by multiplying the local image noise by a fixed detection threshold of 5 standard deviations. This threshold, higher than the one adopted for source detection (Sect. 4.2), was used to compare the BAT sky coverage with those produced with the INTEGRAL data survey. The large BAT field of view, the large geometrical area, and the Swift pointing distribution, which covers the sky randomly and uniformly according to the appearance of GRBs, allowed an unprecedented sensitive and quite uniform sky coverage to be obtained. The 39 month BAT survey covers 90% of the sky down to a flux limit of 2.5×10^{-11} erg cm^{-2} s^{-1} (1.1 mCrab), and 50% of the sky down to 1.8×10^{-11} erg cm^{-2} s^{-1} (0.8 mCrab). In the same figure, the BAT sky coverage is compared with that of INTEGRAL/ISGRI after 44 months of observation (Krivonos et al. 2007).

Figure 6 shows the limiting flux map in Galactic Aitoff projection, with the ecliptic coordinates grid superimposed. The minimum detection limiting flux is not fully uniform on the sky: the Galactic center and the ecliptic plane are characterized by a poorer sensitivity because of high contamination from intense Galactic sources and to the observing constraints on the *Swift* spacecraft. The highest flux sensitivity is achieved close to the ecliptic poles, where a detection flux limit of about 1.1×10^{-11} erg cm^{-2} s^{-1} is reached (~0.5 mCrab).

6. The 39-month catalogue

The complete catalogue of the sources identified in the first 39 months of BAT survey data is reported in Table 2. The table contains the following information:

- Palermo BAT Catalogue (PBC) name of the source (Col. 2), compiled from the BAT coordinates with the precision of 0.1 arcmin on RA.
- Counterpart identification (Col. 3) and source type (Col. 4) coded according to the nomenclature used in SIMBAD.
- RA and Dec of the BAT source in decimal degrees (Cols. 5, 6).
- Error radius (Col. 7), offset with respect to the counterpart position (Col. 8) and significance (Col. 9), obtained for the energy band with the highest significance (a flag in Col. 14 indicates the energy range with the maximum significance).
- Flux in the widest band of detection, averaged over the entire survey period (Col. 10). For most of the sources, this is 14–150 keV. In the other cases, a flag in Col. 14 indicates the appropriate band. To convert count rates into fluxes, we derived a conversion factor for each of the three bands using the corresponding Crab count rate and the Crab spectrum used for BAT calibration purposes, as reported in the BAT calibration status report[4].
- Hardness ratio defined as Rate[30–150 keV]/Rate [14–30 keV], where the hard rate is evaluated as the difference between the count rates in the 14–150 and in the 14–30 energy bands (Col. 11).
- Redshift of the extragalactic sources (Col. 12), from the SIMBAD database (or NED, for the few cases that were not reported in SIMBAD).
- Log of the rest-frame luminosity in the 14–150 keV band for extragalactic objects (Col. 13), calculated using the luminosity distance for sources with redshift >0.01, and using the distance reported in the Nearby Galaxies Catalogue (NBG,

[4] http://swift.gsfc.nasa.gov/docs/swift/analysis/bat_digest.html#calstatus

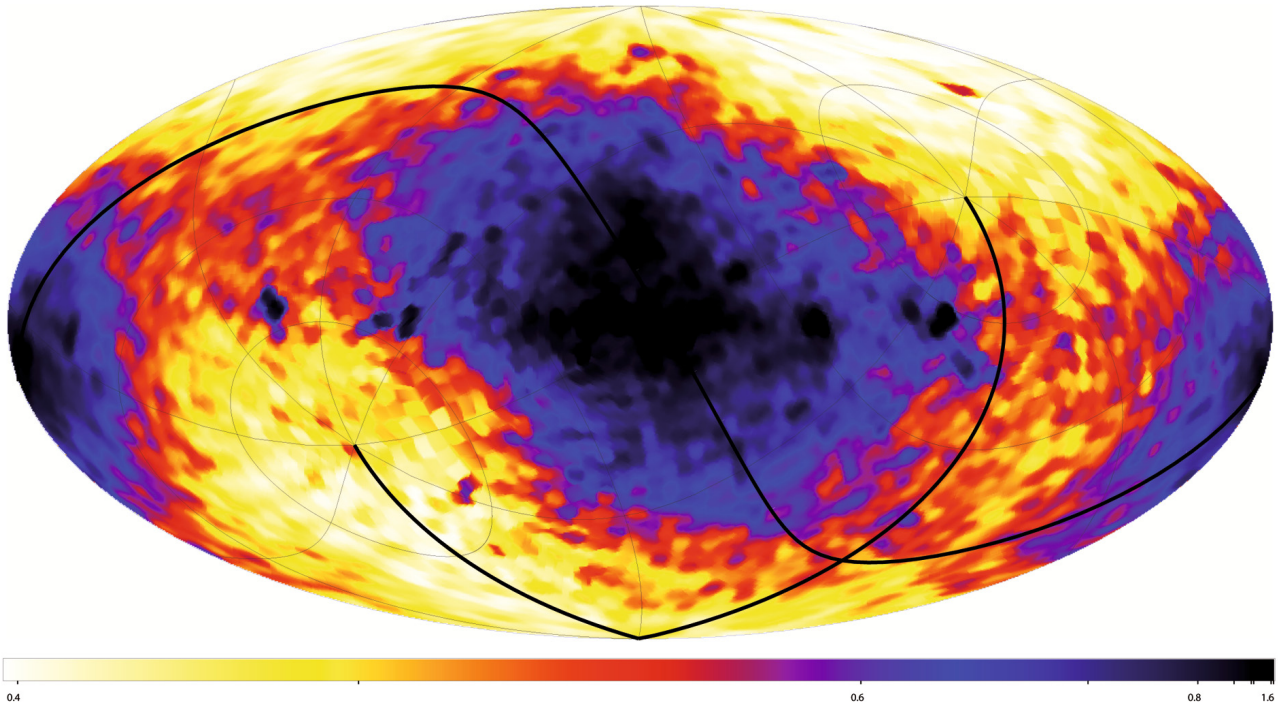

Fig. 6. Map of the limiting flux (in mCrab) of the 39-months BAT-survey data in the 14−150 keV band, projected in Galactic coordinates, with the ecliptic coordinates grid superimposed (the thick lines represents the ecliptica axes). The scale on the colorbar is in mCrab.

Tully 1988) or NED, for the few cases not reported in the NBG catalogue, for sources with redshift <0.01.

– Flag column (Col. 14) with information about: energy band with the highest significance (A), energy band used for the calculation of the flux (B), flag for already known hard X-ray sources (C), position with respect to the Galactic plane ($|b| < 5°$, D), and strategy used for the identification (E, see Sect. 4.3).

6.1. Statistical properties of the catalogue

Table 1 describes the distribution of the 754 sources in our catalogue among different object classes: ~69% of the catalogue consists of extragalactic objects, ~27% are Galactic objects, and ~4% are already known X-ray or gamma-ray emitters whose nature is still to be determined. Figure 7 shows the distribution of all the sources in our catalogue, colour-coded according to the object class, where the size of the symbol is proportional to the 14−150 keV flux (for those sources not detected in the 14−150 keV band, the flux in the widest band of detection has been extrapolated to the 14−150 keV range using the BAT Crab spectrum).

We compared this distribution with the third ISGRI catalogue (Bird et al. 2007). The results are plotted in Fig. 8. We measured a dramatic improvement in the detection of extragalactic objects, both in the nearby Universe (normal galaxies, LINERs) and at greater distances (Seyfert galaxies, QSO, clusters of galaxies). As expected from the sky coverage achieved by the BAT survey data (Fig. 5), most of our identified sources have a flux below 1×10^{-10} erg s^{-1} cm^{-2} and are located outside the Galactic plane. We also detected many Galactic sources that are not included in the ISGRI catalogue, most of which are cataclysmic variables and X-ray binaries. This can be explained in part by the different pointing strategy of the two instruments.

Table 1. Classification of the known sources detected in the BAT survey.

Class	# of sources	% in the catalog
LXB	76	10.1%
HXB	64	8.5%
Pulsars	10	1.3%
SN/SNR	5	0.7%
Cataclysmic variables	46	6.1%
Stars	5	0.7%
Molecolar Cloud	1	0.1%
Galactic (total)	207	27.5%
Seyfert 1 galaxies	235	31.2%
Seyfert 2 galaxies	131	17.4%
LINERs	7	0.9%
QSO	14	1.8%
Blazars	71	9.4%
Galaxy clusters	18	2.4%
Normal galaxies	27	3.6%
Unclassified AGN	16	2.1%
Extragalactic (total)	519	68.8%
Other types	28	3.7%

Other types includes all sources that have a catalogued counterpart but have not been classified yet.

However, Fig. 2 shows that, although most of our newly identified sources (red triangles) are above the Galactic plane, where the ISGRI exposure is low, we also detect a few sources on the Galactic plane most of which we identify as X-ray binaries (1E 1743.1–2852, GRO 1750–27, SAX J1810.8–2609, and XTE J1856+053). We verified that their detections are caused by a transient intense emission observed in the large FoV of BAT.

We detected emission from 18 clusters of galaxies. We verified that for 17 of them the spectral distribution in the 14−150 keV band is consistent with the tail of a thermal

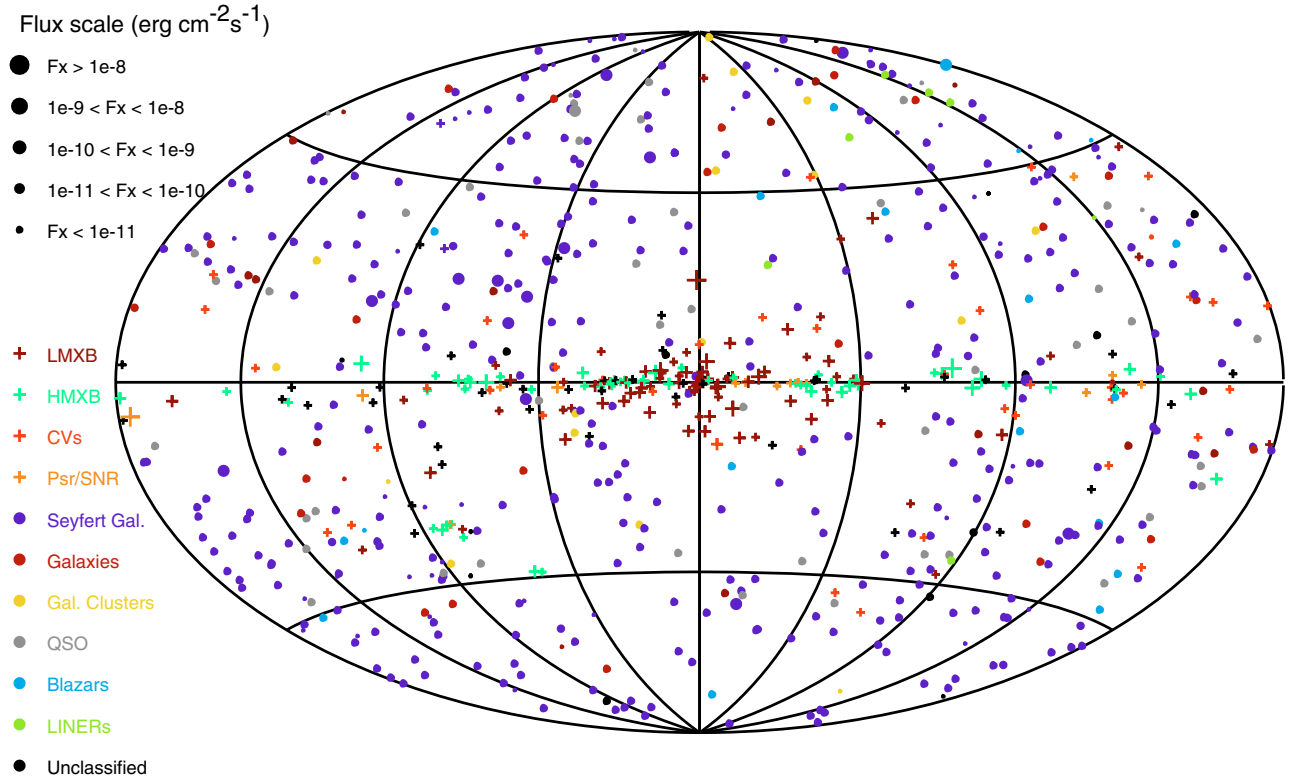

Fig. 7. Map of the sources that we detect in the BAT survey data (Galactic coordinates). Different colors denote different object classes, as detailed in the legend. The size of the symbol is proportional to the source flux in the 14−150 keV band.

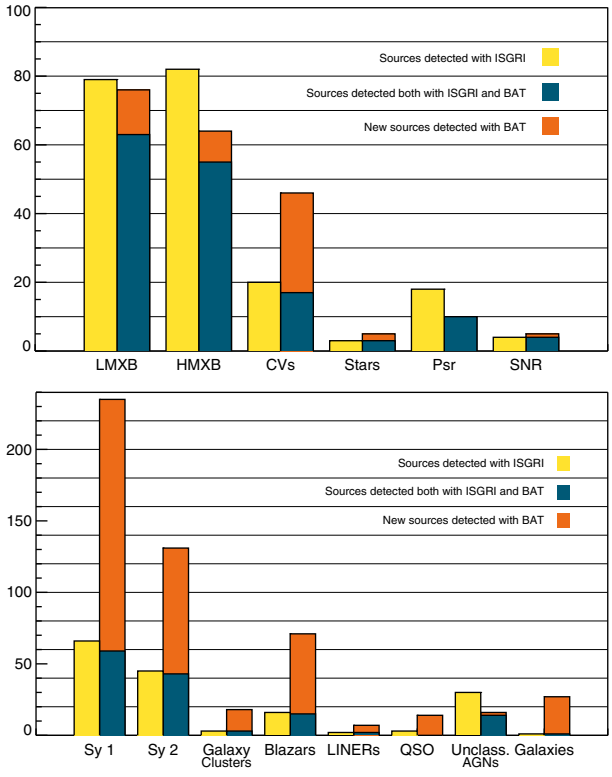

Fig. 8. Comparison between the sources in our catalogue and those reported in the third ISGRI catalogue (Bird et al. 2007). *Top*: galactic sources. *Bottom*: extragalactic sources.

emission with $kT \sim 10$ keV, without evidence of hard non-thermal emission. Only for Abell 2142 did we find evidence of a power law component that could be related to the AGN content of the cluster.

6.2. The extragalactic subsample

The catalogue contains 519 extragalactic objects. Figure 9 shows the redshift distribution of our sample for the main classes of extragalactic objects. Most of the emission-line AGNs are located at $z < 0.1$, but we also detected a few Seyfert 1 galaxies at higher redshift (up to ∼0.29). Seyfert 2 galaxies are detected up to $z \sim 0.4$. Blazars are detected up to $z \sim 3.7$, and QSOs are detected up to $z \sim 2.4$.

We verified the completeness of our sample of 366 emission-line galaxies (i.e., the significance limit down to which we include in the sample all objects above a given flux limit) using the $V/V_{\rm Max}$ test (Schmidt 1968; Huchra & Sargent 1973). This method was developed to test the evolution of complete samples of objects, but can also be used to test the completeness of non-evolving samples. For each source, V is the volume enclosed by the object distance, while $V_{\rm Max}$ is the volume corresponding to the maximum distance where the object could still be revealed in the survey (and thus depends on the limiting flux in the direction of the object). In the case of no evolution, the expected value of $< V/V_{\rm Max} >$, averaged over the entire sample, is 0.5. We assumed the hypothesis of no evolution and uniform distribution in the local Universe. For each source in the sample and for each significance level tested for completeness ($\sigma_{\rm T}$), we computed the quantity $V/V_{\rm Max}$ as $[F/\sigma_{\rm T}\Delta F)]^{-3/2}$, where F is the flux of the source and ΔF is its 1 standard deviation uncertainty. The quantity $< V/V_{\rm Max} >$ was obtained by averaging $V/V_{\rm Max}$ over the number N of all sources in the sample detected with a significance higher than $\sigma_{\rm T}$, and its error is $1/12N$. Figure 10 shows the results of this test: the distribution becomes constant

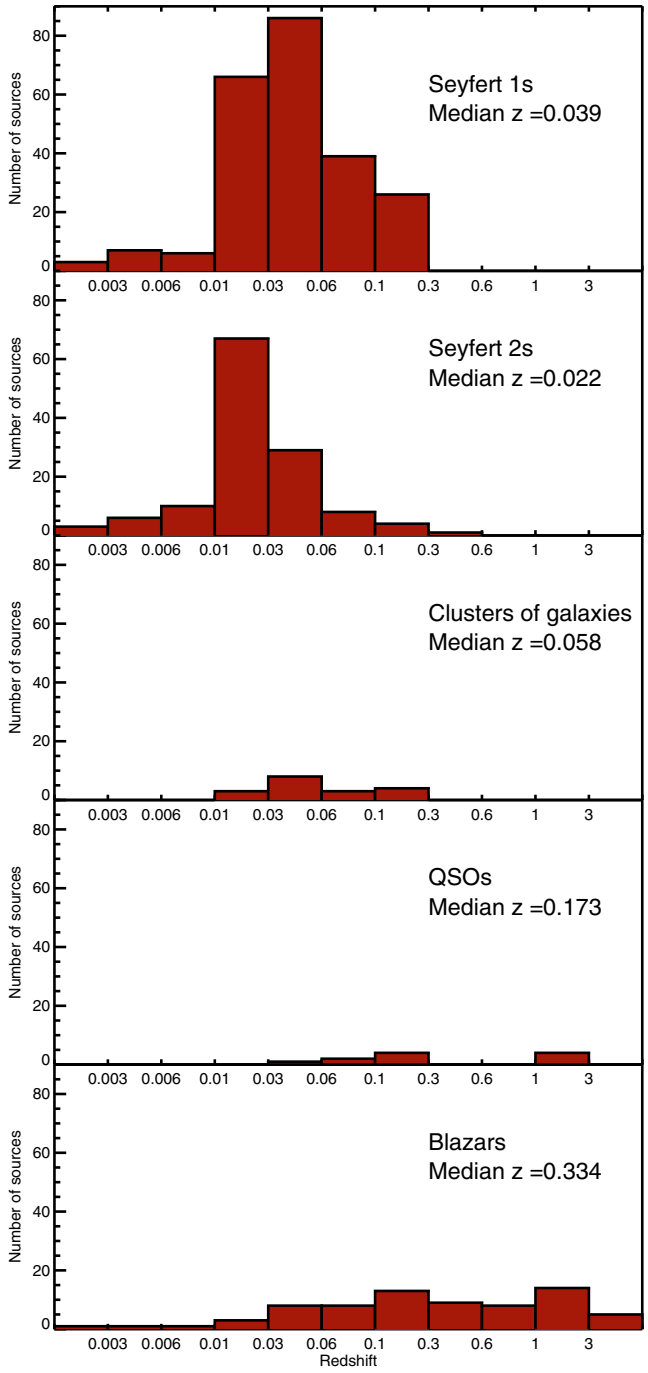

Fig. 9. Redshift distribution of the extragalactic sources in the BAT survey catalogue for different classes of extragalactic sources.

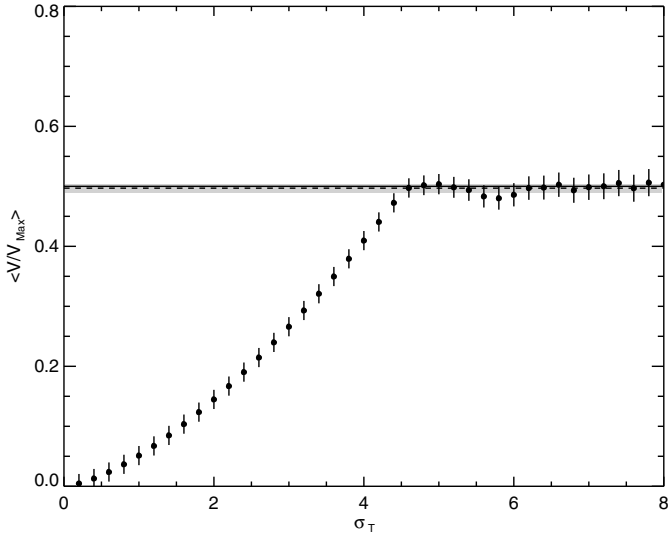

Fig. 10. $\langle V/V_{\rm Max}\rangle$ versus significance for our sample of extragalactic sources. The solid line is the expected value (0.5), the dashed line is the average value for $S/N > 4.5\sigma$, and the shaded area covers the 1σ error for the average value.

at $S/N \gtrsim 4.5\sigma$, with a mean value of 0.497 ± 0.007, consistent with the expected value of 0.5. Thus, we can confidently assume that our sample is complete to our adopted significance threshold of 4.8σ.

6.3. log(N) – log(S) distribution

The $\log(N) - \log(S)$ distribution was evaluated by summing the contributions of all the detected sources firmly identified with extragalactic objects (Table 2) and all the unidentified detections. We selected only sources with $|b| > 5°$: Fig. 2 (orange squares) shows that the detection distribution is uniform above this Galactic latitude limit. The cumulative distribution is weighted by the area in which these sources could have been detected. The following formula was applied:

$$N(>S) = \sum_{S_i>S} \frac{1}{\Omega_i},$$

where N is the total number of detected sources with fluxes greater than S, S_i is the flux of the ith source and Ω_i is the sky coverage associated with the flux S_i (Fig. 5).

To avoid the presence of systematic errors in the determination of the $\log(N) - \log(S)$ caused by spurious source detections and to the large relative uncertainty in the sky coverage at the lower end of the flux scale, we limited the construction of the $\log(N) - \log(S)$ to fluxes greater than $\sim 1.5 \times 10^{-11}$ erg cm^{-2} s^{-1}. The resulting $\log(N) - \log(S)$ distribution contains 330 sources (14 unidentified) and covers a flux range up to 3×10^{-10} erg s^{-1} cm^{-2}.

We applied a linear least-square fit to determine the slope of the $\log(N) - \log(S)$ distribution assuming a power law in the form $N(>S) = K \times (S/S_0)^{-\alpha}$, where S_0 is assumed to be 1×10^{-11} erg cm^{-2} s^{-1}. The fit infers a value of $\alpha = 1.56 \pm 0.06$ and a normalization of 570 ± 24 sources with flux greater than 10^{-11} erg cm^{-2} s^{-1}, corresponding to a density of $(1.38 \pm 0.06) \times 10^{-2}$ deg^{-2}. The single power-law model is found to provide an acceptable description of the data ($\chi^2 = 0.65$; 31 d.o.f.) with a slope consistent with a Euclidean distribution.

The presence of spurious detections in the sample of unidentified sources could introduce a systematic effect in both the slope and the normalization of the $\log(N) - \log(S)$. We expect between 15 and 45 spurious detections to be caused by statistical fluctuations (see Sect. 4.2), which correspond to a percentage between ~7 and ~22% in the sample of the ~208 unidentified sources. This implies that 1–3 unidentified sources among those used in the fit of the $\log(N) - \log(S)$ could be spurious. We checked that their contribution does not introduce any significant systematic errors in the best-fit values.

The integrated flux is $\sim 4.5 \times 10^{-13}$ erg cm^{-2} s^{-1} deg^{-2} corresponding to ~1.4% of the intensity of the X-ray background in

Table 2. BAT survey 39 months catalogue.

	PBC name	ID	Type⋆	RA (deg)	Dec (deg)	Error radius (arcmin)	Offset (arcmin)	SNR	Flux† (erg cm^{-2} s^{-1})	Hardness ratio (R_{30-150}/R_{14-30})	Redshift	log L_{14-150} (erg s^{-1})	Flag‡ A	B	C	D	E
1	PBC J0006.3+2012	Mrk 335	Sy1	1.58873	20.20689	3.10	0.480	11.46	1.9 ± 0.2	1.0 ± 0.3	0.0254	43.34	3	1	n	h	a
2	PBC J0009.3-0034	2MASX J00091156-0036551	Sy2	2.34193	–0.57510	3.89	3.558	5.35	0.9 ± 0.2	...	0.0730	44.17	1	1	n	h	b
3	PBC J0010.4+1059	Mrk 1501	BLA	2.61064	10.99384	2.59	1.579	10.02	1.8 ± 0.2	0.8 ± 0.3	0.0893	44.65	3	1	n	h	a
4	PBC J0018.3+8135	S5 0014+81	BLA	4.58770	81.59197	3.34	2.682	6.75	1.0 ± 0.2	0.6 ± 0.4	3.3660	48.12	1	1	n	h	a
5	PBC J0023.0+6138	IGR J00234+6141	CV*	5.77389	61.64727	3.91	3.795	7.53	1.1 ± 0.2	0.2 ± 0.3	...	...	2	1	y	l	a
6	PBC J0024.9+6407	TYCHO SNR	SNR	6.23328	64.13138	3.26	2.824	6.99	1.1 ± 0.2	0.4 ± 0.3	...	...	3	1	y	l	a
7	PBC J0025.0+6248	IGR J00245+6251	gB	6.27016	62.80854	4.16	4.688	4.85	0.7 ± 0.2	0.2 ± 0.4	...	...	1	1	y	l	a
8	PBC J0025.6+6823	IGR J00256+6821	AG?	6.40185	68.39235	3.47	1.834	6.37	1.0 ± 0.2	0.8 ± 0.5	0.0120	42.50	1	1	n	h	a
9	PBC J0028.9+5917	V709 Cas	DQ*	7.22675	59.29191	1.41	0.724	43.64	7.7 ± 0.2	0.49 ± 0.05	...	...	3	1	y	l	a
10	PBC J0029.3+1317	RBS 0068	Sy1	7.33068	13.28351	4.19	1.677	4.80	0.6 ± 0.1	...	0.1450	44.77	3	3	n	h	c
11	PBC J0033.2+6130	IGR J00335+6126	Sy1	8.31342	61.50171	3.17	4.006	9.62	1.9 ± 0.2	0.9 ± 0.3	0.1050	44.72	1	1	y	l	a
12	PBC J0035.8+5951	1ES 0033+59.5	BLA	8.96774	59.85079	2.68	0.972	12.36	1.9 ± 0.2	0.3 ± 0.2	0.0860	44.57	2	1	y	l	a
13	PBC J0036.3+4539	2MASX J00362092+4539532	Sy1	9.09174	45.66243	3.96	0.238	6.09	1.2 ± 0.2	...	0.0477	43.77	3	1	n	h	b
14	PBC J0037.2+6120	IGR J00370+6122	HXB	9.30329	61.34838	2.88	0.800	11.69	2.0 ± 0.2	1.0 ± 0.3	...	...	3	1	y	l	a
15	PBC J0041.6+2534	NGC 214	GiG	10.42025	25.56853	3.74	5.061	7.52	1.5 ± 0.2	...	0.0150	42.78	1	1	n	h	c
16	PBC J0041.7-0920	ABELL 0085	ClG	10.43030	–9.34827	4.06	1.393	5.04	0.8 ± 0.2	0.6 ± 0.5	0.0521	43.80	2	1	n	h	a
17	PBC J0042.6+4111	4U 0037+39	X	10.65773	41.19100	3.95	1.840	5.24	0.9 ± 0.2	...	...	...	1	1	n	h	a
18	PBC J0042.7+3017	RX J0042.6+3017	Sy1	10.69393	30.29990	3.45	1.274	6.58	1.1 ± 0.2	0.9 ± 0.5	0.1400	44.76	3	1	n	h	b
19	PBC J0042.8-2331	NGC 235A	Sy2	10.71398	–23.52057	1.86	1.272	19.90	3.7 ± 0.2	1.1 ± 0.2	0.0222	43.58	3	1	y	h	a
20	PBC J0048.7+3157	Mrk 348	BLA	12.19016	31.95353	1.11	0.379	57.54	11.2 ± 0.2	0.96 ± 0.06	0.0151	43.72	3	1	y	h	a
21	PBC J0051.8-7318	RX J0052.1-7319	HXB	12.96843	–73.30997	2.93	1.661	12.02	2.0 ± 0.2	0.4 ± 0.2	...	...	3	1	n	h	a
22	PBC J0051.9+1725	Mrk 1148	Sy1	12.99701	17.43206	2.21	1.089	13.01	2.1 ± 0.2	0.7 ± 0.2	0.0642	44.42	3	1	n	h	c
23	PBC J0054.6+2521	RBS 0130	Sy1	13.67128	25.36165	4.37	4.668	4.52	0.3 ± 0.1	...	0.1550	44.85	2	2	n	h	c
24	PBC J0055.3+4612	XSS J00564+4548	CV*	13.83279	46.21383	2.43	1.815	16.50	3.0 ± 0.2	0.5 ± 0.1	...	...	2	1	n	h	c
25	PBC J0056.5+6043	gam Cas	Be*	14.14344	60.72316	1.21	1.063	51.18	7.9 ± 0.2	0.19 ± 0.04	...	...	2	1	y	l	a
26	PBC J0059.8+3150	Mrk 352	Sy1	14.96095	31.83543	2.35	0.761	13.14	2.5 ± 0.2	0.7 ± 0.2	0.0149	43.08	3	1	y	h	a
27	PBC J0100.6-4752	ESO 195-IG 021	Sy1	15.15736	–47.87433	3.32	0.594	6.81	0.9 ± 0.2	0.8 ± 0.5	...	...	3	1	n	h	c
28	PBC J0105.7-1415	RBS 0149	Sy1	16.44535	–14.25433	3.43	2.181	6.48	1.0 ± 0.2	0.6 ± 0.4	0.0670	44.11	3	1	n	h	c
29	PBC J0106.8+0637	2MASX J01064523+0638015	Sy2	16.71979	6.62860	4.29	1.904	4.64	0.7 ± 0.2	...	0.0409	43.55	1	1	n	h	b
30	PBC J0108.8+1320	3C 033	Sy2	17.21265	13.34690	2.87	0.733	11.28	2.3 ± 0.2	1.8 ± 0.5	0.0596	44.16	1	1	n	h	c
31	PBC J0111.1-1616	6dFGS gJ011114.3-161555	Sy1	17.78875	–16.27258	0.00	1.387	6.69	1.3 ± 0.2	...	0.0500	43.81	2	2	n	h	b
32	PBC J0111.5-3804	NGC 424	Sy2	17.89226	–38.07623	2.75	1.379	11.40	2.0 ± 0.2	1.0 ± 0.3	0.0115	42.67	3	1	n	h	a
33	PBC J0113.7+1314	Mrk 975	Sy1	18.43550	13.23966	3.75	2.492	5.67	0.9 ± 0.2	0.9 ± 0.6	0.0494	43.81	3	1	n	h	b
34	PBC J0113.8-1450	Mrk 1152	Sy1	18.45009	–14.84880	2.90	0.534	9.63	1.8 ± 0.2	0.6 ± 0.3	0.0522	44.03	3	1	n	h	a
35	PBC J0114.3-3240	IC 1663	Sy2	18.57513	–32.66833	3.50	2.576	6.65	1.2 ± 0.2	...	0.0118	42.57	1	1	n	h	b
36	PBC J0114.4-5524	NGC 454	Sy2	18.60750	–55.40798	3.19	0.813	9.23	1.6 ± 0.2	1.3 ± 0.5	0.0120	42.65	1	1	y	h	a
37	PBC J0117.1-7326	SMC X-1	HXB	19.28694	–73.44229	0.75	0.276	331.27	45.9 ± 0.2	0.143 ± 0.006	...	...	2	1	y	h	a
38	PBC J0118.0+6517	3A 0114+650	HXB	19.51938	65.29603	1.04	0.334	90.80	16.0 ± 0.2	0.43 ± 0.02	...	...	3	1	y	l	a
39	PBC J0122.3+5004	MCG+08-03-018	G	20.58219	50.07506	3.98	2.649	5.64	0.9 ± 0.2	0.6 ± 0.5	0.0206	43.02	3	1	n	h	c
40	PBC J0123.1+3421	1ES 0120+340	BLA	20.78009	34.35617	3.54	0.623	6.16	0.9 ± 0.2	0.5 ± 0.4	0.2720	45.40	3	1	n	h	c
41	PBC J0123.8-5847	RBS 0194	Sy1	20.96559	–58.79782	1.90	0.905	16.98	2.8 ± 0.2	0.8 ± 0.2	0.0470	44.27	3	1	n	h	a
42	PBC J0123.9-3503	NGC 526	Sy1	20.97878	–35.05627	1.63	0.561	23.84	4.3 ± 0.2	1.1 ± 0.1	0.0192	43.53	1	1	y	h	a
43	PBC J0124.4+3346	NGC 0513	Sy2	21.11426	33.78088	3.14	1.093	10.19	2.0 ± 0.2	1.2 ± 0.4	0.0195	43.15	1	1	n	h	c
44	PBC J0126.0+1518	RHS 10	Sy1	21.50103	15.30966	4.23	0.661	4.74	0.5 ± 0.1	...	0.1110	44.42	3	3	n	h	b
45	PBC J0128.0-1848	RBS 0203	Sy1	22.00957	–18.81051	3.27	1.053	6.96	0.9 ± 0.2	0.6 ± 0.4	0.0430	43.70	3	1	n	h	c
46	PBC J0132.0-3306	ESO 353- G 009	Sy2	23.01577	–33.09999	3.40	3.098	6.55	0.8 ± 0.1	0.9 ± 0.5	0.0165	42.81	3	1	n	h	b
47	PBC J0134.0-3630	NGC 612	rG	23.50479	–36.50449	1.74	0.977	22.04	4.0 ± 0.2	1.4 ± 0.2	0.0299	43.86	1	1	n	h	a
48	PBC J0134.5-0428	RBS 0216	Sy1	23.64721	–4.48073	3.54	2.873	6.18	0.9 ± 0.2	0.6 ± 0.5	0.0790	44.22	3	1	n	h	c
49	PBC J0138.6-4000	ESO 297- G 018	Sy2	24.67064	–40.01276	1.57	0.728	24.19	3.6 ± 0.1	1.0 ± 0.1	0.0252	43.81	3	1	y	h	a
50	PBC J0140.4-5320	2MASX J01402676-5319389	G	25.11661	–53.33582	4.23	0.527	4.75	0.7 ± 0.1	...	...	...	1	1	n	h	c
51	PBC J0146.3+6144	4U 0142+614	Psr	26.57639	61.73474	1.73	1.083	24.85	5.2 ± 0.2	2.6 ± 0.4	...	...	1	1	y	l	a
52	PBC J0152.7-0327	MCG-01-05-047	Sy2	28.18907	–3.46139	2.58	1.257	10.07	1.6 ± 0.2	0.9 ± 0.3	0.0167	43.10	3	1	n	h	a
53	PBC J0154.7-2707	1RXS J015440.5-270659	AGN	28.67879	–27.13114	3.74	1.031	5.68	0.9 ± 0.2	...	0.1510	44.72	3	0	n	h	b
54	PBC J0201.0-0648	NGC 788	Sy2	30.26176	–6.81509	1.51	0.901	30.27	5.9 ± 0.2	1.1 ± 0.1	0.0136	43.33	3	1	y	h	a
55	PBC J0202.9-2400	RBS 0273	Sy1	30.73681	–24.01470	3.61	1.677	5.99	0.8 ± 0.1	...	0.1780	44.97	1	1	n	h	b
56	PBC J0206.3-0016	Mrk 1018	Sy1	31.57732	–0.27684	2.86	1.077	9.49	2.1 ± 0.2	1.4 ± 0.5	0.0426	43.91	3	1	y	h	a
57	PBC J0207.0+2929	RHS 13	rad	31.75435	29.49597	3.79	1.024	5.57	0.9 ± 0.2	0.4 ± 0.4	0.1100	44.44	3	1	n	h	b
58	PBC J0209.4-1010	NGC 835	Sy2	32.35103	–10.17373	4.35	2.272	4.55	0.5 ± 0.1	...	0.0123	42.55	3	3	n	h	a
59	PBC J0209.4+5226	IGR J02097+5222	Sy1	32.36014	52.44562	1.96	1.213	21.26	4.3 ± 0.2	0.8 ± 0.1	0.0492	44.34	1	1	y	h	a
60	PBC J0214.5-0044	Mrk 590	Sy1	33.63866	–0.73508	3.56	1.902	5.31	1.1 ± 0.2	...	0.0265	43.34	3	1	n	h	a
61	PBC J0214.7-6431	RBS 0295	Sy1	33.67610	–64.52047	4.13	1.259	4.91	0.7 ± 0.1	...	0.0740	44.05	1	1	n	h	b
62	PBC J0216.1+5124	2MASX J02162987+5126246	Sy2	34.02882	51.41636	3.09	3.164	7.59	1.5 ± 0.2	1.1 ± 0.4	0.4220	45.97	3	1	n	h	a
63	PBC J0217.4+7349	1ES 0212+735	BLA	34.37040	73.83144	2.49	0.368	10.69	1.9 ± 0.2	1.3 ± 0.4	2.3670	48.02	1	1	y	h	a
64	PBC J0225.0+1848	RBS 315	BLA	36.25686	18.80895	2.61	1.867	9.91	1.7 ± 0.2	1.1 ± 0.4	2.6900	48.11	3	1	n	h	c
65	PBC J0225.4-6314	FRL 296	Sy1	36.37364	–63.24697	3.51	2.663	7.51	1.3 ± 0.2	1.5 ± 0.6	0.0598	43.99	1	1	n	h	c
66	PBC J0226.7-2819	2MASX J02262568-2820588	Sy1	36.67490	–28.32004	4.17	3.976	6.47	1.0 ± 0.2	...	0.0600	43.89	3	1	n	h	b
67	PBC J0228.2+3119	Mrk 1040	Sy1	37.05453	31.32041	1.65	0.652	30.07	6.1 ± 0.2	0.76 ± 0.10	0.0163	43.49	3	1	y	h	a
68	PBC J0231.9-3640	IC 1816	Sy2	37.99192	–36.67282	3.26	1.393	9.39	1.6 ± 0.2	0.8 ± 0.3	0.0170	42.93	3	1	n	h	c
69	PBC J0232.7+2018	1ES 0229+200	BLA	38.18263	20.30858	2.89	1.685	8.44	1.4 ± 0.2	0.7 ± 0.4	0.1396	44.96	3	1	n	h	c
70	PBC J0234.3+3227	NGC 0973	Sy2	38.58036	32.46154	3.12	2.650	7.46	1.4 ± 0.2	1.4 ± 0.6	0.0150	42.94	1	1	y	h	a
71	PBC J0234.7-0846	NGC 985	Sy1	38.67776	–8.76888	2.31	1.651	12.08	1.9 ± 0.2	0.9 ± 0.3	0.0430	44.00	3	1	y	h	a
72	PBC J0235.3-2935	ESO 416-G002	Sy1	38.83300	–29.59368	2.70	1.553	11.58	2.1 ± 0.2	1.2 ± 0.3	0.0591	44.16	3	1	n	h	a

Table 2. continued.

	PBC name	ID	Type*	RA (deg)	Dec (deg)	Error radius (arcmin)	Offset (arcmin)	SNR	Flux† (erg cm^{-2} s^{-1})	Hardness ratio (R_{30-150}/R_{14-30})	Redshift	log L_{14-150} (erg s^{-1})	Flag‡ A B C D E
73	PBC J0238.2-5211	RBS 0335	Sy1	39.55099	–52.19260	2.56	1.128	10.22	1.4 ± 0.1	1.4 ± 0.4	0.0452	43.94	1 1 n h a
74	PBC J0238.8-4038	RBS 0339	Sy1	39.70396	–40.63831	2.83	0.348	8.72	1.3 ± 0.1	0.9 ± 0.4	0.0617	44.17	1 1 n h c
75	PBC J0240.6+6114	GT 0236+610	HXB	40.16095	61.24414	2.61	1.221	11.81	2.5 ± 0.2	0.9 ± 0.3	...	...	1 1 y l a
76	PBC J0241.2-0814	NGC 1052	Sy2	40.30301	–8.24776	2.58	2.018	12.29	2.6 ± 0.2	1.3 ± 0.3	0.0049	42.06	3 1 y h a
77	PBC J0241.5+0709	1ES 0238+069	Sy1	40.39875	7.16616	4.10	1.279	4.96	1.0 ± 0.2	...	0.0272	43.32	1 1 n h c
78	PBC J0242.7-0000	NGC 1068	Sy2	40.67545	–0.01328	2.58	0.319	13.28	2.8 ± 0.2	0.8 ± 0.2	0.0037	41.80	3 1 y h a
79	PBC J0245.0+6228	1ES 0241+622	Sy1	41.25464	62.47726	1.46	0.658	27.75	5.1 ± 0.2	1.0 ± 0.1	0.0445	44.47	3 1 y l a
80	PBC J0245.3+1045	4C +10.08	BLA	41.32499	10.75687	4.39	2.203	4.48	0.9 ± 0.2	...	0.0700	44.13	1 1 n h b
81	PBC J0248.9+2627	2MASX J02485937+2630391	G	42.24030	26.46388	3.26	2.850	7.48	1.7 ± 0.2	...	0.0597	44.19	1 1 n h c
82	PBC J0250.8+5442	2MFGC 2280	AG?	42.70468	54.70889	3.34	0.957	6.74	1.1 ± 0.2	0.8 ± 0.5	0.0150	42.75	1 1 n l a
83	PBC J0250.8-3617	1RXS J025055.4-361640	QSO	42.70677	–36.29198	4.20	1.484	4.78	0.5 ± 0.1	...	1.5362	46.90	3 0 n h b
84	PBC J0251.6-1640	NGC 1125	Sy2	42.92255	–16.67006	4.13	1.196	4.91	0.8 ± 0.2	...	0.0110	42.44	1 1 n h c
85	PBC J0252.4-0832	MCG-02-08-014	Sy2	43.10131	–8.53628	2.88	1.564	11.10	2.1 ± 0.2	0.8 ± 0.3	0.0167	43.03	3 1 y h a
86	PBC J0255.2-0011	NGC 1142	Sy2	43.80866	–0.19313	1.46	0.711	31.64	7.4 ± 0.2	1.2 ± 0.1	0.0288	44.11	1 1 y h a
87	PBC J0256.1+1925	XY Ari	DQ*	44.04704	19.43307	2.33	0.781	16.54	3.2 ± 0.2	0.5 ± 0.1	...	...	3 1 n h c
88	PBC J0256.3-3211	ESO 417- G 006	Sy2	44.08810	–32.18462	2.43	0.127	13.92	2.3 ± 0.2	1.0 ± 0.3	0.0163	43.10	3 1 n h c
89	PBC J0300.2+1627	RHS 17	Sy1	45.06699	16.45644	4.01	3.430	5.13	1.0 ± 0.2	...	0.0350	43.54	1 1 n h b
90	PBC J0303.8-0107	NGC 1194	Sy1	45.96340	–1.11725	2.76	0.941	12.84	2.8 ± 0.2	1.3 ± 0.3	0.0133	42.89	3 1 n h c
91	PBC J0311.3-2046	RBS 0392	Sy1	47.83725	–20.77998	2.84	0.706	8.67	1.5 ± 0.2	1.3 ± 0.5	0.0660	44.28	1 1 n h c
92	PBC J0318.2+6829	2MASX J03181899+6829322	Sy1	49.55286	68.49622	2.64	0.628	11.59	2.1 ± 0.2	0.7 ± 0.2	0.0901	44.59	3 1 y h a
93	PBC J0319.7+4129	NGC 1275	BLA	49.93641	41.49971	1.28	0.963	47.70	7.9 ± 0.2	0.19 ± 0.04	0.0175	43.69	2 1 y h a
94	PBC J0324.7-0300	NGC 1320	Sy2	51.17604	–3.01233	4.00	2.421	6.04	1.1 ± 0.2	...	0.0092	42.27	3 1 n h c
95	PBC J0324.7+3409	1H 0323+342	Sy1	51.18716	34.15801	3.23	1.501	11.22	2.4 ± 0.2	1.1 ± 0.3	0.0629	44.16	1 1 y h a
96	PBC J0325.0-1223	MCG-02-09-040	Sy2	51.25023	–12.39860	0.00	3.438	5.26	1.0 ± 0.2	...	0.0147	42.70	2 2 n h b
97	PBC J0325.1+4042	UGC 02724	Sy2	51.29144	40.71148	3.85	4.738	7.48	1.8 ± 0.2	0.9 ± 0.4	0.0477	43.88	3 1 n h c
98	PBC J0331.1+4353	GK Per	CV*	52.79535	43.89860	1.22	0.401	53.70	9.9 ± 0.2	0.32 ± 0.04	...	...	2 1 y h a
99	PBC J0333.3+3717	IGR J03334+3718	Sy1	53.33251	37.28838	3.02	0.903	10.27	2.0 ± 0.2	0.6 ± 0.2	0.0547	44.10	3 1 y h a
100	PBC J0333.5-3608	NGC 1365	Sy1	53.38638	–36.13346	1.56	0.809	31.18	5.0 ± 0.2	0.9 ± 0.1	0.0055	42.47	3 1 y h a
101	PBC J0333.7-0459	NGC1358	Sy2	53.42520	–4.98349	4.16	6.382	4.86	0.9 ± 0.2	...	0.0134	42.64	1 1 n h a
102	PBC J0334.2-1514	RHS 23	Sy1	53.57479	–15.24032	4.04	1.735	7.30	1.3 ± 0.2	...	0.0351	43.44	3 3 n h a
103	PBC J0334.9+5310	EXO 0331+530	HXB	53.74935	53.17972	0.63	0.400	520.47	87.6 ± 0.2	0.212 ± 0.004	...	...	2 1 y l a
104	PBC J0336.5+3219	NRAO 140	BLA	54.12504	32.32561	3.04	1.048	11.96	2.8 ± 0.2	1.3 ± 0.3	1.2585	47.27	3 1 n h a
105	PBC J0342.0-2114	RBS 0462	Sy1	55.52306	–21.24664	2.05	0.658	14.84	2.4 ± 0.2	1.0 ± 0.2	0.0144	43.15	3 1 y h a
106	PBC J0345.3-3932	2MASX J03451250-3934293	Sy1	56.34057	–39.53379	3.68	3.053	7.63	1.2 ± 0.2	...	0.0430	43.67	1 1 n h b
107	PBC J0349.4-1158	RBS 476	BLA	57.36619	–11.96986	3.33	1.702	10.12	1.7 ± 0.2	0.3 ± 0.2	0.1880	45.21	1 1 y h a
108	PBC J0350.5-5021	ESO 201-IG 004	G	57.62844	–50.35066	3.24	3.144	7.05	1.1 ± 0.2	...	0.0364	43.63	1 1 y h a
109	PBC J0351.6-4030	RBS 0482	Sy1	57.92416	–40.50147	4.20	2.081	4.79	0.7 ± 0.1	0.5 ± 0.5	0.0582	43.84	1 1 n h c
110	PBC J0353.3-6830	RHS 24	BLA	58.33943	–68.50845	2.86	1.670	8.55	1.2 ± 0.1	0.5 ± 0.3	0.0870	44.34	1 1 y h a
111	PBC J0353.5+3713	UGC 02889	G	58.39326	37.21730	3.87	2.877	5.41	1.1 ± 0.2	...	0.0187	42.92	3 1 n h c
112	PBC J0354.0+0250	RBS 0489	Sy1	58.51765	2.84711	3.68	1.938	5.83	0.7 ± 0.1	...	0.0360	43.59	3 3 n h c
113	PBC J0355.3+3102	X Per	HXB	58.84092	31.04448	0.77	0.282	221.60	49.5 ± 0.2	0.81 ± 0.01	...	...	3 1 y h a
114	PBC J0356.6-6252	2MASX J03561995-6251391	AG?	59.15925	–62.88090	4.11	2.406	4.94	0.5 ± 0.1	...	0.1075	44.20	3 3 n h c
115	PBC J0356.9-4040	2MASX J03565655-4041453	G	59.23843	–40.67678	3.16	1.162	8.69	1.6 ± 0.2	0.8 ± 0.3	0.0747	44.30	1 1 y h a
116	PBC J0359.5+5058	4C 50.11	Q?	59.88451	50.98018	4.07	1.053	9.34	1.9 ± 0.2	...	...	...	3 1 n l c
117	PBC J0402.4-1803	ESO 549-G 049	Sy1	60.60231	–18.06520	2.93	1.092	8.26	1.3 ± 0.2	1.7 ± 0.7	0.0262	43.41	3 1 n h c
118	PBC J0402.8+0157	MCG+00-11-007	Sy2	60.71591	1.95081	0.00	1.238	5.68	1.2 ± 0.2	...	0.0127	42.58	3 3 n h b
119	PBC J0405.6-1308	RX J0405.5-1308	BLA	61.42355	–13.14014	3.87	1.871	5.41	0.9 ± 0.2	...	0.5710	46.15	3 1 n h c
120	PBC J0407.2+0341	3C 105	Sy2	61.81504	3.69596	2.59	0.706	12.14	2.9 ± 0.2	0.9 ± 0.2	0.0890	44.70	3 1 y h a
121	PBC J0407.9-1210	RBS 0511	BLA	61.97728	–12.18211	4.24	1.644	4.72	0.6 ± 0.1	...	0.5740	46.12	3 3 n h a
122	PBC J0414.9-0755	1E 0412-0803	Sy1	63.73178	–7.92127	3.18	0.860	7.25	1.3 ± 0.2	0.6 ± 0.3	0.0379	43.72	3 1 n h c
123	PBC J0418.3+3801	3C 111	Sy1	64.58928	38.02349	1.28	0.189	45.11	10.2 ± 0.2	0.93 ± 0.07	0.0485	44.69	3 1 y h a
124	PBC J0419.7-5456	NGC 1566	Sy1	64.94690	–54.93510	3.50	1.931	6.54	0.9 ± 0.2	0.6 ± 0.4	0.0049	41.84	1 1 n h c
125	PBC J0422.4-5613	ESO 157- G 023	Sy2	65.61693	–56.22189	3.57	0.586	6.75	0.8 ± 0.2	...	0.0432	43.68	3 1 n h c
126	PBC J0423.6+0406	2MASX J04234080+0408017	Sy2	65.90762	4.11122	3.17	1.555	9.95	2.5 ± 0.3	1.2 ± 0.4	0.0461	43.89	3 1 n h c
127	PBC J0425.9-5712	RBS 0542	QSO	66.48853	–57.20998	2.55	0.742	10.30	1.2 ± 0.1	0.3 ± 0.2	0.1040	44.63	3 1 n h a
128	PBC J0430.4-5334	RBS 0547	Sy1	67.60258	–53.57330	4.06	3.411	5.04	0.4 ± 0.1	...	0.0397	43.43	3 3 n h a
129	PBC J0431.1-6126	ABELL 3266	ClG	67.77518	–61.44218	2.85	2.259	8.61	1.1 ± 0.2	0.2 ± 0.2	0.0594	44.05	2 1 n h a
130	PBC J0433.1+0521	3C 120	BLA	68.29594	5.35671	1.52	0.144	30.98	8.0 ± 0.3	0.97 ± 0.10	0.0331	44.24	1 1 n h a
131	PBC J0436.3-1021	Mrk 618	Sy1	69.08099	–10.35313	3.33	1.534	6.77	1.0 ± 0.2	0.6 ± 0.4	0.0362	43.58	3 1 n h b
132	PBC J0437.8-4713	RBS 0560	Sy1	69.45275	–47.21727	3.87	3.939	5.40	0.7 ± 0.1	...	0.0520	43.74	3 1 n h c
133	PBC J0438.2-1047	MCG -02-12-050	Sy1	69.56160	–10.79698	3.83	0.164	8.30	1.6 ± 0.2	...	0.0359	43.51	3 1 n h c
134	PBC J0440.2-5937	ESO 118-33	Sy2	70.06174	–59.62806	4.14	3.815	4.80	0.6 ± 0.1	...	0.0577	43.83	3 3 n h b
135	PBC J0440.9+4432	RX J0440.9+4431	HXB	70.24734	44.53536	4.37	0.300	7.12	1.7 ± 0.2	...	...	...	1 1 n l a
136	PBC J0441.3-2707	RBS 0572	Sy1	70.33162	–27.12113	4.11	1.257	4.94	0.8 ± 0.2	...	0.0835	44.22	1 1 n h b
137	PBC J0441.9-0824	RHS 25	Sy1	70.49783	–8.40521	4.34	2.643	4.56	0.3 ± 0.1	...	0.0410	43.67	2 2 n h b
138	PBC J0443.7+2858	UGC 3142	Sy1	70.93417	28.97579	2.65	0.632	13.95	3.9 ± 0.3	0.9 ± 0.2	0.0218	43.53	1 1 y h a
139	PBC J0444.0+2814	2MASX J04440903+2813003	Sy2	71.02279	28.23483	2.33	1.339	11.94	3.1 ± 0.3	1.5 ± 0.4	0.0113	42.93	1 1 n h a
140	PBC J0444.7-2810	RX J0444.6-2810	Sy2	71.18002	–28.17853	2.93	1.465	8.23	1.1 ± 0.2	0.8 ± 0.4	0.1470	44.90	3 1 n h c
141	PBC J0451.6-0347	MCG -01-13-025	Sy1	72.92422	–3.79406	3.22	0.926	11.72	2.8 ± 0.2	...	0.0130	42.79	3 1 y h a
142	PBC J0451.7-5811	RBS 0594	Sy1	72.94930	–58.18852	2.83	0.586	8.71	1.1 ± 0.1	1.2 ± 0.5	0.0910	44.46	3 1 n h c
143	PBC J0452.0+4931	RX J0452.0+4932	Sy1	73.00880	49.53013	1.79	1.032	18.93	3.6 ± 0.2	1.1 ± 0.2	0.0290	43.94	3 1 y l a
144	PBC J0453.3+0404	2MASX J04532576+0403416	Sy2	73.33683	4.08107	2.97	1.663	12.13	3.3 ± 0.3	1.2 ± 0.3	0.0296	43.63	3 1 n h c
145	PBC J0455.9-7532	ESO 033- G 002	Sy2	73.99588	–75.54008	2.70	0.047	9.37	1.3 ± 0.2	0.8 ± 0.3	0.0184	43.11	3 1 y h a

Table 2. continued.

	PBC name	ID	Type*	RA (deg)	Dec (deg)	Error radius (arcmin)	Offset (arcmin)	SNR	Flux† (erg cm^{-2} s^{-1})	Hardness ratio (R_{30-150}/R_{14-30})	Redshift	log L_{14-150} (erg s^{-1})	Flag‡ A B C D E
146	PBC J0457.0+4525	1RXS J045707.4+452751	X	74.27387	45.43040	3.07	2.038	10.32	2.2 ± 0.2	0.5 ± 0.2	...	...	3 1 n l c
147	PBC J0500.7-7041	IGR J05007-7047	HXB	75.18539	–70.69196	2.68	3.085	10.54	1.5 ± 0.2	0.3 ± 0.2	...	...	3 1 y h a
148	PBC J0502.3+0327	1E 0459.5+0327	Sy1	75.58974	3.46153	4.21	5.204	7.21	2.0 ± 0.3	...	0.0159	42.88	3 3 n h c
149	PBC J0502.4+2443	V* V1062 Tau	No*	75.61893	24.73218	3.88	1.467	9.13	2.6 ± 0.3	0.5 ± 0.3	...	...	2 1 n h c
150	PBC J0503.0+2300	1RXS J050258.5+225949	Sy1	75.75658	23.00426	3.64	0.839	5.93	1.6 ± 0.3	...	0.0577	44.21	3 1 n h c
151	PBC J0504.2-7343	IGR J05053-7343	gam	76.06448	–73.72049	3.90	4.460	5.34	0.7 ± 0.2	0.4 ± 0.4	...	...	1 1 y h a
152	PBC J0505.7-2351	2MASX J05054575-2351139	Sy2	76.44971	–23.86203	1.75	0.701	19.69	3.2 ± 0.2	1.1 ± 0.2	0.0350	44.05	1 1 n h a
153	PBC J0506.6-1935	1RXS J050648.5-193651	Sy1	76.66824	–19.59548	4.14	2.219	4.89	0.8 ± 0.2	...	0.0900	44.31	1 1 n h b
154	PBC J0508.1+1724	2MASX J05081967+1721483	Sy2	77.04440	17.40416	3.86	3.267	6.38	1.8 ± 0.3	0.6 ± 0.4	0.0177	43.13	3 1 n h c
155	PBC J0510.8+1629	4U 0517+17	Sy1	77.70303	16.49706	1.88	0.779	21.77	6.6 ± 0.3	0.9 ± 0.1	0.0178	43.61	3 1 y h a
156	PBC J0514.1-4002	1H 0512-401	LXB	78.54694	–40.04926	1.52	0.955	30.37	4.6 ± 0.2	0.38 ± 0.07	...	...	2 1 n h a
157	PBC J0516.1-0009	Mrk 1095	Sy1	79.04830	–0.15333	1.84	0.192	17.92	3.8 ± 0.2	0.9 ± 0.2	0.0336	44.09	3 1 y h a
158	PBC J0516.4-1034	MCG-02-14-009	Sy1	79.10258	–10.57948	3.95	1.372	7.63	1.5 ± 0.2	...	0.0280	43.32	3 1 n h c
159	PBC J0519.4-3240	ESO 362- G 018	Sy1	79.86591	–32.67729	2.02	1.994	15.23	2.3 ± 0.2	1.0 ± 0.2	0.0126	43.01	1 1 n h a
160	PBC J0519.8-4546	PICTOR A	Sy1	79.96823	–45.78220	1.87	0.506	20.44	3.2 ± 0.2	0.8 ± 0.1	0.0342	43.94	1 1 n h a
161	PBC J0520.4-7157	LMC X-2	LXB	80.11213	–71.95819	2.00	0.430	17.86	1.9 ± 0.2	< 0.03	...	...	2 1 n h a
162	PBC J0523.0-3626	RBS 0644	BLA	80.75136	–36.43521	2.44	1.480	11.06	1.6 ± 0.2	0.6 ± 0.2	0.0553	44.17	3 1 n h a
163	PBC J0524.1-1211	LEDA 17233	Sy1	81.02939	–12.18665	3.45	1.213	9.13	1.9 ± 0.2	0.9 ± 0.4	0.0491	43.95	1 1 n h c
164	PBC J0525.4-4559	PKS 0524-460	BLA	81.36746	–45.98814	3.13	2.001	7.45	1.0 ± 0.1	1.4 ± 0.6	0.0424	43.74	1 1 n h c
165	PBC J0525.6+2413	RX J0525.3+2413	CV*	81.40698	24.22637	3.75	3.446	8.15	2.7 ± 0.3	0.7 ± 0.3	...	...	1 1 n h c
166	PBC J0529.3-3249	TV Col	DQ*	82.33624	–32.82527	1.38	1.090	38.84	6.1 ± 0.2	0.40 ± 0.06	...	...	3 1 y h a
167	PBC J0530.9+1333	PKS 0528+134	BLA	82.73608	13.56583	4.28	2.031	5.38	1.6 ± 0.3	...	2.0700	47.68	1 1 n h a
168	PBC J0532.7-6621	LMC X-4	HXB	83.19444	–66.36521	0.80	0.446	214.63	31.4 ± 0.2	0.269 ± 0.009	...	...	2 1 y h a
169	PBC J0534.5+2201	Crab	Psr	83.62907	22.01721	0.55	0.283	4811.15	1985.9 ± 0.4	0.7456 ± 0.0006	...	...	1 1 y h a
170	PBC J0534.7-5800	IGR J05346-5759	CV*	83.68449	–58.00522	2.84	1.140	11.38	1.3 ± 0.2	< 0.06	...	...	2 1 y h a
171	PBC J0538.9+2618	1A 0535+262	HXB	84.72902	26.31300	0.81	0.189	174.49	46.6 ± 0.3	0.42 ± 0.01	...	...	2 1 y l a
172	PBC J0538.9-6404	LMC X-3	HXB	84.73983	–64.07533	2.86	0.441	11.83	2.0 ± 0.2	0.9 ± 0.3	...	...	1 1 n h a
173	PBC J0538.9-4406	PKS 0537-441	BLA	84.74760	–44.10882	4.25	2.134	4.72	0.6 ± 0.1	...	0.8960	46.49	1 1 n h a
174	PBC J0539.8-6943	LMC X-1	HXB	84.95984	–69.73308	2.14	1.182	17.25	3.0 ± 0.2	0.4 ± 0.1	...	...	1 1 y h a
175	PBC J0539.8-2839	PKS 0537-286	BLA	84.96399	–28.66074	2.67	0.703	11.21	2.2 ± 0.2	1.5 ± 0.4	3.1040	48.19	1 1 y h a
176	PBC J0540.0-6921	PSR B0540-69.3	Psr	85.01019	–69.36603	1.97	1.934	20.13	3.6 ± 0.2	1.2 ± 0.2	...	...	1 1 y h a
177	PBC J0541.4-6825	XMMU J054134.7-682550	HXB	85.35213	–68.42186	1.63	1.074	22.37	3.0 ± 0.2	0.21 ± 0.08	...	...	2 1 n h a
178	PBC J0542.7+6052	BY Cam	AM*	85.69649	60.87052	2.35	0.732	13.66	3.0 ± 0.3	0.5 ± 0.2	...	...	2 1 y h a
179	PBC J0543.4-4102	TX Col	DQ*	85.85282	–41.03880	2.50	0.944	12.67	1.9 ± 0.2	0.3 ± 0.2	...	...	2 1 n h c
180	PBC J0543.6-2738	MCG -05-14-012	G	85.90178	–27.63827	3.35	1.095	9.08	1.6 ± 0.2	0.6 ± 0.3	...	...	1 1 n h c
181	PBC J0544.3+5905	2MASX J05442257+5907361	G	86.08633	59.09609	3.73	3.363	5.96	1.6 ± 0.3	...	...	...	1 1 n h c
182	PBC J0550.7-3215	PKS 0548-322	BLA	87.68599	–32.25305	2.35	1.385	11.73	1.8 ± 0.2	0.7 ± 0.2	0.0689	44.41	3 1 n h a
183	PBC J0552.1-0727	NGC 2110	Sy2	88.04263	–7.46249	1.00	0.472	86.26	21.5 ± 0.3	1.07 ± 0.04	0.0075	43.37	1 1 n h a
184	PBC J0552.1+5927	1RXS J055229.5+592842	Sy1	88.04604	59.46057	4.31	2.568	8.05	1.7 ± 0.3	0.4 ± 0.3	0.0405	43.68	3 1 n h b
185	PBC J0554.8+4626	4U 0558+46	Sy1	88.71237	46.44129	1.36	0.472	32.12	6.0 ± 0.2	0.84 ± 0.09	0.0204	43.85	1 1 y h a
186	PBC J0555.9+3948	OA 198	BLA	88.98125	39.81504	4.02	4.743	5.12	1.0 ± 0.2	...	2.3630	47.73	1 1 n h c
187	PBC J0558.0+5353	V405 Aur	DQ*	89.50543	53.89895	2.03	0.086	18.96	3.6 ± 0.2	0.3 ± 0.1	...	...	2 1 n h c
188	PBC J0558.0-3821	H 0557-385	Sy1	89.51728	–38.35059	2.04	1.103	14.97	2.2 ± 0.2	0.7 ± 0.2	0.0339	43.87	3 1 n h a
189	PBC J0559.6-5028	1ES 0558-504	Sy1	89.90740	–50.47260	3.24	2.148	7.06	1.0 ± 0.2	0.7 ± 0.4	0.1370	44.79	3 1 n h a
190	PBC J0602.0+2828	IRAS 05589+2828	Sy1	90.52187	28.46945	2.03	0.985	19.04	5.0 ± 0.3	0.8 ± 0.1	0.0330	44.09	3 1 y l a
191	PBC J0606.0-8636	ESO 5-4	Sy2	91.52424	–86.61494	2.56	1.076	10.23	1.7 ± 0.2	1.2 ± 0.4	0.0063	42.27	1 1 n h a
192	PBC J0615.7+7100	Mrk 3	Sy2	93.93019	71.01530	1.21	1.445	48.89	9.4 ± 0.2	1.24 ± 0.08	0.0134	43.52	1 1 y h a
193	PBC J0617.1+0907	H 0614+091	LXB	94.28369	9.13322	0.85	0.296	161.95	43.1 ± 0.3	0.57 ± 0.01	...	...	3 1 y l a
194	PBC J0623.7-6435	RX J062308.0-643619	BLA	95.94460	–64.59756	4.38	4.069	4.51	0.5 ± 0.1	...	0.1290	44.61	3 3 n h c
195	PBC J0623.8-3212	ESO 426- G 002	Sy2	95.95142	–32.20605	3.00	0.784	12.63	2.2 ± 0.2	1.2 ± 0.3	0.0224	43.40	3 1 n h c
196	PBC J0623.8-6059	ESO 121-IG 028	Sy2	95.96694	–60.99261	2.30	1.205	12.14	1.9 ± 0.2	1.0 ± 0.3	0.0411	43.86	3 1 n h a
197	PBC J0625.2+7336	IGR J06253+7334	CV*	96.30939	73.60435	2.77	0.565	9.93	1.3 ± 0.2	0.1 ± 0.2	...	...	3 1 y h a
198	PBC J0630.9+6340	2MASX J06302561+6340411	Sy2	97.73368	63.66801	4.13	3.387	4.91	0.6 ± 0.1	...	0.0500	43.78	3 3 n h b
199	PBC J0632.0-5403	1ES 0630-540	BLA	98.01952	–54.05547	3.68	1.405	5.83	0.8 ± 0.2	0.3 ± 0.4	0.1930	45.01	3 1 n h b
200	PBC J0632.6+6342	UGC 3478	Sy1	98.16300	63.71342	4.20	2.556	5.60	1.1 ± 0.2	...	0.0124	42.50	1 1 n h a
201	PBC J0635.4-7514	PKS 0637-752	BLA	98.86375	–75.23612	3.99	2.441	5.25	0.8 ± 0.2	...	0.6510	46.25	3 1 y h a
202	PBC J0636.6+3535	1RXS J063631.9+353573	CV*	99.17133	35.58371	3.79	1.967	7.86	1.7 ± 0.2	0.5 ± 0.3	...	...	3 1 n h b
203	PBC J0640.2-2554	ESO 490-IG026	Sy1	100.05178	–25.90328	2.16	0.581	16.98	3.3 ± 0.2	0.9 ± 0.2	0.0258	43.60	3 1 y h a
204	PBC J0640.5-4322	2MASX J06403799-4321211	G	100.13644	–43.37186	3.94	1.354	8.58	1.6 ± 0.2	...	...	...	3 3 y h a
205	PBC J0641.3+3251	CGCG 145-004	G	100.34478	32.86021	3.05	2.339	7.74	1.5 ± 0.2	1.1 ± 0.5	0.0470	43.99	3 1 y h a
206	PBC J0652.1+7425	Mrk 6	Sy1	103.02712	74.42196	1.73	0.489	23.96	4.4 ± 0.2	0.9 ± 0.1	0.0186	43.50	3 1 y h a
207	PBC J0655.8+3958	UGC 03601	Sy1	103.95802	39.98190	3.31	1.090	11.78	2.4 ± 0.2	0.7 ± 0.2	0.0172	43.08	3 1 n h b
208	PBC J0658.3-0712	RX J065817.7-071228	X	104.57674	–7.20671	1.87	0.187	17.33	2.8 ± 0.2	0.2 ± 0.1	...	...	2 1 n l a
209	PBC J0658.4-5553	RX J0658.4-5557	ClG	104.61763	–55.89742	4.38	2.941	4.50	0.3 ± 0.1	...	0.2960	45.44	2 2 n h c
210	PBC J0709.2-3601	PKS 0707-35	G	107.31702	–36.02909	2.88	0.557	8.48	1.4 ± 0.2	2.0 ± 0.8	0.1108	44.73	1 1 n h c
211	PBC J0710.2+5909	1H 0658+595	BLA	107.55034	59.16202	3.80	2.687	5.56	0.9 ± 0.2	0.7 ± 0.5	0.1250	44.65	1 1 n h b
212	PBC J0717.9+4405	RX J0718.0+4405	Sy1	109.49387	44.09904	2.76	0.597	9.07	1.4 ± 0.2	0.5 ± 0.3	0.0610	44.20	3 1 n h c
213	PBC J0718.7+6558	V* HS Cam	AM*	109.68320	65.98037	4.02	3.284	5.10	0.8 ± 0.2	0.6 ± 0.5	...	...	1 1 n h b
214	PBC J0726.5-3553	LEDA 96373	Sy2	111.63921	–35.89796	3.23	1.515	10.17	1.9 ± 0.2	...	0.0296	43.50	1 1 y h a
215	PBC J0726.6+3700	1RXS J072635.3+370006	QSO	111.66588	37.00967	3.87	1.054	5.39	1.0 ± 0.2	...	0.1900	45.11	3 1 n h b
216	PBC J0727.3-2404	1RXS J072720.8-240629	X	111.82922	–24.08079	3.88	1.693	5.38	0.9 ± 0.2	...	...	...	1 1 n l a
217	PBC J0728.9-2605	3A 0726-260	HXB	112.24020	–26.09179	2.43	1.353	15.10	2.3 ± 0.2	0.1 ± 0.1	...	...	2 1 n l a
218	PBC J0731.5+0955	BG CMi	DQ*	112.88268	9.92797	2.51	0.992	13.74	2.9 ± 0.2	0.3 ± 0.1	...	...	2 1 y h a

Table 2. continued.

	PBC name	ID	Type*	RA (deg)	Dec (deg)	Error radius (arcmin)	Offset (arcmin)	SNR	Flux† (erg cm^{-2} s^{-1})	Hardness ratio (R_{30-150}/R_{14-30})	Redshift	log L_{14-150} (erg s^{-1})	Flag‡ A B C D E
219	PBC J0732.6-1331	SWIFT J0732.5-1331	CV*	113.16088	–13.53206	2.50	0.899	14.29	2.8 ± 0.2	0.5 ± 0.2	...	...	3 1 n l a
220	PBC J0739.6-3143	SWIFT J0739.7-3144	X	114.91034	–31.72996	3.10	1.185	13.83	2.5 ± 0.2	1.4 ± 0.3	...	...	3 1 y l a
221	PBC J0742.4+4948	Mrk 79	Sy1	115.60992	49.80320	2.08	1.107	19.83	3.5 ± 0.2	0.5 ± 0.1	0.0220	43.56	3 1 y h a
222	PBC J0743.1-2546	SWIFT J0743.0-2543	X	115.79167	–25.77863	2.93	1.589	10.41	2.1 ± 0.2	0.6 ± 0.2	...	...	1 1 y l a
223	PBC J0744.1+2915	MCG+05-19-001	Sy2	116.03722	29.25091	0.00	0.262	8.41	1.9 ± 0.2	...	0.0159	42.78	3 3 n h b
224	PBC J0745.0-5258	V* V436 Car	DQ*	116.26553	–52.97683	4.16	1.648	5.54	0.6 ± 0.1	...	...	...	2 2 n h b
225	PBC J0746.4+2548	OI +273	BLA	116.61086	25.81589	2.48	0.184	10.78	2.0 ± 0.2	1.8 ± 0.5	2.9793	48.29	1 1 n h a
226	PBC J0747.4+6055	Mrk 10	Sy1	116.86690	60.93186	3.01	0.176	7.89	1.2 ± 0.2	1.0 ± 0.4	0.0292	43.48	1 1 n h c
227	PBC J0747.5-1920	4U 0739-19	ClG	116.87582	–19.34621	3.50	3.118	7.70	1.2 ± 0.2	...	0.1028	44.49	2 3 n l a
228	PBC J0748.6-6744	EXO 0748-676	LXB	117.15228	–67.74304	0.82	0.624	179.29	30.3 ± 0.2	0.63 ± 0.01	...	...	1 1 y h a
229	PBC J0750.6+1231	OI +280	BLA	117.67001	12.52051	3.99	2.748	5.17	0.8 ± 0.2	...	0.8890	46.60	1 1 n h c
230	PBC J0751.2+1445	SWIFT J0750.9+1439	DQ*	117.80929	14.75030	2.08	0.976	18.19	3.3 ± 0.2	0.2 ± 0.1	...	...	2 1 n h a
231	PBC J0752.1+1935	2MASX J07521780+1935423	Sy1	118.04833	19.58654	4.16	1.553	4.69	0.8 ± 0.2	...	0.1172	44.64	3 3 n h b
232	PBC J0752.9+4557	1RXS J075243.6+455653	Sy1	118.22643	45.96241	3.84	1.931	5.46	0.9 ± 0.2	...	0.0600	43.99	1 1 n h c
233	PBC J0759.7-3844	IGR J07597-3842	Sy1	119.93464	–38.73559	1.86	0.526	22.36	4.5 ± 0.2	0.8 ± 0.1	0.0400	44.16	1 1 y l a
234	PBC J0759.9+2324	MCG +04-19-017	Sy2	119.98394	23.41600	3.06	1.672	8.47	1.9 ± 0.2	1.1 ± 0.5	0.0296	43.56	3 1 n h c
235	PBC J0800.2+2637	IC 486	Sy1	120.05240	26.62090	3.34	1.902	9.12	2.0 ± 0.2	1.3 ± 0.4	0.0272	43.46	1 1 n h c
236	PBC J0802.0-4946	ESO 209-12	Sy1	120.52305	–49.77196	3.09	1.337	10.70	2.2 ± 0.2	0.7 ± 0.2	0.0395	43.75	3 1 y h a
237	PBC J0804.0+0506	Mrk 1210	Sy2	121.01718	5.10874	1.93	0.516	16.49	3.1 ± 0.2	0.9 ± 0.2	0.0135	43.20	1 1 n h a
238	PBC J0804.7+1048	MCG+02-21-013	Sy2	121.18034	10.80000	4.00	1.630	6.90	1.5 ± 0.2	...	0.0343	43.54	1 1 n h b
239	PBC J0805.4+6146	VIPS 0069	BLA	121.36999	61.77803	3.99	2.607	5.16	0.7 ± 0.2	...	3.0400	47.87	1 1 n l c
240	PBC J0811.3+7601	RBS 0693	Sy1	122.83299	76.03101	2.94	1.537	8.21	1.1 ± 0.1	0.4 ± 0.3	0.1000	44.53	3 1 y h a
241	PBC J0814.4+0421	2MASX J08142529+0420324	G	123.60365	4.36518	3.49	1.507	7.15	1.6 ± 0.2	...	0.0330	43.55	1 1 n h c
242	PBC J0816.8+1800	2MASX J08165108+1802496	Sy1	124.20686	18.00771	4.18	2.439	4.85	0.6 ± 0.1	...	0.1580	44.81	3 3 n h b
243	PBC J0818.1+0121	1RXS J081815.0+012215	Sy1	124.53683	1.36476	4.11	1.566	4.95	0.9 ± 0.2	...	0.0800	44.32	3 1 n h c
244	PBC J0823.0-0454	FAIRALL 0272	G	125.75989	–4.91566	2.46	1.195	10.91	2.0 ± 0.2	1.7 ± 0.5	0.0218	43.42	1 1 n h a
245	PBC J0826.3-7033	1ES 0826-703	X	126.57810	–70.56373	3.51	2.180	7.02	1.2 ± 0.2	0.4 ± 0.3	...	...	2 1 n h c
246	PBC J0832.6+3706	RBS 707	Sy1	128.17430	37.11599	3.48	3.350	6.34	0.9 ± 0.2	0.6 ± 0.4	0.0920	44.38	1 1 n h c
247	PBC J0835.3-4511	Vela Pulsar	Psr	128.83591	–45.18714	1.13	0.642	71.17	13.5 ± 0.2	0.86 ± 0.05	...	...	3 1 y l a
248	PBC J0838.3+4837	EI UMa	DN*	129.58429	48.62525	2.05	0.608	18.79	3.4 ± 0.2	0.6 ± 0.1	...	...	3 1 n h c
249	PBC J0838.4-3558	FAIRALL 1146	Sy1	129.60313	–35.97490	2.57	1.623	10.16	1.7 ± 0.2	0.7 ± 0.3	0.0317	43.70	3 1 y l a
250	PBC J0838.6-4831	USNO-B1.0 0414-00125587	CV*	129.65353	–48.53153	3.50	2.086	10.76	2.1 ± 0.2	0.9 ± 0.3	...	...	1 1 n l b
251	PBC J0839.7-1214	3C 206	Sy1	129.93419	–12.24953	3.13	1.608	11.10	2.1 ± 0.2	0.7 ± 0.2	0.1978	45.28	3 1 y h a
252	PBC J0840.0+2948	4C 29.30	Sy2	130.01706	29.80382	3.75	0.872	6.38	1.2 ± 0.2	...	0.0647	44.05	3 1 n h b
253	PBC J0841.4+7053	S5 0836+71	BLA	130.36632	70.88821	1.61	0.503	23.06	3.5 ± 0.2	1.4 ± 0.2	2.1720	48.19	1 1 y h a
254	PBC J0842.2+0759	RX J0842.1+0759	Sy1	130.55507	7.99940	3.67	1.679	6.63	1.3 ± 0.2	...	0.1300	44.79	1 1 n h b
255	PBC J0843.6+3553	2MASX J08434495+3549421	Sy2	130.90590	35.88482	3.66	3.707	6.94	1.2 ± 0.2	...	0.0535	43.86	3 1 n h b
256	PBC J0845.2-3530	SWIFT J0845.0-3531	X	131.30219	–35.50058	4.22	2.016	7.83	1.3 ± 0.2	...	...	...	3 1 y l a
257	PBC J0855.6+7812	NGC 2655	LIN	133.91064	78.21089	4.22	0.766	4.58	0.9 ± 0.2	...	0.0047	41.65	1 1 n h a
258	PBC J0855.9+0049	2MASX J08555426+0051110	Sy1	133.98479	0.82705	0.00	1.645	6.66	1.3 ± 0.2	...	0.0523	43.94	2 2 n h b
259	PBC J0902.1-4033	Vela X-1	HXB	135.52834	–40.55265	0.57	0.123	2340.86	398.4 ± 0.2	0.2725 ± 0.0008	...	...	2 1 y l a
260	PBC J0902.2+6004	Mrk 18	G	135.55325	60.07507	3.62	4.913	6.94	1.2 ± 0.2	...	0.0109	42.45	1 1 y h a
261	PBC J0902.6-4813	IGR J09026-4812	gam	135.66902	–48.22909	2.36	0.784	11.65	1.9 ± 0.2	1.0 ± 0.3	...	...	3 1 y l a
262	PBC J0902.6-6815	NGC 2788A	AGN	135.67323	–68.25965	3.36	1.995	6.69	1.0 ± 0.2	...	0.0137	42.61	3 1 n h a
263	PBC J0904.5+5535	2MASX J09043699+5536025	Sy1	136.14954	55.59506	3.57	0.373	8.43	1.3 ± 0.2	...	0.0371	43.52	3 1 y h a
264	PBC J0908.8-0940	4U 0900-09	ClG	137.21297	–9.66736	2.51	1.858	12.47	2.1 ± 0.2	0.2 ± 0.2	0.0535	44.07	2 1 n h a
265	PBC J0909.2+0350	SDSS J090920.23+034940.0	QSO	137.31367	3.84553	3.61	1.630	5.99	1.0 ± 0.2	...	1.7995	47.33	1 0 n h b
266	PBC J0911.4+4528	2MASX J09112999+4528060	Sy2	137.85933	45.47018	2.91	0.666	8.33	1.2 ± 0.2	0.6 ± 0.3	0.0268	43.28	3 1 n h a
267	PBC J0916.2-6218	SWIFT J0917.2-6221	Sy1	139.06474	–62.30518	2.36	1.379	14.20	2.8 ± 0.2	0.6 ± 0.2	0.0571	44.25	1 1 y h a
268	PBC J0918.4+1619	Mrk 704	Sy1	139.60696	16.32457	2.23	1.157	16.64	2.5 ± 0.2	0.5 ± 0.2	0.0292	43.69	3 1 n h a
269	PBC J0919.7+5523	RBS 0766	Sy1	139.94736	55.39048	4.14	2.135	4.89	0.7 ± 0.1	...	0.1226	44.52	1 1 n h b
270	PBC J0919.9+3712	IC 2461	G	139.98050	37.20952	3.18	1.232	9.34	1.8 ± 0.2	1.0 ± 0.3	0.0075	42.28	1 1 n h c
271	PBC J0920.4-5512	H 0918-549	LXB	140.11418	–55.20506	1.26	0.126	48.05	8.1 ± 0.2	0.52 ± 0.05	...	...	3 1 y l a
272	PBC J0920.8-0803	MCG -01-24-012	Sy2	140.21539	–8.06621	1.96	1.477	16.03	3.0 ± 0.2	1.0 ± 0.2	0.0198	43.53	1 1 n h a
273	PBC J0923.7+2255	RBS 0770	Sy1	140.93579	22.92268	2.14	0.895	13.72	2.3 ± 0.2	1.1 ± 0.3	0.0326	43.85	3 1 n h a
274	PBC J0924.0-3141	1RXS J092418.0-314212	Sy1	141.00308	–31.68889	3.02	1.496	7.86	1.3 ± 0.2	0.4 ± 0.3	0.0422	43.82	1 1 n h c
275	PBC J0925.2+5216	Mrk 110	Sy1	141.31607	52.28065	1.57	0.567	29.58	4.9 ± 0.2	0.79 ± 0.10	0.0353	44.10	1 1 y h a
276	PBC J0926.1+1245	Mrk 705	Sy1	141.53746	12.76142	3.10	2.139	7.28	1.4 ± 0.2	0.5 ± 0.3	0.0280	43.45	3 1 n h a
277	PBC J0927.1+2301	NGC 2885	Sy1	141.79355	23.02175	4.08	1.856	4.99	0.8 ± 0.2	...	0.0250	43.18	3 1 n h b
278	PBC J0930.6+4954	RBS 0782	BLA	142.65817	49.90274	4.29	3.701	4.64	0.3 ± 0.1	...	0.1880	44.95	2 2 n h c
279	PBC J0934.7-2155	ESO 565-19	Sy2	143.68114	–21.92694	3.42	0.111	7.40	1.3 ± 0.2	0.8 ± 0.5	0.0157	42.97	1 1 n h c
280	PBC J0945.7-1419	NGC 2992	Sy1	146.42947	–14.33332	2.54	0.484	10.33	2.0 ± 0.2	1.2 ± 0.4	0.0077	42.51	1 1 y h a
281	PBC J0947.6+0725	3C 227	Sy1	146.91605	7.42536	2.87	1.318	8.51	1.7 ± 0.2	0.6 ± 0.3	0.0865	44.51	3 1 y h a
282	PBC J0947.6-3056	MCG-05-23-016	Sy2	146.92079	–30.94757	1.00	0.176	85.32	16.6 ± 0.2	0.72 ± 0.03	0.0082	43.34	3 1 y h a
283	PBC J0949.2+4036	4C 40.24	BLA	147.30640	40.60399	4.15	4.920	5.64	0.6 ± 0.1	...	1.2520	46.80	3 3 n h c
284	PBC J0952.1-0648	NGC 3035	Sy1	148.03586	–6.80447	3.83	3.756	8.64	1.6 ± 0.2	...	0.0145	42.72	1 1 n h b
285	PBC J0954.8+3724	IC 2515	Sy2	148.71001	37.41000	4.21	2.183	4.78	0.4 ± 0.1	...	0.0193	42.80	3 3 n h c
286	PBC J0955.1+6904	SN 1993J	SN*	148.79083	69.07005	3.66	3.262	7.03	1.2 ± 0.2	...	...	...	3 1 n h a
287	PBC J0959.4-2249	NGC 3081	Sy2	149.87402	–22.83063	1.58	0.266	29.85	6.1 ± 0.2	1.1 ± 0.1	0.0079	42.90	1 1 n h a
288	PBC J0959.6-3113	2MASX J09594263-3112581	Sy1	149.91045	–31.22115	3.85	0.926	8.42	1.6 ± 0.2	0.8 ± 0.4	0.0370	43.62	1 1 n h b
289	PBC J1002.0+5539	4C 55.19	Sy2	150.50587	55.65230	2.50	1.736	12.35	2.1 ± 0.2	1.2 ± 0.3	0.0037	41.80	1 1 n h c
290	PBC J1009.7-4248	SWIFT J1009.3-4250	Sy2	152.43893	–42.80688	2.33	0.630	16.30	3.0 ± 0.2	0.9 ± 0.2	0.0330	43.80	3 1 y h a
291	PBC J1009.7-5816	GRO J1008-57	HXB	152.44897	–58.27465	1.09	1.079	56.06	9.9 ± 0.2	0.35 ± 0.04	...	...	3 1 y l a
292	PBC J1010.9-5748	IGR J10109-5746	Sy*	152.73660	–57.81139	2.35	0.938	15.37	2.8 ± 0.2	0.3 ± 0.1	...	...	2 1 y l a
293	PBC J1013.4-3559	AM 1011-354	Sy2	153.37263	–35.99292	3.51	2.017	6.24	1.1 ± 0.2	...	0.0283	43.39	1 1 n h c

Table 2. continued.

	PBC name	ID	Type*	RA (deg)	Dec (deg)	Error radius (arcmin)	Offset (arcmin)	SNR	Flux† (erg cm^{-2} s^{-1})	Hardness ratio (R_{30-150}/R_{14-30})	Redshift	log L_{14-150} (erg s^{-1})	Flag‡ A B C D E
294	PBC J1021.8-0326	RBS 857	Sy1	155.46709	–3.43895	3.35	3.097	6.70	1.1 ± 0.2	1.1 ± 0.6	0.0409	43.75	1 1 n h c
295	PBC J1023.5+1951	NGC 3227	Sy1	155.87566	19.86061	1.15	0.280	56.01	9.6 ± 0.2	0.91 ± 0.06	0.0036	42.40	3 1 y h a
296	PBC J1024.6-2332	RR 183	Sy2	156.15343	–23.54085	4.24	1.397	4.72	0.7 ± 0.2	...	0.0123	42.50	1 1 n h b
297	PBC J1031.8-3451	NGC 3281	Sy2	157.96021	–34.85741	1.53	0.399	29.76	6.1 ± 0.2	1.0 ± 0.1	0.0114	43.22	1 1 y h a
298	PBC J1031.8-1417	RBS 0880	QSO	157.97392	–14.28980	2.34	0.550	11.80	1.8 ± 0.2	0.8 ± 0.3	0.0860	44.62	3 1 n h a
299	PBC J1037.7-5649	4U 1036-56	HXB	159.43849	–56.83131	2.97	2.471	13.74	2.6 ± 0.2	0.8 ± 0.2	...	...	3 1 y l a
300	PBC J1038.8-4947	SWIFT J1038.8-4942	Sy1	159.70503	–49.78740	2.94	0.754	12.28	2.4 ± 0.2	0.8 ± 0.2	0.0600	44.21	3 1 y h a
301	PBC J1040.4-4624	IGR J10404-4625	Sy2	160.11478	–46.40918	2.66	1.230	12.85	2.5 ± 0.2	0.8 ± 0.2	0.0240	43.45	3 1 y h a
302	PBC J1043.4+1105	SDSS J104326.47+110524.2	QSO	160.85365	11.08498	3.65	0.497	5.90	0.8 ± 0.2	...	0.0480	43.64	3 1 n h b
303	PBC J1043.8+7025	MCG+12-10-067	Sy2	160.96632	70.41809	3.57	1.601	6.09	0.8 ± 0.1	0.3 ± 0.3	0.0332	43.41	3 1 n h b
304	PBC J1044.1+8054	S5 1039+81	QSO	161.04086	80.91360	3.62	0.547	5.97	0.9 ± 0.2	...	1.2600	46.91	1 0 n h b
305	PBC J1044.8+3813	SDSS J104442.15+381257.2	QSO	161.21275	38.22656	4.14	1.862	4.89	0.6 ± 0.1	...	2.0741	47.26	3 0 n h b
306	PBC J1046.6+2557	UGC 05881	GiG	161.65364	25.95403	2.76	1.870	9.07	1.4 ± 0.2	1.4 ± 0.5	0.0204	43.22	1 1 n h c
307	PBC J1048.6-2508	NGC 3393	Sy2	162.15910	–25.14727	3.40	3.448	6.55	1.0 ± 0.2	...	0.1250	44.62	1 1 n h c
308	PBC J1049.4+2258	Mrk 417	Sy2	162.35719	22.97811	2.28	1.447	12.34	1.7 ± 0.2	1.2 ± 0.3	0.0328	43.73	3 1 n h a
309	PBC J1052.6+1037	2MASX J10523297+1036205	Sy1	163.15466	10.61994	3.93	1.329	6.10	1.0 ± 0.2	...	0.0880	44.28	3 1 n h c
310	PBC J1059.9+6505	2MASX J10594361+6504063	Sy2	164.98451	65.09007	3.68	1.868	5.82	0.8 ± 0.1	...	0.0840	44.22	3 1 n h b
311	PBC J1101.0+1102	Mrk 728	Sy1	165.25308	11.04626	3.97	0.254	6.67	1.1 ± 0.2	...	0.0360	43.40	3 1 n h c
312	PBC J1103.6-2329	1H 1100-230	BLA	165.90213	–23.49373	3.69	0.271	5.80	0.9 ± 0.2	0.3 ± 0.3	0.1860	45.04	2 1 n h a
313	PBC J1104.4+3813	Mrk 421	BLA	166.10942	38.21949	1.00	0.672	87.35	12.8 ± 0.2	0.39 ± 0.02	0.0300	44.37	3 1 n h a
314	PBC J1106.4+7234	NGC 3516	Sy1	166.60585	72.57288	1.13	1.679	54.33	9.0 ± 0.2	0.84 ± 0.06	0.0088	43.14	3 1 n h a
315	PBC J1113.7+0930	Mrk 732	Sy1	168.43257	9.50916	3.05	4.856	7.77	1.1 ± 0.2	0.8 ± 0.4	0.0293	43.45	1 1 n h c
316	PBC J1117.2-2903	1RXS J111704.0-290232	Sy1	169.30714	–29.05886	4.42	2.378	4.45	0.4 ± 0.1	...	0.0715	44.07	2 2 n h b
317	PBC J1117.9+4803	XTE J1118+480	LXB	169.48860	48.05103	3.96	2.430	6.96	1.1 ± 0.2	1.3 ± 0.6	...	...	1 1 n h a
318	PBC J1118.4-5438	IGR J11187-5438	gam	169.60588	–54.63694	4.00	2.412	8.36	1.6 ± 0.2	...	...	...	1 1 y h a
319	PBC J1120.9-4316	H 1118-429	Sy1	170.23660	–43.27034	3.65	1.663	5.90	1.1 ± 0.2	...	0.0567	44.04	1 1 n h a
320	PBC J1121.2-6037	Cen X-3	HXB	170.31631	–60.62385	0.66	0.055	599.10	95.8 ± 0.2	0.059 ± 0.003	...	...	2 1 y l a
321	PBC J1125.4+5424	Mrk 0040	Sy1	171.37410	54.40469	3.16	1.665	7.33	1.0 ± 0.1	0.7 ± 0.4	0.0206	43.07	1 1 n h c
322	PBC J1127.4+1908	RX J1127.2+1909	Sy1	171.86559	19.14232	3.48	2.698	8.02	1.3 ± 0.2	0.6 ± 0.3	0.1000	44.45	3 1 y h a
323	PBC J1127.5-2913	ESO 439-9	Sy2	171.88710	–29.22993	4.36	2.621	6.04	1.2 ± 0.2	...	0.0251	43.16	1 1 n h b
324	PBC J1130.1-1449	OM -146	BLA	172.53641	–14.81795	2.37	0.557	11.60	2.2 ± 0.2	1.3 ± 0.4	1.1870	47.34	1 1 n h a
325	PBC J1131.0-6256	IGR J11305-6256	HXB	172.77208	–62.94403	2.01	0.319	21.57	4.0 ± 0.2	0.32 ± 0.09	...	...	3 1 y l a
326	PBC J1132.9+1017	4C +10.33	BLA	173.24261	10.29749	3.75	2.100	5.67	0.8 ± 0.2	...	0.0410	43.61	3 1 n h b
327	PBC J1136.4+2134	Mrk 739	Sy1	174.11215	21.57923	3.15	1.147	7.36	1.0 ± 0.2	0.6 ± 0.4	0.0300	43.40	3 1 n h c
328	PBC J1137.2+6735	RBS 1004	BLA	174.30367	67.59340	4.17	4.343	4.84	0.7 ± 0.1	0.6 ± 0.5	0.1350	44.63	2 1 n h c
329	PBC J1139.0-3744	NGC 3783	Sy1	174.75148	–37.74152	1.13	0.334	60.87	14.1 ± 0.2	0.91 ± 0.05	0.0096	43.40	3 1 y h a
330	PBC J1139.0+5911	RBS 1011	Sy1	174.75975	59.19750	2.71	0.849	12.05	1.9 ± 0.2	0.9 ± 0.3	0.0600	44.11	3 1 y h a
331	PBC J1139.6+3157	NGC 3786	Sy1	174.90343	31.95250	3.00	2.857	9.35	1.3 ± 0.2	0.6 ± 0.3	0.0100	42.47	1 1 n h b
332	PBC J1141.2+2156	RBS 1019	Sy1	175.30974	21.94202	3.91	0.452	5.32	0.7 ± 0.2	...	0.0630	43.94	3 1 n h b
333	PBC J1143.6+7141	SWIFT J1142.7+7149	DQ*	175.90649	71.69883	2.31	0.593	15.76	1.9 ± 0.2	0.1 ± 0.1	...	...	2 1 n h a
334	PBC J1144.1-6106	IGR J11435-6109	HXB	176.03122	–61.11120	2.53	1.043	18.69	3.5 ± 0.2	0.7 ± 0.2	...	...	3 1 y l a
335	PBC J1144.4+3652	RBS 1024	Sy1	176.11256	36.87804	3.98	0.723	5.18	0.7 ± 0.1	...	0.0400	43.53	1 1 n h c
336	PBC J1144.9+7940	RHS 33	Sy1	176.22502	79.67973	2.25	1.008	12.68	1.7 ± 0.2	0.9 ± 0.3	0.0153	43.05	3 1 y h a
337	PBC J1145.7-1826	RBS 1030	Sy1	176.43826	–18.44119	2.02	1.367	15.26	2.6 ± 0.2	1.0 ± 0.2	0.0329	43.91	3 1 y h a
338	PBC J1145.9+7422	2MASX J11462959+7421289	Sy2	176.49478	74.37868	3.69	2.326	5.80	0.6 ± 0.1	...	0.0560	43.75	3 1 n h b
339	PBC J1147.5-6157	1E 1145.1-6141	HXB	176.87863	–61.95808	0.90	0.367	161.28	30.3 ± 0.2	0.41 ± 0.01	...	...	3 1 y l a
340	PBC J1149.2-0413	RBS 1037	Sy1	177.32335	–4.22373	4.30	3.475	4.62	0.6 ± 0.1	...	0.0850	44.25	3 3 n h b
341	PBC J1152.2-1122	RBS 1044	Sy1	178.05464	–11.36932	4.05	2.363	5.04	0.9 ± 0.2	...	0.0490	43.80	1 1 n h b
342	PBC J1153.4+4930	RBS 1046	BLA	178.37216	49.50038	3.47	1.372	6.37	0.8 ± 0.1	...	0.3340	45.55	1 1 n h a
343	PBC J1158.1+5527	NGC 3998	LIN	179.54074	55.45241	3.05	1.903	11.12	1.7 ± 0.2	0.9 ± 0.3	0.0036	41.64	1 1 n h a
344	PBC J1201.0+0647	CGCG 041-020	Sy2	180.26166	6.78993	2.53	1.561	10.41	1.6 ± 0.2	1.1 ± 0.4	0.0359	43.78	3 1 n h a
345	PBC J1201.3-0340	Mrk 1310	Sy1	180.32762	–3.66675	3.52	1.266	5.11	1.0 ± 0.2	0.7 ± 0.5	0.0196	42.96	3 1 n h c
346	PBC J1202.8-5349	IGR J12026-5349	Sy2	180.70969	–53.82763	2.03	0.616	19.80	3.9 ± 0.2	0.7 ± 0.1	0.0283	43.83	1 1 y h a
347	PBC J1203.1+4430	NGC 4051	Sy1	180.79076	44.51309	1.83	1.102	18.74	3.2 ± 0.2	0.5 ± 0.1	0.0021	41.51	3 1 y h a
348	PBC J1204.4+2018	NGC 4074	Sy2	181.10553	20.30725	2.77	1.153	9.02	1.3 ± 0.1	1.3 ± 0.5	0.0225	43.27	1 1 y h a
349	PBC J1204.7+3108	UGC 07064	Sy1	181.19118	31.14042	3.94	2.274	5.26	0.4 ± 0.1	...	0.0250	42.99	3 3 n h c
350	PBC J1206.2+5244	NGC 4102	LIN	181.56427	52.74236	2.47	2.208	13.33	2.2 ± 0.2	1.2 ± 0.3	0.0028	41.55	3 1 y h a
351	PBC J1207.6+3353	7C 1205+3409	rG	181.90329	33.88649	4.11	0.961	4.94	0.5 ± 0.1	...	0.0788	44.09	3 3 n h c
352	PBC J1207.9+4306	NGC 4117	Sy2	181.98459	43.10007	4.24	2.434	4.73	0.7 ± 0.2	...	0.0029	41.21	1 1 n h b
353	PBC J1209.1+4702	Mrk 0198	Sy2	182.29366	47.04599	2.84	0.955	8.66	1.2 ± 0.1	1.4 ± 0.5	0.0245	43.30	1 1 n h c
354	PBC J1209.5+4342	NGC 4138	Sy1	182.37637	43.71407	2.31	1.746	15.15	2.9 ± 0.2	1.1 ± 0.2	0.0029	41.62	1 1 y h a
355	PBC J1210.5+3924	NGC 4151	Sy1	182.63246	39.40598	0.75	0.184	246.03	37.6 ± 0.2	1.04 ± 0.01	0.0032	42.90	3 1 y h a
356	PBC J1210.7+3819	KUG 1208+386	GiG	182.69434	38.32501	2.69	0.815	9.45	1.3 ± 0.2	0.8 ± 0.3	0.0227	43.28	3 1 n h c
357	PBC J1212.8+0703	IGRJ 12131+0700	Sy1	183.22400	7.05920	4.27	4.080	4.68	0.7 ± 0.2	...	0.2095	41.99	1 1 n h a
358	PBC J1212.9-6453	4U 1210-64	HXB	183.22630	–64.89564	3.46	0.658	10.94	1.9 ± 0.2	0.1 ± 0.2	...	...	2 1 n l a
359	PBC J1214.2+2932	Was 49	Sy1	183.55112	29.54366	3.65	1.502	8.23	1.3 ± 0.2	0.7 ± 0.3	0.0640	43.96	3 1 y h a
360	PBC J1215.8+5046	Mrk 1469	Sy1	183.96851	50.77435	0.00	3.821	5.60	1.0 ± 0.2	...	0.0312	43.25	3 3 n h c
361	PBC J1216.9-2615	ESO 505-31	Sy2	184.24518	–26.25084	3.88	2.464	5.27	1.3 ± 0.2	...	0.0403	43.71	1 1 n h b
362	PBC J1217.1+0712	NGC 4235	Sy1	184.27641	7.21300	2.78	1.530	9.32	2.0 ± 0.2	1.5 ± 0.5	0.0077	42.39	1 1 n h c
363	PBC J1218.4+2949	Mrk 766	Sy1	184.62291	29.83114	2.37	1.271	14.45	2.1 ± 0.2	0.5 ± 0.2	0.0126	42.75	3 1 y h a
364	PBC J1218.9+4718	NGC 4258	LIN	184.72964	47.30855	3.00	0.494	10.96	1.8 ± 0.2	1.0 ± 0.3	0.0015	40.86	3 1 y h a
365	PBC J1221.8+7519	Mrk 205	Sy1	185.45032	75.32202	3.37	0.729	8.93	1.1 ± 0.2	0.2 ± 0.2	0.0700	44.15	2 1 n h a
366	PBC J1222.3+0415	4C 04.42	BLA	185.58986	4.25689	3.22	2.164	7.26	1.5 ± 0.2	...	0.9650	46.88	3 1 y h a
367	PBC J1223.4+0240	Mrk 50	Sy1	185.85086	2.66868	3.02	0.626	8.60	1.8 ± 0.2	0.9 ± 0.4	0.0231	43.35	3 1 y h a

Table 2. continued.

	PBC name	ID	Type*	RA (deg)	Dec (deg)	Error radius (arcmin)	Offset (arcmin)	SNR	Flux† (erg cm^{-2} s^{-1})	Hardness ratio (R_{30-150}/R_{14-30})	Redshift	log L_{14-150} (erg s^{-1})	Flag‡ A B C D E
368	PBC J1223.9+4042	SDSS J122358.97+404409.3	QSO	185.99078	40.70899	3.44	1.630	6.44	0.8 ± 0.1	0.8 ± 0.5	0.0964	44.25	3 0 n h b
369	PBC J1224.8+2122	4C +21.35	BLA	186.22160	21.37864	3.59	0.302	6.06	0.8 ± 0.1	...	0.4350	45.82	3 1 n h a
370	PBC J1225.7+3331	NGC 4395	Sy1	186.43011	33.51800	2.97	2.088	11.31	1.9 ± 0.2	1.1 ± 0.3	0.0010	40.51	3 1 y h a
371	PBC J1225.7+1240	NGC 4388	Sy2	186.43855	12.66964	0.92	0.613	102.58	20.3 ± 0.2	1.07 ± 0.03	0.0084	43.46	1 1 y h a
372	PBC J1226.6-6246	GX 301-2	HXB	186.66063	–62.77081	0.59	0.110	1551.20	292.2 ± 0.3	0.123 ± 0.001	...	...	2 1 y l a
373	PBC J1228.0-4854	XSS J12270-4859	CV*	187.00999	–48.91053	2.57	1.050	12.49	3.0 ± 0.2	1.1 ± 0.3	...	...	1 1 y h a
374	PBC J1229.1+0202	3C 273	BLA	187.27650	2.04772	0.86	0.292	139.02	29.6 ± 0.2	1.14 ± 0.03	0.1583	46.26	3 1 y h a
375	PBC J1231.9+2013	RBS 1125	Sy1	187.99770	20.23182	4.03	4.529	5.09	0.6 ± 0.1	...	0.0640	43.89	3 1 n h b
376	PBC J1232.2-4216	1RXS J123212.3-421745	Sy1	188.05376	–42.27178	4.07	1.545	5.71	1.3 ± 0.2	...	0.1000	44.47	3 1 n h c
377	PBC J1234.7-6434	IGR J12349-6434	Sy*	188.69917	–64.56965	1.79	0.780	29.32	6.6 ± 0.3	0.52 ± 0.08	...	...	3 1 y l a
378	PBC J1235.5-3954	NGC 4507	Sy2	188.89040	–39.91012	1.14	0.550	63.02	14.6 ± 0.2	0.89 ± 0.05	0.0117	43.60	3 1 y h a
379	PBC J1238.8-2719	ESO 506- G 027	Sy2	189.71558	–27.32387	1.63	1.152	22.42	4.6 ± 0.2	1.1 ± 0.2	0.0252	43.92	3 1 n h a
380	PBC J1239.1-1612	IGR J12391-1612	Sy2	189.78006	–16.20324	2.38	1.427	14.22	3.1 ± 0.2	1.0 ± 0.2	0.0367	43.94	3 1 y h a
381	PBC J1239.6-0520	NGC 4593	Sy1	189.91920	–5.33581	1.50	0.585	31.52	6.6 ± 0.2	0.9 ± 0.1	0.0090	43.03	3 1 y h a
382	PBC J1240.6-3334	1ES 1238-332	Sy1	190.17406	–33.56771	3.69	1.106	5.79	1.1 ± 0.2	...	0.0500	43.91	1 1 n h c
383	PBC J1241.5-5749	IGR J12415-5750	Sy2	190.37613	–57.83113	2.78	0.622	14.40	3.2 ± 0.2	0.9 ± 0.2	0.0242	43.53	1 1 y h a
384	PBC J1246.5+5432	NGC 4686	G	191.64784	54.54395	2.27	0.870	12.65	2.2 ± 0.2	1.2 ± 0.3	0.0167	43.11	3 1 n h c
385	PBC J1249.8-5906	3A 1246-588	LXB	192.45297	–59.10614	1.58	1.638	35.18	7.4 ± 0.2	0.54 ± 0.07	...	...	3 1 y l a
386	PBC J1252.3-2914	EX Hya	DQ*	193.08485	–29.24268	2.24	0.960	14.92	3.2 ± 0.3	0.2 ± 0.1	...	...	2 1 n h a
387	PBC J1253.3-4137	ESO 323-32	Sy2	193.33243	–41.62855	3.86	0.528	5.42	1.0 ± 0.2	...	0.0159	42.86	3 1 y h a
388	PBC J1256.1-0547	3C 279	BLA	194.04514	–5.79737	2.59	0.491	12.60	3.2 ± 0.3	1.0 ± 0.3	0.5362	46.47	1 1 y h a
389	PBC J1257.7-6917	1H 1254-690	LXB	194.42622	–69.29657	1.33	0.632	47.11	6.8 ± 0.2	0.03 ± 0.04	...	...	2 1 y h a
390	PBC J1259.5+2756	Coma Cluster	ClG	194.88933	27.94817	1.44	3.890	36.91	3.7 ± 0.2	< 0.05	0.0231	43.66	2 1 y h a
391	PBC J1301.2-6136	GX 304-1	HXB	195.30661	–61.61546	2.52	0.918	16.26	3.2 ± 0.2	0.4 ± 0.1	...	...	3 1 n l a
392	PBC J1302.1-6356	IGR J13020-6359	HXB	195.54649	–63.94546	2.01	1.978	21.62	4.8 ± 0.2	0.6 ± 0.1	...	...	3 1 y l a
393	PBC J1302.8+1622	Mrk 783	Sy1	195.70276	16.38159	3.75	2.899	7.99	1.4 ± 0.2	...	0.0670	44.07	1 1 y h a
394	PBC J1304.0-1019	NGC 4939	Sy2	196.02100	–10.32205	3.71	2.517	5.52	1.1 ± 0.2	...	0.0103	42.52	3 1 n h c
395	PBC J1304.0+5347	IGR J13038+5348	Sy1	196.02338	53.79128	2.09	0.919	15.96	2.5 ± 0.2	1.0 ± 0.2	0.0298	43.67	3 1 y h a
396	PBC J1304.2-0533	NGC 4941	Sy2	196.06079	–5.55030	4.21	0.383	6.02	1.6 ± 0.3	...	0.0037	41.56	1 1 n h a
397	PBC J1305.4-4928	NGC 4945	Sy2	196.35863	–49.46954	1.09	0.078	73.06	18.3 ± 0.3	1.52 ± 0.07	0.0019	42.12	1 1 y h a
398	PBC J1306.5-4025	ESO 323-77	Sy2	196.64583	–40.42824	2.43	1.815	14.53	3.3 ± 0.2	0.9 ± 0.2	0.0149	43.16	1 1 y h a
399	PBC J1309.0+1138	NGC 4992	Sy2	197.27386	11.64738	1.81	0.796	18.56	3.0 ± 0.2	1.5 ± 0.3	0.0252	43.73	1 1 n h a
400	PBC J1310.7-5551	IGR J13109-5552	Sy1	197.68118	–55.86078	3.12	0.154	10.37	2.5 ± 0.2	...	0.1040	44.75	1 1 y h a
401	PBC J1313.0-1108	RBS 1233	Sy1	198.26985	–11.14374	3.60	0.969	6.02	1.3 ± 0.2	0.8 ± 0.5	0.0343	43.64	1 1 n h b
402	PBC J1315.2+4423	Mrk 248	Sy2	198.81517	44.39318	2.91	0.859	8.33	1.1 ± 0.1	0.5 ± 0.3	0.0353	43.63	3 1 y h a
403	PBC J1318.2-6259	IGR J13186-6257	gam	199.56624	–62.98454	3.23	3.246	9.32	2.1 ± 0.2	0.7 ± 0.3	...	...	1 1 y l a
404	PBC J1320.6+6014	RBS 1252	Sy1	200.16286	60.23888	4.38	1.183	4.51	0.6 ± 0.1	...	0.1000	44.27	1 1 n h b
405	PBC J1322.4-1644	MCG-03-34-063	Sy2	200.61143	–16.74400	2.58	2.827	10.74	2.3 ± 0.2	0.4 ± 0.2	0.0167	43.19	3 1 n h a
406	PBC J1325.4-4301	Cen A	BLA	201.36745	–43.01937	0.72	0.105	368.00	84.5 ± 0.2	0.976 ± 0.009	0.0018	42.74	1 1 y h a
407	PBC J1326.4-6207	4U 1323-62	LXB	201.61169	–62.12960	1.01	1.154	84.78	19.3 ± 0.2	0.59 ± 0.03	...	...	3 1 y l a
408	PBC J1331.2-2523	RHS 37	Sy1	202.80685	–25.39996	3.81	0.146	5.52	1.2 ± 0.2	...	0.0264	43.39	1 1 n h c
409	PBC J1332.0+1116	2MASX J13315225+1116496	Sy1	203.00609	11.27332	3.77	2.304	7.56	1.5 ± 0.2	...	0.0910	44.38	3 1 n h b
410	PBC J1333.3-3400	ESO 383-18	Sy2	203.33310	–34.01167	3.86	1.346	8.60	1.9 ± 0.2	0.3 ± 0.2	0.0130	42.73	2 1 y h a
411	PBC J1334.5-2324	ESO 509-66	Sy2	203.64436	–23.41187	4.10	2.362	6.55	1.7 ± 0.3	...	0.0446	43.77	1 1 n h c
412	PBC J1335.8+0301	NGC 5231	AGN	203.95845	3.02554	3.14	1.655	8.57	1.6 ± 0.2	0.6 ± 0.3	0.0216	43.21	1 1 n h c
413	PBC J1335.8-3417	1H 1334-340	Sy1	203.97183	–34.28806	1.81	0.464	18.50	4.1 ± 0.2	0.6 ± 0.1	0.0078	42.85	1 1 y h a
414	PBC J1338.1+0432	NGC 5252	Sy2	204.54378	4.54433	1.57	1.374	28.58	6.0 ± 0.2	1.2 ± 0.1	0.0222	43.79	3 1 y h a
415	PBC J1341.2-1439	RBS 1303	Sy1	205.30513	–14.65268	3.14	0.492	7.43	1.4 ± 0.2	...	0.0417	43.85	3 1 n h b
416	PBC J1341.2+3022	Mrk 268	Sy2	205.31233	30.36730	2.99	1.049	11.32	1.8 ± 0.2	0.9 ± 0.3	0.0404	43.72	3 1 y h a
417	PBC J1341.9+3537	NGC 5273	Sy1	205.48656	35.63315	4.29	2.691	4.57	0.5 ± 0.1	...	0.0035	41.35	3 3 n h b
418	PBC J1344.2+1934	2MASX J13441569+1933596	G	206.07095	19.56813	4.30	4.571	7.29	1.3 ± 0.2	...	...	...	1 1 n h c
419	PBC J1345.4+4141	NGC 5290	G	206.35364	41.68343	3.79	2.049	7.14	1.1 ± 0.2	...	0.0086	42.30	1 1 n h c
420	PBC J1347.4-3254	ABELL 3571	ClG	206.87143	–32.90324	3.47	2.247	6.35	1.1 ± 0.2	0.1 ± 0.3	0.0414	43.65	2 1 n h b
421	PBC J1347.5-6035	4U 1344-60	Sy1	206.88101	–60.59861	1.56	0.687	36.39	8.0 ± 0.2	0.79 ± 0.08	0.0130	43.41	1 1 y l a
422	PBC J1348.7+2635	ABELL 1795	ClG	207.18561	26.59277	4.02	3.595	5.10	0.3 ± 0.1	...	0.0624	44.04	2 2 n h a
423	PBC J1349.2-3018	IC 4329A	Sy1	207.32405	–30.31039	1.00	0.331	88.60	24.0 ± 0.3	0.83 ± 0.03	0.0160	44.07	1 1 y h a
424	PBC J1349.8+0205	RX J1349.8+0204	Sy1	207.46144	2.09790	3.33	1.245	6.77	1.3 ± 0.2	0.7 ± 0.4	0.0328	43.61	1 1 n h c
425	PBC J1351.5-1815	RBS 1323	Sy1	207.89159	–18.25744	4.08	1.976	5.00	1.1 ± 0.2	...	0.0120	42.64	3 1 n h b
426	PBC J1353.1+6918	Mrk 279	Sy1	208.28001	69.31242	1.74	0.418	22.56	3.8 ± 0.2	1.1 ± 0.2	0.0306	43.87	3 1 n h a
427	PBC J1354.3-3746	PGC 049418	Sy2	208.58514	–37.77275	3.36	0.926	6.68	1.4 ± 0.2	0.8 ± 0.5	0.0516	44.03	3 1 n h a
428	PBC J1355.8+3833	Mrk 0464	Sy1	208.95427	38.55485	2.70	1.495	9.40	1.4 ± 0.1	1.2 ± 0.4	0.0507	44.01	1 1 n h c
429	PBC J1400.7-6323	IGR J14003-6326	gam	210.19054	–63.39278	3.76	3.393	9.65	2.1 ± 0.2	0.5 ± 0.2	...	...	3 1 y l a
430	PBC J1408.2-3023	2MASX J14080674-3023537	Sy1	212.06598	–30.39067	4.19	1.922	6.03	1.3 ± 0.3	...	0.0236	43.28	1 1 n h b
431	PBC J1413.2-6519	Circinus Galaxy	Sy2	213.30536	–65.32830	0.98	0.880	99.84	21.6 ± 0.2	0.82 ± 0.03	0.0014	41.91	3 1 y l a
432	PBC J1413.2-0312	NGC 5506	BLA	213.31001	–3.21058	0.99	0.218	77.30	19.6 ± 0.3	0.75 ± 0.03	0.0060	43.15	3 1 y h a
433	PBC J1414.2+1219	1RXS J141409.8+121836	QSO	213.56500	12.31940	4.41	1.491	4.47	0.6 ± 0.1	...	0.4558	45.62	3 0 n h b
434	PBC J1416.8-4639	IGR J14175-4641	Sy2	214.20912	–46.66321	3.65	2.988	8.31	2.2 ± 0.3	...	0.0760	44.41	1 1 y h a
435	PBC J1417.9+2508	NGC 5548	Sy1	214.49156	25.13824	1.69	0.385	26.98	5.4 ± 0.2	1.0 ± 0.1	0.0166	43.48	1 1 y h a
436	PBC J1419.4-2639	RHS 39	Sy1	214.85828	–26.65148	2.35	0.938	17.17	4.5 ± 0.3	1.1 ± 0.2	0.0222	43.60	3 1 y h a
437	PBC J1421.1-6243	H 1417-624	HXB	215.27979	–62.73145	3.61	2.090	8.94	1.8 ± 0.2	0.2 ± 0.2	...	...	2 1 n l a
438	PBC J1421.4+4748	RBS 1378	Sy1	215.36588	47.80225	2.98	0.796	8.03	1.2 ± 0.1	1.5 ± 0.6	0.0720	44.27	1 1 n h a
439	PBC J1426.0+3748	ABELL 1914	ClG	216.50131	37.80708	4.03	1.193	5.09	0.3 ± 0.1	...	0.1710	44.97	2 2 n h c
440	PBC J1427.4+1952	Mrk 813	Sy1	216.86951	19.87586	4.13	2.824	4.92	0.8 ± 0.2	0.5 ± 0.4	0.1310	44.64	3 1 n h c
441	PBC J1428.6+4239	H 1426+428	BLA	217.16380	42.65468	2.59	1.723	11.62	1.8 ± 0.2	0.7 ± 0.2	0.1290	44.87	3 1 n h a
442	PBC J1429.2+0119	Mrk 1383	Sy1	217.30269	1.32764	3.03	2.966	7.84	1.6 ± 0.2	1.3 ± 0.5	0.0860	44.56	1 1 n h b

Table 2. continued.

	PBC name	ID	Type*	RA (deg)	Dec (deg)	Error radius (arcmin)	Offset (arcmin)	SNR	Flux† (erg cm^{-2} s^{-1})	Hardness ratio (R_{30-150}/R_{14-30})	Redshift	log L_{14-150} (erg s^{-1})	Flag‡ A B C D E
443	PBC J1429.8-6711	IGR J14298-6715	LXB	217.45323	–67.19478	4.23	4.748	6.78	1.4 ± 0.2	...	...	...	3 3 y h a
444	PBC J1434.9+4839	RBS 1407	Sy1	218.72563	48.65292	3.17	0.608	7.29	0.9 ± 0.1	0.5 ± 0.4	0.0410	43.64	3 1 n h b
445	PBC J1436.3+5848	Mrk 817	Sy1	219.07803	58.80375	2.34	0.729	11.82	1.5 ± 0.1	0.9 ± 0.3	0.0312	43.63	3 1 n h c
446	PBC J1439.0+1413	2MASX J14391186+1415215	G	219.76900	14.23305	3.95	3.863	5.24	0.8 ± 0.2	...	...	...	1 1 n h c
447	PBC J1440.9+5330	Mrk 477	Sy2	220.24268	53.50606	3.69	2.998	5.79	0.7 ± 0.1	...	0.0380	43.48	3 1 n h a
448	PBC J1442.4-1714	NGC 5728	Sy2	220.61559	–17.24790	1.72	0.968	21.99	6.4 ± 0.3	1.2 ± 0.2	0.0094	43.05	1 1 y h a
449	PBC J1446.6-6416	IGR J14471-6414	Sy1	221.66554	–64.26871	3.82	2.532	6.18	1.2 ± 0.2	...	0.0530	43.97	3 1 y l a
450	PBC J1449.0-5533	IGR J14493-5534	AGN	222.25575	–55.56605	3.24	2.861	7.06	1.6 ± 0.2	0.8 ± 0.5	...	...	1 1 y l a
451	PBC J1451.2-5539	IGR J14515-5542	Sy2	222.82178	–55.65489	2.64	2.616	14.63	4.1 ± 0.3	1.0 ± 0.2	0.0180	43.33	1 1 y l a
452	PBC J1453.0+2553	RX J1453.1+2554	G	223.26154	25.89366	2.86	1.478	8.56	1.4 ± 0.2	0.9 ± 0.4	...	...	3 1 n h c
453	PBC J1453.5-5522	IGR J14536-5522	CV*	223.37582	–55.37833	3.52	1.868	9.20	2.8 ± 0.3	0.5 ± 0.2	...	...	2 1 y l a
454	PBC J1455.1-5132	IGR J14552-5133	Sy1	223.79524	–51.54427	4.09	1.952	8.23	2.2 ± 0.3	...	0.0160	42.94	1 1 y h a
455	PBC J1457.8-4306	IC 4518	Sy2	224.46944	–43.10536	2.60	2.380	9.98	2.1 ± 0.2	0.5 ± 0.3	0.0160	43.18	3 1 y h a
456	PBC J1503.9+1027	Mrk 841	Sy1	225.98579	10.45653	2.50	1.595	10.60	2.1 ± 0.2	0.8 ± 0.3	0.0364	43.91	1 1 n h a
457	PBC J1506.6+0349	2MASX J15064412+0351444	G	226.65204	3.82672	4.00	2.863	5.30	1.1 ± 0.2	...	...	...	3 1 n h c
458	PBC J1509.4-6649	IGR J15094-6649	CV*	227.35425	–66.82104	2.79	0.159	12.11	2.4 ± 0.2	0.2 ± 0.2	...	...	2 1 y h a
459	PBC J1510.8+0545	ABELL 2029	ClG	227.71558	5.76119	3.24	1.732	7.07	1.0 ± 0.2	< 0.2	0.0774	44.26	2 1 n h c
460	PBC J1512.0-2118	RBS 1473	Sy1	228.00632	–21.31100	3.25	0.544	7.02	1.8 ± 0.3	0.7 ± 0.4	0.0443	44.02	3 1 n h b
461	PBC J1512.8-0906	PKS 1510-08	BLA	228.20403	–9.10167	2.48	0.400	10.75	2.6 ± 0.2	1.5 ± 0.5	0.3599	46.15	1 1 n h a
462	PBC J1513.8-8123	2MASX J15144217-8123377	Sy1	228.47337	–81.38692	2.95	1.860	10.75	1.5 ± 0.2	0.4 ± 0.3	...	...	3 1 n h c
463	PBC J1513.8-5909	PSR B1509-58	Psr	228.47343	–59.15364	1.08	0.976	77.44	19.2 ± 0.2	0.98 ± 0.05	...	...	1 1 y l a
464	PBC J1515.2+4202	NGC 5899	LIN	228.80011	42.04249	3.21	1.670	7.83	1.4 ± 0.2	1.0 ± 0.4	0.0085	42.34	3 1 n h c
465	PBC J1517.7-2419	Ap Lib	BLA	229.44090	–24.33106	4.01	2.624	5.12	1.4 ± 0.3	...	0.0490	43.99	3 1 n h c
466	PBC J1520.6-5710	Cir X-1	LXB	230.16652	–57.17210	1.16	0.334	59.26	11.2 ± 0.3	0.04 ± 0.03	...	...	2 1 y l a
467	PBC J1533.4-0844	1E 1530-085	Sy2	233.37047	–8.73427	2.91	2.857	8.34	2.1 ± 0.3	0.9 ± 0.4	0.0230	43.51	1 1 n h c
468	PBC J1536.0+5754	Mrk 290	Sy1	234.00989	57.90701	2.75	1.357	10.79	1.8 ± 0.2	1.4 ± 0.4	0.0296	43.51	3 1 n h a
469	PBC J1536.1-5749	IGR J15359-5750	gam	234.04422	–57.82164	3.49	2.554	7.44	1.6 ± 0.3	...	...	...	1 1 y l a
470	PBC J1542.4-5222	H 1538-522	HXB	235.61090	–52.37747	0.89	0.725	149.15	33.9 ± 0.2	0.19 ± 0.01	...	...	2 1 y l a
471	PBC J1546.5+6931	2MASX J15462424+6929102	G	236.63815	69.52399	4.21	3.724	4.77	0.5 ± 0.1	...	...	...	3 3 n h c
472	PBC J1547.3+2050	4C 21.45	Sy1	236.84962	20.83874	4.06	4.996	5.03	0.6 ± 0.1	...	0.2640	45.37	3 3 n h c
473	PBC J1547.9-6233	4U 1543-624	LXB	236.98810	–62.55989	1.57	0.571	36.09	6.7 ± 0.2	0.14 ± 0.05	...	...	2 1 y h a
474	PBC J1548.1-4528	IGR J15479-4529	CV*	237.04102	–45.48055	1.57	0.820	34.26	8.4 ± 0.3	0.49 ± 0.07	...	...	3 1 y h a
475	PBC J1548.4-1344	NGC 5995	Sy2	237.12299	–13.74846	2.95	1.242	9.92	3.0 ± 0.4	0.6 ± 0.3	0.0250	43.65	1 1 y h a
476	PBC J1555.5+1109	PG 1553+113	BLA	238.89127	11.16346	4.21	2.753	4.77	1.0 ± 0.2	0.3 ± 0.4	...	...	2 1 n h a
477	PBC J1557.7-5425	H 1553-542	HXB	239.43919	–54.42502	2.46	0.841	16.89	3.9 ± 0.3	0.3 ± 0.1	...	...	2 1 n l a
478	PBC J1558.4+2713	ABELL 2142	ClG	239.61826	27.22837	2.64	2.739	9.76	1.5 ± 0.2	0.4 ± 0.2	0.0899	44.59	2 1 n h a
479	PBC J1559.4+2556	SWIFT J1559.5+2553	Sy*	239.87094	25.93589	1.53	0.977	30.08	6.2 ± 0.2	0.49 ± 0.07	...	...	3 1 n h a
480	PBC J1601.0-6044	1H 1556-605	LXB	240.25290	–60.74547	2.82	0.471	12.98	2.6 ± 0.3	0.1 ± 0.1	...	...	2 1 y h a
481	PBC J1612.1-6037	IGR J16119-6036	Sy1	243.02875	–60.63256	2.76	1.900	11.66	2.9 ± 0.3	0.5 ± 0.2	0.0158	43.13	3 1 y h a
482	PBC J1612.7-5225	H 1608-522	LXB	243.19197	–52.42426	0.80	0.474	241.78	63.3 ± 0.3	0.61 ± 0.01	...	...	1 1 y l a
483	PBC J1614.1+6542	Mrk 876	Sy1	243.54457	65.71315	4.13	1.439	4.90	0.5 ± 0.1	...	0.1200	44.54	3 3 n h c
484	PBC J1614.4-6050	ABELL 3627	ClG	243.60663	–60.83481	4.02	2.062	7.48	1.5 ± 0.3	...	0.0162	42.93	3 3 n h c
485	PBC J1616.5-4957	IGR J16167-4957	CV*	244.14120	–49.96606	3.93	0.994	12.85	3.2 ± 0.3	0.5 ± 0.2	...	...	3 1 y l a
486	PBC J1617.8+3224	4C 32.51	Sy1	244.46895	32.41375	3.65	3.089	7.28	1.5 ± 0.2	...	0.1517	44.91	1 1 n h b
487	PBC J1618.5-5926	WKK 6471	Sy1	244.63680	–59.43859	4.08	1.077	5.00	1.1 ± 0.2	...	0.0350	43.60	3 1 n h a
488	PBC J1619.5-4946	IGR J16195-4945	HX?	244.88121	–49.76785	2.99	1.564	14.88	3.2 ± 0.3	0.2 ± 0.1	...	...	2 1 y l a
489	PBC J1619.5-2807	IGR J16194-2810	LXB	244.89807	–28.12538	2.88	2.955	13.89	4.0 ± 0.3	0.5 ± 0.2	...	...	3 1 y h a
490	PBC J1619.9-1538	Sco X-1	LXB	244.97778	–15.64214	0.55	0.150	4507.25	2387.0 ± 0.7	0.0218 ± 0.0001	...	...	2 1 y h a
491	PBC J1620.3+8101	MCG+14-08-004	Sy2	245.09547	81.02960	2.63	2.692	8.32	1.4 ± 0.2	0.4 ± 0.3	...	...	3 1 n h c
492	PBC J1620.8-5130	IGR J16207-5129	HXB	245.20256	–51.51277	2.43	0.760	18.08	4.8 ± 0.3	0.5 ± 0.1	...	...	3 1 y l a
493	PBC J1625.5+8530	VII Zw 653	Sy1	246.37715	85.50495	4.43	0.610	4.43	0.3 ± 0.1	...	0.0629	43.99	2 2 n h b
494	PBC J1626.0-2952	PKS 1622-29	BLA	246.51421	–29.87462	4.29	1.173	4.65	1.4 ± 0.3	...	0.8149	46.73	1 1 n h a
495	PBC J1626.5-5155	SWIFT J1626.6-5156	HXB	246.63135	–51.93035	2.14	1.025	19.53	4.3 ± 0.3	0.04 ± 0.09	...	...	2 1 y l a
496	PBC J1627.9-4911	H 1624-490	LXB	246.99832	–49.18477	1.26	0.979	58.10	11.8 ± 0.3	0.02 ± 0.03	...	...	2 1 y l a
497	PBC J1628.0+5145	Mrk 1498	Sy1	247.02367	51.76632	2.10	0.591	19.30	3.6 ± 0.2	1.0 ± 0.2	0.0556	44.31	3 1 y h a
498	PBC J1628.1-4839	IGR J16283-4838	HXB	247.02614	–48.65155	2.34	0.752	21.60	5.3 ± 0.3	0.4 ± 0.1	...	...	3 1 y l a
499	PBC J1631.7-4848	IGR J16318-4848	HXB	247.93288	–48.81008	0.83	0.870	173.76	44.4 ± 0.3	0.56 ± 0.02	...	...	3 1 y l a
500	PBC J1632.0-4751	IGR J16320-4751	HXB	248.00879	–47.85451	0.95	1.180	112.36	29.4 ± 0.3	0.33 ± 0.02	...	...	3 1 y l a
501	PBC J1632.2-6727	4U 1626-67	LXB	248.05656	–67.46353	0.87	0.323	155.60	26.8 ± 0.2	0.06 ± 0.01	...	...	2 1 y h a
502	PBC J1632.7-4727	IGR J16328-4726	gam	248.17848	–47.45155	3.42	1.027	11.39	4.8 ± 0.3	3.1 ± 0.8	...	...	3 1 y l a
503	PBC J1638.5-2058	1RXSJ163830.9-205520	AGN	249.63292	–20.97947	4.37	3.366	4.53	1.5 ± 0.3	...	0.0269	43.48	1 1 n h a
504	PBC J1638.5-6421	IGR J16377-6423	ClG	249.64517	–64.36086	2.47	2.187	14.61	2.7 ± 0.3	0.1 ± 0.1	0.0500	44.20	2 1 y h a
505	PBC J1639.1-4641	IGR J16393-4643	HXB	249.79294	–46.69981	1.70	0.867	38.65	10.4 ± 0.3	0.11 ± 0.04	...	...	3 1 y l a
506	PBC J1640.9-5344	H 1636-536	LXB	250.24306	–53.74683	0.85	0.501	165.21	41.4 ± 0.3	0.27 ± 0.01	...	...	2 1 y l a
507	PBC J1641.7-4532	IGR J16418-4532	HXB	250.44786	–45.54793	2.10	0.767	28.52	8.2 ± 0.3	0.35 ± 0.08	...	...	3 1 y l a
508	PBC J1643.0+3951	4C 39.48	BLA	250.75140	39.86289	3.89	3.187	5.36	0.9 ± 0.2	...	0.5930	46.20	1 1 n h c
509	PBC J1645.8-4536	GX 340+0	LXB	251.45810	–45.60397	0.73	0.581	383.12	97.2 ± 0.3	0.008 ± 0.004	...	...	2 1 y l a
510	PBC J1648.2-4511	IGR J16479-4514	HXB	252.06552	–45.18373	2.21	1.953	26.30	7.8 ± 0.3	0.39 ± 0.09	...	...	3 1 y l a
511	PBC J1648.3-3034	IGR J16482-3036	Sy1	252.07918	–30.57235	2.86	2.302	13.91	4.0 ± 0.3	1.1 ± 0.3	0.0310	43.92	1 1 y h a
512	PBC J1649.4-4349	IGR J16493-4348	LX?	252.35638	–43.81733	2.48	0.273	16.58	4.8 ± 0.3	0.5 ± 0.1	...	...	3 1 y l a
513	PBC J1649.8-3305	IGR J16500-3307	CV*	252.46718	–33.09388	4.33	2.288	10.16	2.7 ± 0.3	...	...	...	1 1 y h a
514	PBC J1650.6+0434	NGC 6230	Sy2	252.66219	4.56987	3.79	2.854	5.57	1.2 ± 0.2	...	0.0325	43.58	3 1 n h c
515	PBC J1651.9-5914	ESO 138-1	Sy2	252.99258	–59.23731	3.36	4.892	9.47	2.3 ± 0.3	...	0.0091	42.56	3 1 y h a
516	PBC J1652.2+5554	MCG+09-28-001	Sy2	253.07460	55.90911	3.32	0.273	8.02	1.5 ± 0.2	...	0.0290	43.43	1 1 n h c

Table 2. continued.

	PBC name	ID	Type*	RA (deg)	Dec (deg)	Error radius (arcmin)	Offset (arcmin)	SNR	Flux† (erg cm^{-2} s^{-1})	Hardness ratio (R_{30-150}/R_{14-30})	Redshift	log L_{14-150} (erg s^{-1})	Flag‡ A B C D E
517	PBC J1653.0+0223	NGC 6240	LIN	253.26155	2.39526	2.06	1.000	18.74	4.9 ± 0.3	1.1 ± 0.2	0.0243	43.77	1 1 y h a
518	PBC J1653.8+3945	Mrk 501	BLA	253.45061	39.75972	2.08	0.784	22.97	4.4 ± 0.2	0.5 ± 0.1	0.0336	43.99	3 1 y h a
519	PBC J1653.9-3950	GRO J1655-40	LXB	253.48779	–39.84532	1.37	0.590	62.19	17.5 ± 0.3	0.72 ± 0.05	...	...	3 1 y l a
520	PBC J1656.0-5202	IGR J16558-5203	Sy1	254.01791	–52.04258	2.90	1.145	12.83	3.2 ± 0.3	0.7 ± 0.2	0.0540	44.28	3 1 y h a
521	PBC J1656.2-3303	SWIFT J1656.3-3302	QSO	254.05182	–33.05803	2.63	1.583	18.41	5.0 ± 0.3	1.3 ± 0.3	2.4000	48.35	1 1 y h a
522	PBC J1657.8+3520	Her X-1	LXB	254.46025	35.33956	0.63	0.213	632.36	99.5 ± 0.2	0.120 ± 0.003	...	...	2 1 y h a
523	PBC J1700.2-4221	AX J1700.2-4220	HXB	255.06839	–42.35731	3.78	1.079	13.47	3.9 ± 0.3	0.6 ± 0.2	...	...	1 1 y l a
524	PBC J1700.8-4139	OAO 1657-415	HXB	255.20674	–41.65610	0.76	0.134	301.21	88.3 ± 0.3	0.478 ± 0.008	...	...	3 1 y l a
525	PBC J1701.0-4610	XTE J1701-462	LXB	255.25725	–46.18292	0.91	0.592	132.26	32.3 ± 0.3	0.00 ± 0.01	...	...	2 1 y l a
526	PBC J1702.8-4847	GX 339-4	LXB	255.71030	–48.78911	0.76	0.164	216.96	67.7 ± 0.3	0.97 ± 0.02	...	...	1 1 y l a
527	PBC J1703.9-3750	4U 1700-377	HXB	255.98592	–37.84074	0.64	0.206	1255.55	336.8 ± 0.3	0.468 ± 0.002	...	...	3 1 y l a
528	PBC J1704.0+7836	ABELL 2256	ClG	256.01288	78.61470	3.46	6.243	6.38	0.4 ± 0.1	...	0.0581	44.05	2 2 n h a
529	PBC J1705.7-3625	GX 349+2	LXB	256.43671	–36.42181	0.73	0.097	664.56	140.3 ± 0.3	0.016 ± 0.001	...	...	2 1 y l a
530	PBC J1706.2-6143	SWIFT J1706.6-6146	X	256.55762	–61.72909	1.87	1.100	17.44	4.1 ± 0.2	0.8 ± 0.2	...	...	3 1 n h c
531	PBC J1706.2-4302	H 1702-429	LXB	256.56186	–43.03912	0.93	0.219	152.26	45.6 ± 0.3	0.45 ± 0.01	...	...	3 1 y l a
532	PBC J1706.5+2358	4U 1700+24	LXB	256.63510	23.97188	3.15	0.479	11.79	2.5 ± 0.2	0.6 ± 0.2	...	...	1 1 n h a
533	PBC J1708.8-3219	4U 1705-32	LXB	257.21292	–32.32247	2.79	0.902	18.24	5.1 ± 0.3	0.5 ± 0.1	...	...	1 1 y l a
534	PBC J1708.8-4406	H 1705-440	LXB	257.21954	–44.10624	0.82	0.406	173.13	46.3 ± 0.3	0.117 ± 0.010	...	...	2 1 y l a
535	PBC J1709.4-3624	IGR J17091-3624	XB*	257.35260	–36.40780	2.35	3.546	36.98	10.8 ± 0.3	0.86 ± 0.08	...	...	1 1 y l a
536	PBC J1710.2-2807	XTE J1710-281	LXB	257.56531	–28.13160	2.19	0.744	22.47	5.8 ± 0.3	0.6 ± 0.1	...	...	3 1 y h a
537	PBC J1712.3-2320	Oph Cluster	ClG	258.09961	–23.34907	1.43	0.967	43.64	10.4 ± 0.3	0.06 ± 0.04	0.0280	44.22	2 1 y h a
538	PBC J1712.4-4050	4U 1708-40	LXB	258.11768	–40.84512	3.15	0.846	13.74	3.7 ± 0.3	0.2 ± 0.1	...	...	2 1 y l a
539	PBC J1712.6-2415	V2400 Oph	DQ*	258.15021	–24.26535	2.16	1.182	20.50	5.8 ± 0.3	0.30 ± 0.10	...	...	3 1 y h a
540	PBC J1712.6-3737	SAX J1712.6-3739	LXB	258.15451	–37.63066	2.18	0.975	35.30	10.2 ± 0.3	0.47 ± 0.07	...	...	3 1 y l a
541	PBC J1717.1-6249	NGC 6300	Sy2	259.28189	–62.82583	1.52	1.032	34.09	7.3 ± 0.2	0.82 ± 0.09	0.0037	42.30	3 1 y h a
542	PBC J1719.5+4858	Arp 102B	BLA	259.87872	48.97905	2.83	2.686	8.60	1.8 ± 0.2	0.9 ± 0.3	0.0250	43.39	3 1 n h a
543	PBC J1719.6-4100	IGR J17195-4100	CV*	259.91815	–41.01368	2.89	0.847	15.69	4.3 ± 0.3	0.2 ± 0.1	...	...	2 1 y l a
544	PBC J1720.1-3116	IGR J17200-3116	HXB	260.04553	–31.27227	3.77	1.258	12.41	3.7 ± 0.3	0.3 ± 0.2	...	...	2 1 y l a
545	PBC J1723.5+3631	RBS 1645	Sy1	260.88589	36.52710	4.13	2.386	4.92	0.8 ± 0.2	...	0.0400	43.59	1 1 n h b
546	PBC J1725.2-3616	IGR J17252-3616	HXB	261.31674	–36.28168	1.55	0.935	43.43	12.4 ± 0.3	0.25 ± 0.04	...	...	3 1 y l a
547	PBC J1725.5-3256	IGR J17254-3257	LXB	261.38580	–32.94731	3.72	1.557	11.22	3.2 ± 0.3	...	...	...	1 1 y l a
548	PBC J1727.6-3047	4U 1722-30	LXB	261.90067	–30.79953	1.05	0.652	126.26	35.8 ± 0.3	0.55 ± 0.02	...	...	1 1 y l a
549	PBC J1730.3-0559	IGR J17303-0601	CV*	262.59283	–5.99002	1.91	0.256	26.23	6.6 ± 0.3	0.6 ± 0.1	...	...	3 1 y h a
550	PBC J1731.7-1657	3A 1728-169	LXB	262.93921	–16.95700	0.83	0.403	207.05	43.3 ± 0.3	0.019 ± 0.003	...	...	2 1 y h a
551	PBC J1731.9-3349	GX 354-0	LXB	262.99637	–33.82764	0.76	0.556	335.86	96.6 ± 0.3	0.234 ± 0.006	...	...	2 1 y l a
552	PBC J1732.0-2444	GX 1+4	LXB	263.00879	–24.74156	0.75	0.240	420.97	112.9 ± 0.3	0.718 ± 0.007	...	...	1 1 y l a
553	PBC J1735.4-3256	IGR J17354-3255	gam	263.85269	–32.93444	3.72	0.780	9.64	2.9 ± 0.3	0.5 ± 0.2	...	...	3 1 y l a
554	PBC J1735.7+2047	MCG+03-45-003	Sy2	263.92798	20.79123	4.22	2.361	6.55	1.3 ± 0.2	...	0.0241	43.24	1 1 n h b
555	PBC J1737.4-2908	GRS 1734-292	Sy1	264.36417	–29.13481	1.93	0.213	33.42	10.3 ± 0.3	0.78 ± 0.09	0.0214	43.97	1 1 y l a
556	PBC J1737.7-5953	ESO 139-12	Sy2	264.44336	–59.89243	3.88	3.063	7.02	1.8 ± 0.3	...	0.0174	42.97	3 1 n h c
557	PBC J1738.2-2700	SLX 1735-269	LXB	264.56979	–27.00564	1.26	0.700	70.77	21.4 ± 0.3	0.63 ± 0.04	...	...	1 1 y l a
558	PBC J1738.9-4427	4U 1735-444	LXB	264.74500	–44.45039	0.81	0.092	339.22	66.9 ± 0.3	< 0.003	...	...	2 1 y h a
559	PBC J1740.6-2819	SLX 1737-282	LXB	265.15558	–28.32333	1.90	1.641	30.53	9.6 ± 0.3	0.63 ± 0.08	...	...	1 1 y l a
560	PBC J1741.3+0349	RX J1741.4+0348	Sy1	265.34604	3.83097	4.23	1.666	4.74	1.2 ± 0.2	...	0.0300	43.48	1 1 n h b
561	PBC J1741.8-1210	IGR J17418-1212	Sy1	265.47342	–12.16823	3.56	1.791	11.80	3.1 ± 0.3	...	0.0370	43.88	3 1 y h a
562	PBC J1743.0-3620	XTE J1743-363	gam	265.75159	–36.33700	3.76	0.470	10.63	2.5 ± 0.3	0.3 ± 0.2	...	...	1 1 y l a
563	PBC J1743.6+6252	2MASXJ17431735+6250207	Sy2	265.91876	62.88182	3.70	3.667	5.78	0.9 ± 0.2	0.9 ± 0.5	0.0335	43.48	1 1 n h b
564	PBC J1744.0-2942	1E 1740.7-2942	LXB	266.02197	–29.71543	0.95	2.885	133.18	38.8 ± 0.3	0.94 ± 0.03	...	...	1 1 y l a
565	PBC J1745.7-2930	1A 1742-294	LXB	266.44437	–29.50015	1.16	4.201	59.70	19.4 ± 0.3	0.29 ± 0.03	...	...	2 1 y l a
566	PBC J1746.1-3214	IGR J17464-3213	LXB	266.54578	–32.24360	2.86	1.235	14.16	4.5 ± 0.3	0.7 ± 0.2	...	...	3 1 y l a
567	PBC J1746.2-2853	1E 1743.1-2852	LXB	266.55923	–28.88615	1.51	1.279	34.64	12.1 ± 0.4	0.02 ± 0.04	...	...	3 1 n l a
568	PBC J1747.2-2721	IGR J17473-2721	gam	266.82452	–27.36473	3.53	1.236	12.44	4.1 ± 0.4	...	...	...	1 1 y l a
569	PBC J1747.4-3001	SLX 1744-299	LXB	266.85300	–30.02287	1.39	0.310	30.61	18.2 ± 0.3	1.00 ± 0.07	...	...	3 1 y l a
570	PBC J1747.6-2820	IGR J17475-2822	MoC	266.91599	–28.34551	3.18	7.801	7.27	3.1 ± 0.4	0.7 ± 0.4	...	...	1 1 y l a
571	PBC J1748.1-2634	GX 3+1	LXB	267.04568	–26.58299	0.91	3.542	169.04	41.6 ± 0.4	0.01 ± 0.01	...	...	2 1 y l a
572	PBC J1748.7-3253	IGR J17488-3253	Sy1	267.19885	–32.89507	3.15	1.942	11.84	3.3 ± 0.3	0.9 ± 0.3	0.0200	43.45	3 1 y l a
573	PBC J1749.4-2820	IGR J17497-2821	LXB	267.36441	–28.33916	1.89	2.511	29.85	10.1 ± 0.4	1.0 ± 0.1	...	...	1 1 y l a
574	PBC J1749.6-2639	GRO J1750-27	HXB	267.40424	–26.65818	2.82	5.629	13.35	5.9 ± 0.4	0.16 ± 0.02	...	...	2 1 n l a
575	PBC J1750.2-3703	1H 1746-370	LXB	267.57205	–37.05915	1.51	1.006	37.04	8.6 ± 0.3	0.03 ± 0.05	...	...	2 1 y h a
576	PBC J1750.9-3116	GRS 1747-312	LXB	267.72614	–31.28317	3.17	1.952	13.21	3.9 ± 0.3	0.3 ± 0.2	...	...	3 1 y l a
577	PBC J1753.4-0126	SWIFT J1753.5-0127	LXB	268.36658	–1.44652	0.72	0.318	394.24	108.8 ± 0.3	1.15 ± 0.01	...	...	1 1 y h a
578	PBC J1758.5-2122	IGR J17586-2129	gam	269.64111	–21.37315	3.54	2.935	10.23	3.3 ± 0.3	0.4 ± 0.2	...	...	3 1 y l a
579	PBC J1759.7-2201	IGR J17597-2201	LXB	269.92703	–22.03095	2.59	0.773	19.23	5.8 ± 0.3	0.3 ± 0.1	...	...	3 1 y l a
580	PBC J1800.0+6634	NGC 6552	Sy2	270.00861	66.58048	4.23	2.124	4.74	0.7 ± 0.2	...	0.0265	43.13	1 1 n h c
581	PBC J1800.5+0810	V2301 OPH	NL*	270.13766	8.18089	3.91	0.868	5.79	0.6 ± 0.1	...	...	...	2 2 n h c
582	PBC J1801.1-2505	GX 5-1	LXB	270.28549	–25.09039	0.70	0.677	612.15	146.1 ± 0.3	< 0.002	...	...	2 1 y l a
583	PBC J1801.2-2544	GRS 1758-258	LXB	270.30124	–25.74685	0.79	0.388	359.73	106.1 ± 0.3	1.11 ± 0.01	...	...	1 1 y l a
584	PBC J1801.6-2030	GX 9+1	LXB	270.41418	–20.50517	0.78	2.189	262.17	63.7 ± 0.3	0.011 ± 0.002	...	...	2 1 y l a
585	PBC J1802.7-1454	IGR J18027-1455	Sy1	270.69550	–14.91040	3.87	0.309	11.81	3.4 ± 0.3	...	0.0350	43.92	3 1 y l a
586	PBC J1802.9-2016	IGR J18027-2016	HXB	270.73093	–20.26691	2.38	3.401	14.15	9.3 ± 0.3	1.2 ± 0.2	...	...	1 1 y l a
587	PBC J1805.1+1243	NVSS J180508+124256	QSO	271.29510	12.72249	4.25	0.644	4.71	0.7 ± 0.2	...	0.1707	44.87	3 0 n h b
588	PBC J1807.9+0551	V* V426 Oph	DN*	271.98260	5.86542	3.26	1.030	10.03	2.0 ± 0.2	0.2 ± 0.2	...	...	2 1 n h b
589	PBC J1808.5-2025	SGR 1806-20	Psr	272.14313	–20.42577	2.62	1.464	16.66	4.9 ± 0.3	0.8 ± 0.2	...	...	1 1 y l a
590	PBC J1810.6-2609	SAX J1810.8-2609	LXB	272.67166	–26.15210	2.15	0.729	27.26	7.6 ± 0.3	0.48 ± 0.09	...	...	3 1 n l a
591	PBC J1813.6-1753	IGR J18135-1751	SNR	273.40790	–17.89938	3.48	3.988	14.70	4.2 ± 0.3	...	...	...	1 1 y l a

Table 2. continued.

	PBC name	ID	Type*	RA (deg)	Dec (deg)	Error radius (arcmin)	Offset (arcmin)	SNR	Flux† (erg cm^{-2} s^{-1})	Hardness ratio (R_{30-150}/R_{14-30})	Redshift	log L_{14-150} (erg s^{-1})	Flag‡ A B C D E
592	PBC J1814.5-1709	GX 13+1	LXB	273.63599	–17.15660	0.90	0.264	181.53	40.1 ± 0.3	0.034 ± 0.009	...	...	2 1 y l a
593	PBC J1815.1-1205	4U 1812-12	LXB	273.77686	–12.09116	1.02	0.322	175.75	50.0 ± 0.3	0.78 ± 0.02	...	...	1 1 y l a
594	PBC J1816.0-1402	GX 17+2	LXB	274.00458	–14.03613	0.71	0.074	690.44	164.2 ± 0.3	0.000 ± 0.002	...	...	2 1 y l a
595	PBC J1816.0+4952	AM Her	AM*	274.01758	49.87377	3.56	1.511	7.17	1.0 ± 0.2	0.1 ± 0.3	...	...	3 1 n h a
596	PBC J1817.7-3300	XTE J1817-330	LXB	274.42542	–33.00713	2.00	0.759	24.76	7.8 ± 0.3	0.7 ± 0.1	...	...	1 1 y h a
597	PBC J1821.5+6421	1ES 1821+643	Sy1	275.39767	64.35571	2.78	2.469	8.98	1.4 ± 0.2	0.9 ± 0.4	0.2970	45.69	3 1 n h a
598	PBC J1823.6-3021	H 1820-303	LXB	275.91812	–30.35822	0.77	0.178	423.74	103.2 ± 0.3	< 0.004	...	...	1 1 y h a
599	PBC J1824.3-5622	IGR J18244-5622	Sy2	276.09216	–56.37068	2.41	1.087	15.70	3.8 ± 0.3	0.7 ± 0.2	0.0169	43.34	1 1 y h a
600	PBC J1825.3-0001	H 1822-000	LXB	276.34058	–0.02095	1.64	0.545	29.82	5.1 ± 0.3	< 0.02	...	...	2 1 y h a
601	PBC J1825.7-3706	3A 1822-371	LXB	276.44849	–37.10214	0.78	0.251	249.29	55.4 ± 0.3	0.098 ± 0.007	...	...	2 1 y h a
602	PBC J1829.4-2347	Ginga 1826-24	LXB	277.36813	–23.79502	0.78	0.221	587.45	154.4 ± 0.3	0.614 ± 0.005	...	...	1 1 y h a
603	PBC J1829.6+4845	3C 380	BLA	277.41263	48.75422	3.58	1.292	6.06	1.0 ± 0.2	1.0 ± 0.6	0.6919	46.41	3 1 n h c
604	PBC J1831.0+0928	2MASX J18305065+0928414	G	277.76520	9.48046	4.43	3.223	7.09	1.6 ± 0.2	...	...	...	1 1 n h c
605	PBC J1833.5-1033	SNR 021.5-00.9	Psr	278.38458	–10.56269	2.12	0.720	23.39	7.0 ± 0.3	0.7 ± 0.1	...	...	3 1 y l a
606	PBC J1833.7-2102	PKS 1830-211	BLA	278.43671	–21.03819	2.39	1.789	20.35	5.6 ± 0.3	1.2 ± 0.2	2.5070	48.42	1 1 y h a
607	PBC J1835.0+3241	3C 382	Sy1	278.75208	32.69692	1.55	0.610	31.93	6.6 ± 0.2	0.87 ± 0.10	0.0581	44.66	3 1 y h a
608	PBC J1835.7-3259	XB 1832-330	LXB	278.93164	–32.98809	1.19	0.379	69.94	18.7 ± 0.3	0.76 ± 0.04	...	...	3 1 y h a
609	PBC J1836.9-5925	1H 1828-593	Sy2	279.24756	–59.42310	3.73	1.263	5.70	1.1 ± 0.2	...	0.0194	43.09	1 1 n h a
610	PBC J1838.0-0655	AX J1838.0-0655	SNR	279.51385	–6.91991	2.45	1.016	15.75	4.6 ± 0.3	0.7 ± 0.2	...	...	1 1 y l a
611	PBC J1838.4-6525	H 1834-653	Sy2	279.60498	–65.41833	1.38	0.774	31.24	6.4 ± 0.2	0.80 ± 0.10	0.0132	43.50	3 1 y h a
612	PBC J1839.9+0502	Ser X-1	LXB	279.99066	5.03908	0.78	0.205	224.66	37.9 ± 0.3	0.025 ± 0.004	...	...	2 1 y l a
613	PBC J1841.0-0538	IGR J18410-0535	HXB	280.26245	–5.63463	3.75	2.377	8.67	2.7 ± 0.3	0.7 ± 0.3	...	...	3 1 y l a
614	PBC J1841.3-0456	PSR B1841-04	Psr	280.34317	–4.93756	2.12	0.755	21.15	6.4 ± 0.3	1.8 ± 0.3	...	...	1 1 y l a
615	PBC J1842.0+7946	3C 390.3	Sy1	280.52322	79.77036	1.33	0.164	38.53	7.8 ± 0.2	0.87 ± 0.08	0.0561	44.72	3 1 y h a
616	PBC J1844.8-6224	ESO140-43	Sy1	281.20758	–62.40071	2.42	2.214	15.30	3.4 ± 0.2	0.6 ± 0.2	0.0141	43.11	1 1 n h c
617	PBC J1844.9-0433	IGR J18450-0435	HXB	281.24237	–4.56503	2.65	0.931	12.99	3.9 ± 0.3	0.6 ± 0.2	...	...	1 1 y l a
618	PBC J1845.5+7212	2MASX J18452628+7211008	Sy2	281.38458	72.20068	3.60	1.114	5.56	1.0 ± 0.2	0.7 ± 0.5	0.0461	43.77	1 1 n h c
619	PBC J1845.6+0051	Ginga 1843+009	HXB	281.41214	0.85972	1.87	0.573	25.12	6.5 ± 0.3	0.55 ± 0.10	...	...	3 1 y l a
620	PBC J1846.3-0258	PSR J1846-0258	Psr	281.58301	–2.97161	3.06	1.155	11.65	3.7 ± 0.3	1.0 ± 0.3	...	...	3 1 y l a
621	PBC J1847.4-7831	H 1846-786	Sy1	281.85178	–78.51771	4.03	1.447	10.73	2.0 ± 0.2	0.7 ± 0.3	0.0743	44.15	1 1 n h a
622	PBC J1848.2-0311	IGR J18483-0311	HXB	282.06717	–3.18850	2.04	1.209	22.36	7.2 ± 0.3	0.6 ± 0.1	...	...	3 1 y l a
623	PBC J1848.3-0045	IGR J18485-0047	gam	282.08875	–0.75635	3.64	2.153	7.88	2.3 ± 0.3	1.1 ± 0.5	...	...	3 1 y l a
624	PBC J1848.8-0002	IGR J18490-0000	gam	282.21588	–0.04286	3.80	3.230	9.21	2.6 ± 0.3	...	...	...	1 1 y l a
625	PBC J1853.0-0841	3A 1850-087	LXB	283.26639	–8.69426	1.36	0.722	40.81	12.2 ± 0.3	0.72 ± 0.07	...	...	3 1 y l a
626	PBC J1854.9-3109	V* V1223 Sgr	DQ*	283.74954	–31.15807	1.30	0.598	46.03	13.1 ± 0.3	0.31 ± 0.04	...	...	3 1 n h a
627	PBC J1855.5-0236	XTE J1855-026	HXB	283.87604	–2.60549	1.08	0.273	68.79	19.6 ± 0.3	0.48 ± 0.03	...	...	3 1 y l a
628	PBC J1856.0+1537	IGR J18559+1535	Sy1	284.00473	15.62249	3.16	0.909	12.20	3.0 ± 0.2	1.0 ± 0.3	0.0840	44.56	3 1 y h a
629	PBC J1856.6+0518	XTE J1856+053	LXB	284.16721	5.30547	2.51	1.498	14.69	3.8 ± 0.3	1.1 ± 0.2	...	...	3 1 n l a
630	PBC J1857.4-7830	2E 1849.2-7832	Sy1	284.35208	–78.50396	3.05	2.205	11.61	2.1 ± 0.2	1.0 ± 0.3	0.0420	43.77	3 1 n h b
631	PBC J1858.6+0324	XTE J1858+034	HXB	284.67151	3.40731	4.31	1.949	6.11	1.5 ± 0.3	...	...	...	2 2 y l a
632	PBC J1900.1-2454	HETE J1900.1-2455	LXB	285.03979	–24.91414	0.91	0.778	152.67	38.5 ± 0.3	0.69 ± 0.02	...	...	3 1 y h a
633	PBC J1901.6+0127	XTE J1901+014	XB*	285.41077	1.45471	2.08	1.153	19.56	5.3 ± 0.3	0.8 ± 0.1	...	...	3 1 y l a
634	PBC J1907.2+0918	SGR 1900+14	Psr	286.81879	9.31031	4.34	0.895	7.48	2.1 ± 0.3	...	...	...	3 3 y l a
635	PBC J1907.2-2048	V1082SGR	CV*	286.82068	–20.81646	3.92	0.813	6.00	1.8 ± 0.3	0.4 ± 0.3	...	...	2 1 n h c
636	PBC J1909.6+0950	H 1907+097	HXB	287.41315	9.83342	0.94	0.362	113.43	25.1 ± 0.3	0.12 ± 0.02	...	...	2 1 y l a
637	PBC J1910.7+0735	4U 1909+07	HXB	287.69769	7.59589	1.01	0.139	100.97	25.2 ± 0.3	0.42 ± 0.02	...	...	2 1 y l a
638	PBC J1911.2+0035	Aql X-1	LXB	287.80695	0.58527	1.30	0.584	47.26	11.2 ± 0.2	0.58 ± 0.06	...	...	3 1 y l a
639	PBC J1911.8+0459	SS 433	HXB	287.96478	4.99149	1.18	0.724	61.95	14.1 ± 0.2	0.38 ± 0.03	...	...	2 1 y l a
640	PBC J1914.0+0951	IGR J19140+0951	HXB	288.52234	9.86335	1.28	1.203	62.50	15.5 ± 0.3	0.41 ± 0.03	...	...	2 1 y l a
641	PBC J1915.1+1056	GRS 1915+105	LXB	288.79938	10.94210	0.59	0.216	1897.92	431.4 ± 0.3	0.320 ± 0.001	...	...	2 1 y l a
642	PBC J1918.7-0513	4U 1916-053	LXB	289.69040	–5.22980	1.13	0.655	68.63	17.1 ± 0.3	0.50 ± 0.03	...	...	3 1 y h a
643	PBC J1920.9+4358	4U 1919+44	ClG	290.24796	43.97611	2.12	2.694	20.53	2.7 ± 0.2	0.01 ± 0.09	0.0559	44.23	2 1 n h a
644	PBC J1921.3-5842	ESO 141-55	Sy1	290.33630	–58.70839	2.05	2.407	18.92	4.2 ± 0.2	0.8 ± 0.2	0.0366	44.05	3 1 n h a
645	PBC J1922.6-1716	SWIFT J1922.7-1716	gam	290.66843	–17.27866	1.83	0.881	23.63	5.9 ± 0.3	0.6 ± 0.1	...	...	3 1 y h a
646	PBC J1924.4-2913	OV -236	BLA	291.10501	–29.22380	4.22	5.742	4.76	1.3 ± 0.3	...	0.3520	45.83	1 1 y h a
647	PBC J1924.4+5014	CH Cyg	Sy*	291.12061	50.23541	3.23	0.843	11.26	2.0 ± 0.2	0.3 ± 0.2	...	...	2 1 n h c
648	PBC J1930.1+3411	[ILC2007] 32	Sy1	292.53448	34.18452	3.27	1.168	6.96	1.3 ± 0.2	0.6 ± 0.4	0.0629	44.18	3 1 n h a
649	PBC J1933.8+3254	1RXS J193347.6+325422	Sy1	293.46338	32.91162	3.71	0.868	5.75	1.3 ± 0.2	0.8 ± 0.5	0.0580	44.11	3 1 n h a
650	PBC J1937.4-0613	IGR J19378-0617	Sy1	294.36865	–6.22544	4.23	1.231	4.75	0.8 ± 0.2	...	0.0105	42.57	3 3 y h a
651	PBC J1938.2-5107	1H 1927-516	Sy1	294.55365	–51.12950	3.94	2.392	5.25	1.0 ± 0.2	...	0.0400	43.66	3 1 n h b
652	PBC J1940.2-1024	RX J1940.2-1025	AM*	295.06082	–10.41343	1.86	0.983	22.23	5.0 ± 0.3	0.4 ± 0.1	...	...	3 1 y h a
653	PBC J1942.6-1019	NGC 6814	Sy1	295.65240	–10.32181	1.83	0.945	23.46	5.5 ± 0.3	0.7 ± 0.1	0.0052	42.48	3 1 y h a
654	PBC J1943.9+2118	RX J1943.9+2118	X	295.97647	21.30228	2.88	0.269	8.47	1.8 ± 0.2	1.0 ± 0.4	...	...	1 1 y l a
655	PBC J1947.2+4448	CXOU J194719.3+444942	AGN	296.81897	44.81174	3.24	1.122	7.06	1.4 ± 0.2	0.8 ± 0.4	0.0530	44.07	1 1 n h a
656	PBC J1949.5+3011	KS 1947+300	HXB	297.39267	30.19237	1.99	1.018	26.07	5.7 ± 0.2	0.59 ± 0.09	...	...	3 1 y l a
657	PBC J1952.2+0230	3C 403	Sy2	298.07098	2.50191	3.24	0.660	9.75	2.2 ± 0.2	1.1 ± 0.4	0.0590	44.23	1 1 y h a
658	PBC J1955.6+3205	3A 1954+319	LXB	298.92053	32.09107	0.90	0.451	132.72	30.7 ± 0.3	0.34 ± 0.01	...	...	2 1 y l a
659	PBC J1958.2+3232	V* V2306 Cyg	CV*	299.55118	32.54526	3.62	0.467	8.85	2.3 ± 0.3	...	...	...	2 2 n l c
660	PBC J1958.3+3512	Cyg X-1	HXB	299.58990	35.20245	0.55	0.055	5189.52	1611.4 ± 0.3	1.0140 ± 0.0006	...	...	1 1 y l a
661	PBC J1959.2+1143	4U 1957+115	LXB	299.81223	11.72551	3.87	2.447	9.93	2.0 ± 0.2	0.4 ± 0.2	...	...	2 1 n h a
662	PBC J1959.4+4044	Cygnus A	Sy2	299.87054	40.73691	1.35	0.210	32.68	6.9 ± 0.2	0.89 ± 0.09	0.0561	44.81	1 1 y h a
663	PBC J1959.8+6509	1ES 1959+650	BLA	299.96326	65.15565	2.03	1.007	15.09	2.3 ± 0.2	0.4 ± 0.1	0.0480	44.20	3 1 y h a
664	PBC J2000.3+3211	IGR J20006+3210	HXB	300.09317	32.19520	2.30	0.343	18.11	4.5 ± 0.3	0.5 ± 0.1	...	...	3 1 y l a
665	PBC J2000.9-1812	2MASX J20005575-1810274	Sy1	300.22836	–18.20279	3.82	1.724	6.73	1.4 ± 0.3	...	0.0374	43.71	3 1 n h b

Table 2. continued.

	PBC name	ID	Type*	RA (deg)	Dec (deg)	Error radius (arcmin)	Offset (arcmin)	SNR	Flux† (erg cm^{-2} s^{-1})	Hardness ratio (R_{30-150}/R_{14-30})	Redshift	log L_{14-150} (erg s^{-1})	Flag‡ A B C D E
666	PBC J2006.9-3433	ESO 399-20	Sy1	301.72864	–34.55195	3.99	0.526	5.18	1.2 ± 0.3	0.3 ± 0.4	0.0249	43.37	2 1 y h a
667	PBC J2008.9-6105	NGC 6860	Sy1	302.23026	–61.09177	2.26	1.180	12.50	2.6 ± 0.2	0.9 ± 0.3	0.0148	43.22	3 1 n h a
668	PBC J2011.8-5650	ABELL 3667	ClG	302.96671	–56.84073	3.97	5.698	5.20	1.0 ± 0.2	0.3 ± 0.4	0.0552	43.95	2 1 n h c
669	PBC J2018.1-5539	2MASX J20180125-5539312	Sy2	304.54568	–55.65283	2.86	1.405	9.97	2.5 ± 0.3	0.8 ± 0.3	0.0602	44.30	1 1 n h c
670	PBC J2018.6+4041	IGR J20187+4041	Sy2	304.65863	40.69527	3.79	0.715	11.08	2.3 ± 0.2	0.7 ± 0.3	...	...	2 1 y l a
671	PBC J2028.6+2544	IGR J20286+2544	Sy2	307.15765	25.73381	2.00	0.617	23.02	4.9 ± 0.2	1.1 ± 0.2	0.0142	43.28	3 1 y h a
672	PBC J2032.2+3738	EXO 2030+375	HXB	308.06000	37.63888	0.65	0.178	605.59	134.9 ± 0.3	0.389 ± 0.004	...	...	2 1 y l a
673	PBC J2032.4+4057	Cyg X-3	HXB	308.10861	40.96038	0.61	0.167	1303.85	240.9 ± 0.2	0.285 ± 0.002	...	...	2 1 y l a
674	PBC J2033.5+2144	4C +21.55	QSO	308.38181	21.74850	2.52	1.472	10.49	2.1 ± 0.2	1.2 ± 0.4	0.1735	45.23	1 1 n h c
675	PBC J2037.1+4149	SWIFT J2037.2+4151	X	309.28403	41.83277	3.00	0.468	14.15	2.1 ± 0.2	...	...	...	2 2 n l c
676	PBC J2042.6+7508	4C 74.26	Sy1	310.67087	75.14629	1.90	0.776	17.62	3.4 ± 0.2	0.6 ± 0.1	0.1039	44.97	3 1 y h a
677	PBC J2044.0+2834	RX J2044.0+2833	Sy1	310.99991	28.56754	3.66	1.332	7.79	1.4 ± 0.2	...	0.0500	43.98	1 1 n h c
678	PBC J2044.1-1043	Mrk 509	Sy1	311.04306	–10.72743	1.59	0.273	27.53	6.9 ± 0.3	0.9 ± 0.1	0.0343	44.25	3 1 n h a
679	PBC J2052.0-5704	IC 5063	Sy2	313.00775	–57.07801	1.87	0.530	23.37	5.9 ± 0.3	1.1 ± 0.2	0.0112	43.15	1 1 n h a
680	PBC J2103.6+4544	SAX J2103.5+4545	HXB	315.90576	45.74971	1.65	0.311	31.41	5.5 ± 0.2	0.32 ± 0.07	...	...	2 1 y l a
681	PBC J2109.0-0940	RBS 1727	Sy1	317.26688	–9.68192	3.43	1.605	6.47	1.2 ± 0.2	0.6 ± 0.4	0.0270	43.40	3 1 n h b
682	PBC J2113.7+8206	S5 2116+81	Sy1	318.44354	82.10099	2.56	1.363	13.05	2.5 ± 0.2	1.0 ± 0.3	0.0860	44.61	3 1 y h a
683	PBC J2117.6+5137	IGR J21178+5139	AG?	319.40488	51.61994	3.22	2.466	8.82	1.8 ± 0.2	1.1 ± 0.4	...	...	3 1 y l a
684	PBC J2119.7+3329	1RXS J211928.4+333259	X	319.94946	33.49755	4.26	5.109	5.59	0.8 ± 0.1	...	...	...	3 3 n h c
685	PBC J2123.6+4217	V2069 Cyg	CV*	320.91681	42.28775	3.43	1.176	10.70	1.7 ± 0.2	0.2 ± 0.2	...	...	2 1 y h a
686	PBC J2123.8+2502	3C 433	Sy2	320.95697	25.04633	4.31	1.821	8.74	1.8 ± 0.2	...	0.1017	44.45	3 3 n h c
687	PBC J2124.6+5058	IGR J21247+5058	Sy1	321.16321	50.97489	1.06	0.338	73.31	14.1 ± 0.2	0.87 ± 0.04	0.0200	44.04	3 1 y l a
688	PBC J2127.7+5657	IGR J21277+5656	Sy1	321.93326	56.95460	2.04	0.628	18.76	3.3 ± 0.2	0.4 ± 0.1	0.0140	43.09	3 1 y l a
689	PBC J2129.2-1537	PKS 2126-158	BLA	322.31549	–15.63300	3.65	1.104	9.66	2.3 ± 0.3	...	3.2680	48.16	3 1 n h a
690	PBC J2129.9+1210	4U 2129+12	LXB	322.49344	12.17620	1.45	0.523	41.04	7.9 ± 0.2	0.43 ± 0.06	...	...	2 1 n h a
691	PBC J2131.8-3343	RBS 1756	Sy1	322.97260	–33.72404	2.16	1.904	13.50	2.8 ± 0.2	1.0 ± 0.2	0.0297	43.85	1 1 n h a
692	PBC J2133.9+5106	IGR J21335+5105	CV*	323.47504	51.10607	1.73	1.931	27.17	5.0 ± 0.2	0.36 ± 0.08	...	...	3 1 y l a
693	PBC J2134.8-2727	1RXS J213445.2-272551	Sy1	323.70593	–27.45967	4.04	1.987	5.08	1.1 ± 0.2	...	0.0670	44.17	3 1 n h c
694	PBC J2136.0+4728	RX J2135.9+4728	Sy1	324.00583	47.47871	3.00	1.212	9.84	1.9 ± 0.2	0.9 ± 0.4	0.0252	43.37	3 1 y l a
695	PBC J2136.4-6225	RBS 1763	Sy1	324.10950	–62.42773	2.87	1.705	8.51	1.6 ± 0.2	0.7 ± 0.3	0.0589	44.23	3 1 n h c
696	PBC J2138.4+3205	2MASX J21383340+3205060	Sy1	324.61588	32.09181	3.66	1.262	6.60	1.4 ± 0.2	...	0.0250	43.27	1 1 n h c
697	PBC J2139.6+5955	1RXS J213944.3+595016	X	324.90106	59.92457	4.18	5.305	4.60	0.4 ± 0.1	...	...	...	2 2 n h c
698	PBC J2142.7+4334	SS Cyg	DN*	325.69604	43.57811	1.69	0.906	31.33	5.4 ± 0.2	0.27 ± 0.07	...	...	2 1 y h a
699	PBC J2144.6+3819	Cyg X-2	LXB	326.17172	38.32140	0.72	0.016	522.55	72.7 ± 0.2	< 0.001	...	...	2 1 y h a
700	PBC J2146.4-3051	6dFGS gJ214636.1-305141	Sy1	326.62216	–30.85698	4.20	1.470	4.79	1.0 ± 0.2	...	0.0753	44.23	1 1 n h c
701	PBC J2148.0+0657	4C +06.69	BLA	327.02130	6.95571	3.77	0.313	5.61	1.1 ± 0.2	...	0.9900	46.75	1 1 n h c
702	PBC J2148.2-3455	NGC 7130	EmG	327.06842	–34.92590	4.37	1.718	5.73	1.3 ± 0.2	...	0.0160	42.78	1 1 n h a
703	PBC J2152.0-3027	PKS 2149-306	BLA	328.00406	–30.46292	1.75	1.182	25.05	5.7 ± 0.2	1.5 ± 0.2	2.3450	48.31	1 1 n h a
704	PBC J2153.7+1745	ABELL 2390	ClG	328.44708	17.75164	3.94	5.771	5.26	0.4 ± 0.1	...	0.2310	45.23	2 2 n h b
705	PBC J2200.7+1033	Mrk 520	Sy1	330.18033	10.55374	2.56	0.476	10.20	1.7 ± 0.2	0.9 ± 0.3	0.0272	43.56	3 1 y h a
706	PBC J2202.0-3152	NGC 7172	Sy2	330.51105	–31.86799	1.19	0.299	51.60	11.9 ± 0.2	1.05 ± 0.07	0.0086	43.23	1 1 y h a
707	PBC J2202.7+4217	BL Lac	BLA	330.69327	42.29334	2.92	1.095	12.54	2.5 ± 0.2	1.2 ± 0.3	0.0688	44.32	3 1 y h a
708	PBC J2203.3+3148	4C 31.63	BLA	330.83301	31.80374	4.14	2.792	6.04	1.2 ± 0.2	...	0.2980	45.45	3 3 n h c
709	PBC J2204.4+0336	2MASX J22041914+0333511	Sy2	331.11621	3.60697	3.37	3.375	8.12	1.7 ± 0.2	1.7 ± 0.7	0.0611	44.14	3 1 n h b
710	PBC J2207.9+5430	3A 2206+543	HXB	331.99344	54.50954	0.97	0.621	101.04	20.0 ± 0.2	0.50 ± 0.02	...	...	3 1 y l a
711	PBC J2209.2-4710	NGC 7213	BLA	332.31357	–47.16808	2.06	0.184	17.13	3.5 ± 0.2	1.1 ± 0.2	0.0059	42.43	3 1 n h a
712	PBC J2211.9+1843	RBS 1828	BLA	332.98495	18.72362	4.36	1.691	4.53	0.8 ± 0.2	...	0.0699	44.07	3 1 n h b
713	PBC J2213.9+1242	V* RU Peg	DN*	333.48291	12.71647	3.02	1.814	10.13	1.0 ± 0.2	< 0.01	...	...	2 1 n h b
714	PBC J2214.7-3849	RBS 1835	Sy1	333.69174	–38.82517	4.00	1.354	5.14	0.9 ± 0.2	...	0.0392	43.63	3 1 n h c
715	PBC J2217.1+1410	Mrk 304	Sy1	334.28870	14.17319	4.31	4.024	4.61	0.6 ± 0.1	...	0.0662	44.04	3 3 n h b
716	PBC J2217.9-0820	FO Aqr	DQ*	334.48920	-8.33788	1.46	0.941	30.89	6.0 ± 0.2	0.25 ± 0.06	...	...	2 1 y h a
717	PBC J2219.8+2613	RX J2219.8+2613	BLA	334.95767	26.22725	3.78	0.173	5.59	1.0 ± 0.2	...	0.0850	44.33	3 1 n h b
718	PBC J2223.8-0206	3C 445	Sy1	335.95773	–2.11250	2.09	0.548	17.71	3.8 ± 0.2	0.9 ± 0.2	0.0563	44.43	1 1 n h a
719	PBC J2227.0+3623	MCG+06-49-019	Sy1	336.76569	36.39199	4.32	1.890	7.88	1.7 ± 0.2	...	0.0211	42.99	3 3 n h b
720	PBC J2229.4+6647	IGR J22292+6647	AGN	337.36761	66.79736	3.94	1.786	7.43	1.5 ± 0.2	...	...	...	3 1 y h a
721	PBC J2229.6-0831	PKS 2227-08	BLA	337.42233	–8.51841	4.09	1.830	4.98	0.9 ± 0.2	...	1.5615	47.27	1 1 n h c
722	PBC J2232.4+1144	4C +11.69	BLA	338.11536	11.73350	3.01	2.141	7.91	1.5 ± 0.2	1.1 ± 0.5	1.0370	47.02	1 1 n h a
723	PBC J2234.8-2541	ESO 533-50	Sy2	338.70361	–25.69987	4.02	1.419	5.27	1.0 ± 0.2	...	0.0263	43.22	3 1 n h b
724	PBC J2235.6-2601	NGC 7314	Sy1	338.92114	–26.03266	1.99	1.548	17.22	3.3 ± 0.2	0.8 ± 0.2	0.0047	42.22	3 1 y h a
725	PBC J2236.0+3358	NGC7319	Sy2	339.00406	33.97384	2.51	0.575	10.58	1.9 ± 0.2	1.1 ± 0.3	0.0221	43.43	3 1 y h a
726	PBC J2236.7-1232	Mrk 915	Sy1	339.19135	–12.54211	2.72	0.231	13.46	3.0 ± 0.2	1.4 ± 0.3	0.0240	43.48	1 1 y h a
727	PBC J2240.2+0802	RHS 59	Sy1	340.05978	8.04542	3.33	0.832	6.76	1.2 ± 0.2	1.1 ± 0.6	0.0250	43.34	1 1 n h b
728	PBC J2245.8+3939	3C 452	Sy2	341.45032	39.66523	2.61	1.350	13.37	2.9 ± 0.2	1.6 ± 0.3	0.0810	44.55	1 1 y h a
729	PBC J2251.8+2215	87GB 224928.1+220114	BLA	342.97150	22.26663	4.03	1.626	5.71	1.0 ± 0.2	...	3.6680	48.11	3 1 n h c
730	PBC J2253.9+1609	3C 454.3	BLA	343.48819	16.16178	1.36	0.826	41.15	8.3 ± 0.2	1.5 ± 0.1	0.8590	47.44	1 1 y h a
731	PBC J2254.0-1734	RBS 1913	Sy1	343.52182	–17.57691	1.41	0.343	30.01	5.6 ± 0.2	0.9 ± 0.1	0.0639	44.84	3 1 y h a
732	PBC J2254.3+1146	MCG+02-58-032	Sy2	343.58633	11.78212	4.08	0.255	8.47	1.6 ± 0.2	...	0.0285	43.38	1 1 n h b
733	PBC J2255.3-0310	AO Psc	DQ*	343.82910	–3.18121	1.89	0.312	20.41	2.9 ± 0.2	< 0.03	...	...	2 1 n h c
734	PBC J2258.9+4055	MCG +07 -47 -002	Sy1	344.73630	40.92973	3.22	0.253	7.78	1.6 ± 0.2	1.0 ± 0.4	0.0171	43.04	1 1 n h c
735	PBC J2259.6+2454	RBS 1922	Sy1	344.91025	24.90242	2.74	1.573	9.17	1.6 ± 0.2	0.8 ± 0.3	0.0338	43.73	3 1 n h c
736	PBC J2302.1+1558	NGC 7465	LIN	345.53625	15.98235	4.03	2.109	9.05	1.7 ± 0.2	...	0.0065	42.06	1 1 n h b
737	PBC J2303.3+0852	NGC 7469	Sy1	345.82596	8.87315	1.67	0.615	28.28	5.8 ± 0.2	0.9 ± 0.1	0.0158	43.43	3 1 y h a
738	PBC J2304.7-0841	Mrk 926	Sy1	346.18387	–8.68914	1.28	0.261	36.74	6.1 ± 0.2	0.90 ± 0.08	0.0471	44.60	1 1 y h a

Table 2. continued.

	PBC name	ID	Type⋆	RA (deg)	Dec (deg)	Error radius (arcmin)	Offset (arcmin)	SNR	Flux† (erg cm^{-2} s^{-1})	Hardness ratio (R_{30-150}/R_{14-30})	Redshift	log L_{14-150} (erg s^{-1})	Flag‡ A B C D E
739	PBC J2304.8+1217	NGC 7479	Sy2	346.20084	12.29863	4.30	2.526	4.63	0.8 ± 0.2	...	0.0079	42.04	3 1 n h c
740	PBC J2307.2+0433	RBS 1944	Sy1	346.82056	4.55890	3.58	3.548	6.08	0.9 ± 0.2	0.8 ± 0.6	0.0420	43.66	3 1 n h c
741	PBC J2318.3-4221	NGC 7582	Sy2	349.59927	–42.36063	1.52	0.600	31.07	5.6 ± 0.2	0.9 ± 0.1	0.0052	42.49	3 1 n h a
742	PBC J2318.9+0014	Mrk 530	Sy1	349.72592	0.24491	2.11	0.603	14.09	2.5 ± 0.2	0.9 ± 0.2	0.0292	43.78	3 1 y h a
743	PBC J2319.6+2616	RX J2319.5+261	CV*	349.90530	26.27489	3.52	1.852	7.04	1.2 ± 0.2	0.6 ± 0.4	...	...	3 1 n h c
744	PBC J2323.3+5849	Cas A	SNR	350.84976	58.82223	1.33	0.813	41.18	7.5 ± 0.2	0.31 ± 0.05	...	...	2 1 y l a
745	PBC J2325.4-3827	RBS 2004	Sy1	351.36133	–38.46166	3.84	1.004	5.46	0.9 ± 0.2	0.5 ± 0.4	0.0358	43.52	3 1 n h c
746	PBC J2325.8+2152	RHS 61	Sy1	351.46313	21.88039	3.40	0.962	9.16	1.8 ± 0.2	0.8 ± 0.3	0.1200	44.74	1 1 n h a
747	PBC J2327.4+0939	PKS J2327+0940	BLA	351.86725	9.65903	3.47	1.476	9.60	2.0 ± 0.2	...	1.8430	47.55	1 1 n h c
748	PBC J2329.0+0329	NGC 7682	Sy2	352.25446	3.49787	3.71	2.252	5.64	1.2 ± 0.2	...	0.0170	42.97	1 1 n h c
749	PBC J2331.0+7123	IGR J23308+7120	Sy2	352.75507	71.38662	3.32	3.236	6.81	1.1 ± 0.2	0.8 ± 0.5	0.0370	43.53	3 1 y h a
750	PBC J2333.9-2343	RBS 2022	Sy?	353.47760	–23.72896	4.12	0.153	4.92	0.7 ± 0.2	...	0.0478	43.58	1 0 n h b
751	PBC J2341.9+3036	MCG+05-55-047	G	355.47964	30.61338	3.19	1.884	8.57	1.5 ± 0.2	1.0 ± 0.4	0.0174	43.02	3 1 n h c
752	PBC J2351.7-0109	4C -01.61	Sy1	357.94022	–1.15795	3.83	2.629	7.33	1.5 ± 0.2	...	0.1740	44.99	1 1 n h b
753	PBC J2359.1-6055	2MASX J23590436-6054594	Sy2	359.78470	–60.92285	4.40	0.617	5.79	0.9 ± 0.2	...	0.1014	44.36	2 3 n h b
754	PBC J2359.1-3035	H 2356-309	BLA	359.79602	–30.58918	4.08	2.385	5.00	0.6 ± 0.1	...	0.1671	44.90	3 3 n h b

⋆ The source type is coded according to the nomenclature used in SIMBAD. † Flux is in units of 10^{-11} erg cm^{-2} s^{-1}. ‡ Flag A: energy band with highest significance (1 = 14−150 keV; 2 = 14−30 keV; 3 = 14−70 keV); Flag B: energy band used for the calculation of the flux (1 = 14−150 keV; 2 = 14−30 keV; 3 = 14−70 keV); Flag C: y if already reported as hard X-ray source; Flag D: l if the source has $|b| < 5°$, h if the source has $|b| > 5°$; Flag E: strategy used for the identification (see Sect. 4.3).

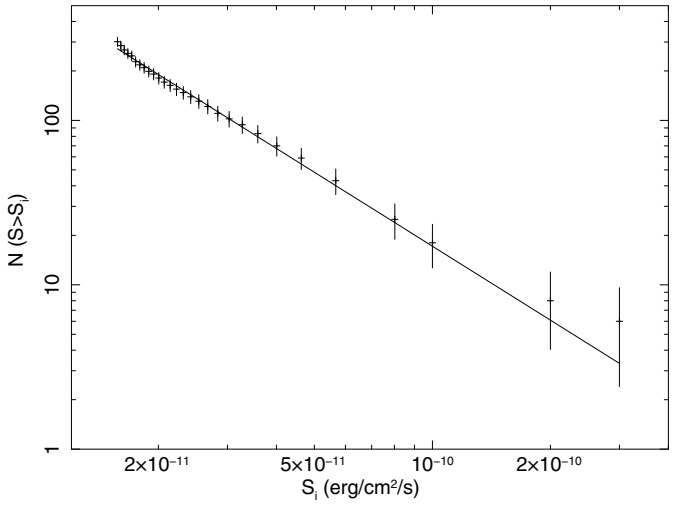

Fig. 11. log(N) − log(S) distribution for the BAT extragalactic sources.

the 14−170 keV energy band as measured by HEAO-1 (Gruber et al. 1999).

We compared this log(N) − log(S) law with the one derived from *INTEGRAL* data (Krivonos et al. 2007) in the 17−60 keV band. To convert our log(N) − log(S) into the 17−60 keV band, we used the Crab spectral parameters derived by the INTEGRAL analysis (Laurent et al. 2003). We determined a slope of $\alpha = 1.62 \pm 0.08$ and a normalization of 240 ± 12 sources with flux higher than 1 mCrab, corresponding to a density of $(5.8 \pm 0.3) \times 10^{-3}$ deg^{-2}. These parameters are in full agreement with those reported by Krivonos et al. (2007).

7. Conclusions

We have analyzed the BAT hard X-ray survey data of the first 39 months of the *Swift* mission. To complete this analysis we developed a dedicated software (Segreto et al. 2010) that performs data reduction, background subtraction, mosaicking, and source detection for the BAT survey data. This software is completely independent from that developed by the *Swift*-BAT team. It is a single tool that provides all the products relevant to the BAT survey sources (e.g., images, spectra, and light curves).

The large BAT field of view, the large geometrical area, and the *Swift* pointing strategy have allowed us to obtain an unprecedented, very sensitive, and quite uniform sky coverage that has provided a significant increase in sources detected in the hard X-ray sky. The survey flux limit is 2.5×10^{-11} erg cm^{-2} s^{-1} (1.1 mCrab) for 90% of the sky and 1.8×10^{-11} erg cm^{-2} s^{-1} (0.8 mCrab) for 50% of the sky.

We have derived a catalogue of 754 identified sources detected above a significance threshold of 4.8 standard deviations. The association of these sources with their counterparts has been performed in three alternative strategies: cross-correlation with the INTEGRAL General Reference Catalogue and with previously published BAT catalogues (Markwardt et al. 2005; Tueller et al. 2008; Ajello et al. 2008a); analysis of soft X-ray field observations with *Swift*-XRT, *XMM-Newton*, *Chandra*, *BeppoSAX*; and cross-correlation with the SIMBAD catalogues of Seyfert galaxies, QSOs, LINERs, Blazars, cataclysmic variables, and X-ray binaries. The expected total number of spurious identifications is negligible. A set of 208 detections have not yet been associated with a counterpart. These candidate sources will be the subject of a follow-up campaign with *Swift*-XRT in the near future.

The extragalactic sources represents ∼69% of our catalogue (519 objects), ∼27% are Galactic objects, and ∼4% are already known X-ray or gamma-ray emitters, whose nature is still to be determined. Compared with the 3rd ISGRI catalogue (Bird et al. 2007), we identify 176 more Seyfert galaxies, 26 more normal galaxies, 13 more galaxy clusters, 13 more QSO, 57 more Blazars, and 5 more LINERs. The redshift limit for the detected emission-line AGNs is ∼0.4, with 31 objects with $z > 0.1$. Blazars and QSOs are detected up to $z \sim 3.7$ and $z \sim 2.4$, respectively. Among the Galactic sources, we significantly increase the number of cataclysmic variables detected in the hard X-ray band (29 new objects). We also detect 22 X-ray binaries that are not included in the ISGRI catalogue, even though the total number of X-ray binaries that we detect is lower than the sample included in the ISGRI catalogue.

Based on the extragalactic sources sample and on the achieved sky coverage, we have evaluated the log(N) − log(S)

distribution for fluxes higher than 1.5×10^{-11} erg cm^{-2} s^{-1}. The slope 1.55 ± 0.06 is consistent with a Euclidean distribution. We estimate that the total number of extragalactic sources at $|b| > 5°$ and flux greater than 1.0×10^{-11} erg cm^{-2} s^{-1} is ∼566. Converting this $\log(N) - \log(S)$ into the 17−60 keV band, our results are in full agreement with those reported by Krivonos et al. (2007) for the INTEGRAL survey. The integrated flux of this extragalactic sample is ∼1.4% of the cosmic X-ray background in the 14−150 keV range (Gruber et al. 1999; Churazov et al. 2007; Frontera et al. 2007; Ajello et al. 2008c).

Forthcoming papers will focus on the detection of transient sources, spectral properties of the extragalactic sample, and updates of the catalogue.

Acknowledgements. G.C. acknowledges B. Sacco and M. Ajello for useful discussions that helped to improve this paper, and the referee W. Voges for his helpful comments and suggestions. This research has made use of NASA's Astrophysics Data System Bibliographic Services, of the SIMBAD database, operated at CDS, Strasbourg, France, as well as of the NASA/IPAC Extragalactic Database (NED), which is operated by the Jet Propulsion Laboratory, California Institute of Technology, under contract with the National Aeronautics and Space Administration. This work was supported by contract ASI/INAF I/011/07/0.

References

Ajello, M., Greiner, J., Kanbach, G., et al. 2008a, ApJ, 678, 102
Ajello, M., Rau, A., Greiner, J., et al. 2008b, ApJ, 673, 96
Ajello, M., Greiner, J., Sato, G., et al. 2008c, ApJ, 689, 666
Barthelmy, S. D., Barbier, L. M., Cummings, J. R., et al. 2005, Space Sci. Rev., 120, 143
Bassani, L., Molina, M., Malizia, A., et al. 2006, ApJ, 636, L65
Beckmann, V., Soldi, S., Shrader, C. R., Gehrels, N., & Produit, N. 2006, ApJ, 652, 126
Bird, A. J., Barlow, E. J., Bassani, L., et al. 2004, ApJ, 607, L33
Bird, A. J., Barlow, E. J., Bassani, L., et al. 2006, ApJ, 636, 765
Bird, A. J., Malizia, A., Bazzano, A., et al. 2007, ApJS, 170, 175
Brandt, W. N., & Hasinger, G. 2005, ARA&A, 43, 827
Cappelluti, N., Hasinger, G., Brusa, M., et al. 2007, ApJS, 172, 341
Churazov, E., Sunyaev, R., Revnivtsev, M., et al. 2007, A&A, 467, 529
Cordier, B., Goldwurm, A., Laurent, P., et al. 1991, Adv. Space Res., 11, 169
Fenimore, E. E., & Cannon, T. M. 1978, Appl. Opt., 17, 337
Forman, W., Jones, C., Cominsky, L., et al. 1978, ApJS, 38, 357
Frontera, F., Orlandini, M., Landi, R., et al. 2007, ApJ, 666, 86
Gehrels, N., Chincarini, G., Giommi, P., et al. 2004, ApJ, 611, 1005
Górski, K. M., Hivon, E., Banday, A. J., et al. 2005, ApJ, 622, 759
Gruber, D. E., Matteson, J. L., Peterson, L. E., & Jung, G. V. 1999, ApJ, 520, 124
Huchra, J., & Sargent, W. L. W. 1973, ApJ, 186, 433
Jager, R., Mels, W. A., Brinkman, A. C., et al. 1997, A&AS, 125, 557
Kendall, M. G. 1980, Multivariate analysis (London: Grin & co.)
Krivonos, R., Vikhlinin, A., Churazov, E., et al. 2005, ApJ, 625, 89
Krivonos, R., Revnivtsev, M., Lutovinov, A., et al. 2007, A&A, 475, 775
Laurent, P., Limousin, O., Cadolle-Bel, M., et al. 2003, A&A, 411, L185
Lebrun, F., Leray, J. P., Lavocat, P., et al. 2003, A&A, 411, L141
Markwardt, C. B., Tueller, J., Skinner, G. K., et al. 2005, ApJ, 633, L77
Moretti, A., Campana, S., Lazzati, D., & Tagliaferri, G. 2003, ApJ, 588, 696
Pavlinsky, M. N., Grebenev, S. A., & Sunyaev, R. A. 1992, SvA Lett., 18, 116
Pavlinsky, M. N., Grebenev, S. A., & Sunyaev, R. A. 1994, ApJ, 425, 110
Sazonov, S., Revnivtsev, M., Krivonos, R., Churazov, E., & Sunyaev, R. 2007, A&A, 462, 57
Schmidt, M. 1968, ApJ, 151, 393
Segreto, A., Cusumano, G., Ferrigno, C., et al. 2010, A&A, 510, A47
Skinner, G. K., Ponman, T. J., Hammersley, A. P., & Eyles, C. J. 1987a, Ap&SS, 136, 337
Skinner, G. K., Willmore, A. P., Eyles, C. J., Bertram, D., & Church, M. J. 1987b, Nature, 330, 544
Sunyaev, R. A., Churazov, E. M., Gil'Fanov, M. R., et al. 1991, Adv. Space Res., 11, 177
Tueller, J., Mushotzky, R. F., Barthelmy, S., et al. 2008, ApJ, 681, 113
Tully, R. B. 1988, Nearby Galaxies Catalogue (NBG) (Cambridge University Press)
Ubertini, P., Bazzano, A., Cocchi, M., et al. 1999, Astrophys. Lett. Commun., 38, 301
Ubertini, P., Lebrun, F., Di Cocco, G., et al. 2003, A&A, 411, L131
Winkler, C., Courvoisier, T. J.-L., Di Cocco, G., et al. 2003, A&A, 411, L1
Wood, K. S., Meekins, J. F., Yentis, D. J., et al. 1984, ApJS, 56, 507
Worsley, M. A., Fabian, A. C., Bauer, F. E., et al. 2005, MNRAS, 357, 1281
Worsley, M. A., Fabian, A. C., Bauer, F. E., et al. 2006, MNRAS, 368, 1735
Zdziarski, A. A., Poutanen, J., & Johnson, W. N. 2000, ApJ, 542, 703